REMOTE SENSING AND GEOTECHNICAL INVESTIGATIONS OF EXPANSIVE SOILS

Fekerte Arega Yitagesu

Examining committee:

Prof.dr. V.G. Jetten	University of Twente, ITC
Prof.dr.ir. A. Stein	University of Twente, ITC
Prof.dr. S.M. de Jong	Utrecht University
Prof.dr. E. Pirard	University of Liège, Belgium
Dr. S. Chabrillat	GFZ German Research Centre for Geosciences

ITC dissertation number 201
ITC, P.O. Box 6, 7500 AA Enschede, The Netherlands

ISBN 978-90-6164-326-5
Cover designed by Demeke Ashenafi and Job Duim
Printed by ITC Printing Department
Copyright © 2012 by Fekerte Arega Yitagesu

UNIVERSITY OF TWENTE.

FACULTY OF GEO-INFORMATION SCIENCE AND EARTH OBSERVATION

REMOTE SENSING AND GEOTECHNICAL INVESTIGATIONS OF EXPANSIVE SOILS

DISSERTATION

to obtain
the degree of doctor at the University of Twente,
on the authority of the Rector Magnificus,
prof.dr. H. Brinksma,
on account of the decision of the graduation committee,
to be publicly defended
on Wednesday March 28, 2012 at 14:45 hrs

by

Fekerte Arega Yitagesu

born on February 16, 1975

in Addis Ababa, Ethiopia

This thesis is approved by
Prof. Dr. F.D. van der Meer, promoter
Dr. H.M.A. van der Werff, assistant promoter

Dedicated to my beloved mom!

Acknowledgements

What a precious aptitude (this research)! I have sojourned my PhD journey seemingly alone, but undoubtedly in support and collaboration with numerous individuals and organizations. I would like to take this opportunity to express my most sincere acknowledgments to all who contributed to bring this work to fruition.

First and foremost, I would like to pay my deepest respect and utmost gratitude to my promoter prof. Dr. Freek van der Meer. Your exceedingly generous support and apt guidance provided an endless enthusiasm at each step of my journey through the years. I came to ITC with avid interest to work on expansive soils. You intuitively introduced me to the various aspects of the current research; and I have learnt a lot from your conscientious working style, countless discussion and thorough revisions of my dissertation. The breadth of skills and lessons that I have learnt from you will be amplified over my career. I am truly, greatly indebted to you.

My most sincere thanks go to my co-promoter Dr. Harald van der Werff for immense enthusiasm and unfading interest in my work in addition to your patience and support during writing and presentation of results. Thorough revisions and many fruitful comments helped to substantially improve this thesis. I am indeed privileged to have worked with you and more importantly grateful for all these immeasurable contributions. I also owe an overdue appreciation to Dr. Hagush Seged for being supportive throughout my Ph.D. duration. I have benefited a lot from your constructive comments.

I would like to extend a much deserved thanks to Drs. Boudewijn de Smeth for the enthusiastic advice and support during the tedious laboratory work. I have experienced an excellent working environment in the laboratory courtesy of your support. You were an excellent advisor and role model as your devoted and meticulous working style will have a remarkable influence throughout my career. My heartfelt thanks to Dr. David Rossiter as I have learnt and do treasure the incredible analytical skills that I carefully collated from you. I am indebted to the invaluable contribution of Drs. Christoph Hecker. Your diligent support during the fieldwork and remote sensing laboratory work has been of great value, of course in addition to important discussion of my work. I truly appreciate the generous support of Ir. Wim Verwaal and Ir. Arno Mulder (of TU Delft engineering geology laboratory) as well as Mr. Henk Wilbrink (of ITC).

I would like to acknowledge the ITC research fund, for granting me a scholarship; the Ethiopian Roads Authority (ERA), for providing data and logistic support to carry out a fieldwork in Ethiopia; the Addis Ababa

University (AAU) technology (AAIT) and natural science (School of Earth and Planetary Science) faculties, the geological survey of Ethiopia (GSE), the Ethiopian mapping agency (EMA), Gondwana engineering PLC, Scott Wilson Kirkpatrick and partners Ethiopia for various forms of assistance. I would like to extend my special thanks to prof. Martin Hale, former ITC research coordinator and his successor Dr. Paul van Dijk for their compassion and support. My wholehearted appreciation to Loes Colenbrander, Christie Agema, Theresa van Boogaard, Marie Chantal Metz, Bettine Geerdink, the entire IT (helpdesk), library, travel unit and finance department (especially Marion and Rébanna) staff members for handling and facilitating innumerable issues, which as a whole made my stay at ITC pleasant. I am deeply grateful to the comfort and care that you provided me. I am greatly indebted to Mr. Bekele Negussie who has been consistently supportive. Your encouragement set the initial momentous step of this research. I salute you Beke! I also have a great regard to the contributions of Dr. Dereje, Zerihun Nuru, Gebre (and Misrak), Muse Belew, Daniel Nebro, Getu Segne, Dr. Dagnachew Leggese, Dr. Gezahegn, Tolossa Shagi (Ethiopian Deputy Minister of Mines), Dr. Lulseged Ayalew, Dr. Araya (Dean of AAU natural science faulty) and Dr. Atalay.

I would like to pay a profound tribute to my friends, colleagues, the large Habesha and entire PhD community for their cordiality that made my stay in Enschede memorable. Sumbal, Shruthi, Van, Dr. Zack, Leo, Beatrice, Abel, Sindu, Rita, Alex, Xuanmei, Samantha, Carolina, Adrie, Sharon, Khamarrul, Byron, Roberta, Mila, Shafique, Juan, Getch, Tagel, Dawit, Armindo, Berhanu, Atkilit, Fasil, Tolga, Dr. Jennifer, Wiebke, Anandita, Frederick, Andre, Mariela, Dr. Sekhar, Dr. Prasun, Dr. Tapas, Dr. Pankaj, Dr. Saibal, Nasrullah, Marshal, Sanaz, Pablo, Tam, Yaseen (and Salma), Paresh, Moonjun, Christiano and Peter deserve a very special thanks. Thank you for the moments that I cherish and do remember mostly with a smile. The support of relatives, friends and colleagues from back home is also gratefully acknowledged.

Finally, my loving thanks to my family for their love, unwavering support, understanding and encouragement. My husband (Fikremariam), kids (Ruth and Sam), mother (Teni), brother (Ge) were particularly the sources of inspiration and strength, which brought me towards the completion of this research. To you, my gratitude is endless.

Table of Contents

List of figures

List of tables

Chapter 1

General Introduction

1.1 Problem definition

Soil is an essential component in civil engineering infrastructure development. It often controls the design and cost of construction projects, predominantly lightweight and shallowly founded structures. Therefore, collecting appropriate soil geotechnical information is a crucial aspect in infrastructure planning and development. Soil geotechnical investigation is typically tailored towards determination of soil types, estimating their geotechnical characteristics and performance (Hunt, 1984; Site Investigation Steering Group, 1993a). Requirement for and frequency of further detailed sampling and testing schemes are commonly based on general site information, and preliminary findings collected at the early stages (Gourley et al., 1993; Paige-Green, 2008). Some soils, such as expansive soils, are known to be problematic and require particular attention.

Expansive soils typically exhibit a large amount of volumetric swelling and shrinkage, in response to changes in moisture content. This property can detrimentally influence construction, performance and life time, especially of lightweight civil engineering infrastructure. Major problems are volume changes due to cyclic swelling and shrinkage upon wetting and drying, which can lead to differential heave, settlement and creep; decrease in bearing capacity and shearing strength of soils when saturated; high-erosion susceptibility and instability when exposed in natural slopes, road cuts or open excavations; and difficult workability conditions (both in saturation and dry states). Damage to civil engineering infrastructure are estimated in billions of dollars (Bell, 1999; Gourley et al., 1993; Jones and Holtz, 1973). The problem is global (Bell, 1999; Chen, 1988), although particularly prone are places with significant climatic variation between dry and wet seasons. According to recent documentation, since the realization of expansive soil problems late in 1930's (Chen, 1988), incidences of expansive soils and various associated geotechnical problems are reported from more than 60 countries (Al-Rawas and Goosen, 2006; Shi et al., 2002). For instance, in the continent of North America expansive soils occur in the United States and Canada (Jones and Holtz, 1973; Ross, 1978; Thomas et al., 2000). Oceania, in Australia and New Zealand (Allbrook, 1985; Delaney et al., 1998). Africa, in Ethiopia, Sudan, South Africa, Kenya, Nigeria etc. (Kariuki and Van der Meer, 2004; Morin and Parry, 1971; Omotosho and Ogboin, 2009; Paige-Green, 2008). Asia, in India, China, Saudi Arabia, Jordan, Oman etc. (Al-Rawas, 1999; Dakshanamurty and Raman, 1973; Gadre and

Chandrasekaran, 1994; Runqiu and Lizhou, 2007; Shi et al., 2002). South America, in Ecuador, Mexico, Argentina, Chile, Cuba etc. (Ramana, 1993; Taboada et al., 2001), and in Europe, in Turkey, Spain, Cyprus, Romania, Poland etc. (Nalbantoglu and Tuncer, 2001; Popescu, 1979; Yilmaz, 2006).

Three fundamental issues need to be addressed to fully appraise geotechnical problems related to soil swelling and shrinkage characteristics:

1) Identifying potentially expansive soils.
2) Quantifying geotechnical characteristics of expansive soils.
3) Delineating the spatial occurrence of expansive soils and variability in their geotechnical characteristics.

Information on the presence and type of expansive soils, magnitude and extent of problems at an early stage of project planning and geotechnical investigation often ensures incorporation of appropriate, cost-effective design and construction countermeasures. Classical qualitative and quantitative characterization requires use of combination of several methods (Thomas et al., 2000). Common procedures are mineralogical and chemical analyses, direct soil swelling potential and swelling pressure measurement, and indirect estimation of volume change from soil physical characteristics such as consistency limits and gradation, as well as use of advanced techniques.

1.1.1 Soil geotechnical classification

Soil swelling and shrinkage potential is difficult to measure directly, for it requires sophisticated sampling and laboratory testing procedures. As a result, it is expensive, time-consuming, tedious, and thus not regularly carried out. Instead, indirect evaluation of such characteristics is often performed via establishing correlations with routinely determined parameters such as consistency limits and gradation.

Soil swelling and shrinkage potential is determined, among other sets of factors, by soil constituents primarily the mineralogical composition and amount of clay fraction (Chen, 1988; Gourley et al., 1993; McCormack and Wilding, 1975; Mitchell, 1993; Pascal et al., 2004; Ross, 1978). Thus, geotechnical parameters that are widely used for assessing soil swelling and shrinkage characteristics show some degree of interdependence. On this basis, correlations can be developed for assessing and rating soil swelling and shrinkage potential (Carter and Bentley, 1991; Thomas et al., 2000). Noteworthy, these correlations are often used to derive soil geotechnical parameters such as percent swell (%S), swelling pressure (SP), potential volume change (PVC), expansion index (EI), Coefficient of linear extensibility (COLE) etc. for basing design of structures (ASTM, 2006; Thomas et al., 2000; Yilmaz, 2006).

However, a wide variation in assignment of soils into different swelling and shrinkage potential categories are reported for similar samples while using different methods (Reddy et al., 2009). That is no universally acceptable single method of evaluating and rating soil expansiveness exists. Differences in climatic conditions, topographic setting, parent materials and other environmental factors that determine the nature and property of soils, probably hinder the success in universal applicability of existing classification systems. As described by Galan (2006), properties of clay minerals are mostly origin dependent and may vary from one geographic region to another. Thus, expansive soils formed in a diverse environment may exhibit different characteristics. Related to the foregoing factors, as well as type and relative abundance of clay minerals, interrelationships among soil geotechnical parameters are rather fuzzy than crisp numerical ranges. Thus, an approach that can appropriately model this aspect is required. More important, there is no existing classification or swelling and shrinkage potential rating system for soils of Ethiopia so far. Classifications, formula and systems developed elsewhere are in use particularly in the road construction sector. A drawback is that these systems and formula are developed for soils of specific geographic regions. This emphasizes the necessity of developing a soil geotechnical classification method for rating swelling and shrinkage potential of expansive soils of Ethiopia.

1.1.2 Remote sensing techniques

Identifying problematic areas, materials, and conditions are fundamental steps in geotechnical investigation of project sites. Although, direct soil sampling and testing provides the best information on soil geotechnical characteristics, it is difficult to sample soils continuously in space, for it requires extensive fieldwork, dense sampling and costly in-situ and laboratory analyses. Thus, discrete sampling spots are commonly selected based on expert knowledge and information acquired from literature. Limitations in this approach are twofold. One, wide sampling interval might miss potentially expansive soils. Two, interpolation between sampling locations might not be accurate. Consequently, critical spots with respect to the presence of expansive soils might be overlooked.

Apart from increasing the number of samples, remote sensing techniques can assist in focusing detailed geotechnical sampling and testing program in areas of greater risk with respect to soil swelling and shrinkage problems. This can be achieved since: (1) soil laboratory spectroscopic analysis can be utilized for evaluating soil samples from any depth. It requires a small amount of material per sample for measurement with little sample preparation. As a result, makes dense sampling easier as compared to the requirement of large volume of material per samples to perform conventional geotechnical tests, in addition to the tedious, and time consuming

procedures. (2) Remote sensing image data has a much better potential to provide with a continuous representation of soil masses with an extensive areal coverage than conventional methods. Thus, it can provide with useful information especially at an early stage of project planning, where site information is mainly limited and based on indirect evidences. Several researchers (Chabrillat et al., 2002; Goetz et al., 2001; Kariuki et al., 2003; Kariuki et al., 2004) reported the potential of spectroscopy in the visible-near infrared (VNIR) and short wave infrared (SWIR) wavelength regions for identifying expansive soils and assessing selected geotechnical parameters. Bourguignon et al. (2007) demonstrated the capability of multispectral remote sensing for detecting and mapping expansive clays.

However, only a knowledge driven approach and one-to-one relations were utilized based on specific wavelengths. Quantifying and mapping soil geotechnical parameters directly from multispectral images is not reported. The potential of spectroscopy in the mid-infrared (MIR) wavelength region (longer than 2.5 µm) is not explored for characterizing active clay minerals and expansive soils. In the MIR wavelength region, spectra of minerals exhibit strong, fundamental, molecular vibrational absorption features (Hunt and Salisbury, 1970; Salisbury and D'Aria, 1992b; Salisbury and D'Aria, 1994). Therefore, for a comprehensive understanding of spectral characteristics of active clay minerals and expansive soils, the MIR wavelength region should be investigated, including interrelationships among spectral and geotechnical characteristics of expansive soils.

1.2 Research objectives

The general purpose of this research is to contribute to a better and more comprehensive understanding of the geotechnical and spectral characteristics of expansive soils, with emphasis on interrelationships among these characteristics. Thereby, the aim is to develop quick means of identifying and characterizing (including estimating geotechnical parameters and rating swelling and shrinkage potential) expansive soil, which can add to the improvement in effectiveness of geotechnical investigations of such soils for practical applications. The specific objectives are:

1) To investigate relationships among geotechnical parameters of expansive soils; and establish an empirical prediction model for estimating and rating swelling and shrinkage potential of soils from routinely determined parameters.

2) To investigate the engineering benefits of the VNIR and SWIR laboratory spectroscopic and multispectral remote sensing techniques for identifying expansive soils and quantifying soil geotechnical characteristics; thereby

producing maps showing the spatial distribution of expansive soils and variability in their geotechnical characteristics.

3) To determine spectral characteristics of (pure) active clay minerals (those that are influential in dictating soil swelling and shrinkage characteristics) and mixtures, in the mid infrared (MIR) wavelength region.

4) To establish the potential of spectroscopy in the mid infrared (MIR) wavelength region for characterizing (i.e., identification, classification and estimation of geotechnical parameters) expansive soils.

1.3 Thesis structure

This thesis has eight chapters, each contributing towards the advance in understanding of the geotechnical and spectral characteristics of expansive soils.

Chapter one (this chapter) is a general introduction that outlines the problems and objectives that this research aimed to address.

The second chapter provides descriptions of expansive soils. Main geotechnical problems associated with the presence of expansive soils are presented with supporting illustrative pictures. The principal causative factors of soil swelling and shrinkage characteristics are described. The various stages and aspects of soil geotechnical investigation are discussed. Two study sites used in this thesis are also introduced in this chapter.

The third chapter analyzes relationships among soil geotechnical parameters. An empirical soil swelling and shrinkage potential assessment and classification technique is established. Relatively easy as well as routinely determined geotechnical parameters are used. Additionally, the fuzzy nature of the interrelationships among geotechnical parameters is addressed.

Chapter four presents laboratory spectroscopic analyses of expansive soils in the VNIR and SWIR wavelength region. It deals with spectral characteristics of expansive soils and their relationships with geotechnical parameters.

In chapter five, spectral characteristics of three key clay minerals influential in soil swelling and shrinkage characteristics, are established in the MIR wavelength region. This chapter presents a laboratory experimental investigation on pure naturally occurring active clay minerals such as montmorilllonite, illite, kaolinite, and their proportioned mixtures.

Chapter six is an extension of chapter five. It deals with expansive soils, and identification of clay mineralogical composition of these soils, based on

spectral signatures of active clay minerals established in chapter six. In addition, relationships between spectral characteristics and geotechnical parameters of soils are statistically analyzed.

In chapter seven, multispectral remote sensing image data is investigated to map soil geotechnical parameters. Maps showing a more direct representation of soil swelling and shrinkage potential rather than discrete sampling points are presented. Issues of repeatability of the approach and factors influencing the outputs are also discussed.

Finally, the eighth chapter is a synthesis of the findings of this research. Main conclusions drawn from the study are summarized including outlooks for future research.

Chapter 2

Expansive soils: Problems and the study sites

2.1 Introduction

Geo-hazards such as problem soils present a substantial danger to human life, property, infrastructure and environment. Bell (1999) defined problem soils as natural geo-hazards that are due to detrimental geotechnical properties of soils. Expansive soils fall into these problem soil geo-hazard category. Swelling and shrinkage phenomena in expansive soils can pose severe limitations to lightweight engineering infrastructure. According to Jones and Holtz (1973) and Bell (1999), global damage to infrastructure and associated remediation costs are often of far reaching economic consequences. In particular, with increasing number of the global population and related rapid urbanization and demand of new land for expansion of infrastructure, these soils have become significant problems.

Expansive soils, predominantly black cotton and other clayey soils occur in various parts of Ethiopia. In the central, western, north-western, south-western and some parts of southern and eastern Ethiopia they often occur covering an extensive area. Such soils commonly occur in flat and gently sloping landscapes such as on the highland plateau, low land flood plains and valley floors (Ahmad, 1996; ERA, 2002; Morin and Parry, 1971). These soils are notorious for exhibiting harmful geotechnical characteristics and causing costly hazards particularly in the construction sector (ERA, 2002; Morin and Parry, 1971; Netterberg, 2001). Figure 2-1 shows a typical expansive soil (black cotton soil) with characteristic polygonal desiccation cracks and popcorn texture in dry periods. In wet seasons, these soils become highly plastic, thick, slick, and heavy (Figure 2-2).

Foundations on expansive soils are prone to differential movements, such as uneven heave and settlement. Subgrade conditions for roads on expansive soils are poor, which often impair serviceability of structures resulting in serious consequences to the construction economy (ERA, 2002; LEA, 2006; Morin and Parry, 1971; Netterberg, 2001). This is due to considerable differential volume change and related deformations, decrease in bearing capacity and low-shearing strength that these soils develop when wetted. Thus, the presence of expansive soils in construction sites such as road alignments is problematic, unless proper care is taken during the planning, location, design and construction of such infrastructure. In Ethiopia, broad range of difficulties were experienced in the road construction sector (ERA, 2002), which are challenging reminders of the requirement of careful consideration of expansive soils. Especially, at the early stages of project

planning such as preliminary site investigation, feasibility, and design phases of road projects the presence and characteristics of expansive soils need to be adequately comprehended. Several manifestations of damage on roads are presented in Figures 2-2, 2-3A, 2-3B and 2-3C.

Figure 2-1: Expansive soil (black cotton soil) with typical desiccation cracks and granular appearance during dry periods (a picture taken along the Addis Ababa - Nazret road, near Dukem town). Cracks are often wide (on the order of tens of cm) and deep (on the order of m).

Earth roads on expansive soils can be entirely impassable (Figure 2-2). In such earth roads, slipperiness is another associated difficulty whenever there is rain wetting the riding surface. During dry periods, due to excessive fine particles, dustiness is another problem. The dustiness has an adverse impact on safety in relation to visibility, also health of road users and inhabitants of the road side environment. In developing countries, earth roads (such as rural low-volume roads) constituent a significant portion of the transport system. In Ethiopia, these types of roads serve as the main access roads connecting the rural community. They are particularly essential for the rural community development, flow of commodities, provision of services and facilities, resource management etc.

Figure 2-2: An entirely impassable section of an earth road (northwestern Ethiopia), due to soil expansiveness during rain periods leading to costly maintenance requirements.

Higher standard gravel wearing-course roads, which also make-up a large portion of the road network in developing countries, can also be severely affected. The effect can range to the extent of complete inaccessibility impeding all-weather functionality of these roads as well.

As far as paved roads are concerned, differential movements and related cyclic changes in strength and stiffness of expansive soils can induce distortions and formation of cracks onto pavement structures (Figures 2-3A and 2-3B).

In general, structural damage to roads located in areas where subgrade material is expansive, often require extensive maintenance work (Chen, 1988; Nelson and Miller, 1992) that often exceed the initial road construction costs (Omotosho and Ogboin, 2009).


(A)


(B)

Figure 2-3: Typical damage due to soil swelling and shrinking characteristics showing distress on lightweight and shallowly founded infrastructure. (A) Road surface deformation and formation of potholes, corrugation and ruts. (B) Formation of longitudinal cracks due to the presence of expansive soils beneath the road embankment. (C) Road side ditch clogging due to slumping of expansive soil from bare back slope. (D) Cracks in the wall of a residential building, due to hogging and sagging following cyclic swelling and shrinkage of expansive soils beneath the foundation.

Cut slopes on expansive soils are susceptible to instabilities and slope movements. Massive landslide problems, in various parts of the country, among other triggering factors, are also related to occurrences of expanding clay horizons within sedimentary sequences and deeply weathered basalt (Abebe et al., 2010; Ayalew, 1999; Van Den Eeckhaut et al., 2009). At places where these soils are overlain by stiff material, the stiffness contrast can lead to larger problems. The problems are aggravated by an action of water in exposed slopes due to increasing pore water pressure. Clogging of road-side ditches and culverts are common difficulties that often require high clearing and maintenance cost allocation. Figure 2-3C shows slope and road-side ditch clogging problems. From an environmental perspective, erosion vulnerability is an utmost concern. Scouring of drainage structures and gully formation related to concentrated runoff from road drainage structures are critical problems, which very often require costly mitigation measures.

Distress is typical to small scale (low-rise) buildings. Cracks, ranging from hairline (of the order of a few mm) to extensive (of the order of tens of cm) and tilting are evident (Figure 2-3D). The cracks can be vertical, horizontal and diagonal. The Bole Senior Secondary School in Addis Ababa city is a notable example that has been seriously damaged by soil swelling and shrinkage prior to serving its intended design life.

2.2 Geotechnical investigation

Geotechnical investigation is a crucial aspect in any civil engineering infrastructure development. It is performed to evaluate critically, among other factors, soil conditions that can affect the cost-effectiveness, design, safe implementation and performance of proposed infrastructure (Site Investigation Steering Group, 1993a, b). Thus, it is a prerequisite for formulating optimal design parameters and necessary counteracting measures to ensure the aforementioned.

As descried by Hunt (1984), subsequent to a project planning, geotechnical investigation involves and is an integral part of the following phases:

- Preliminary investigation phase, where direct and ancillary information about project sites will be collected. This encompasses desk study, such as reviewing available documentations and literature.
- Reconnaissance survey phase of project sites, where any engineering and environmental difficulties that are likely to be encountered will be determined.
- Feasibility study stage where the engineering, environmental and economic aspects of proposed projects will be assessed. At this stage, the benefits, as well as impacts of project implementation, will also be identified.

- Detailed investigation and testing scheme, where thorough investigation of project sites will be carried out including sampling, various in-situ and laboratory analyses.
- Design phase.
- Project implementation (construction) phase.

The first two phases are required to provide appropriate information to allow for sufficient appraisal of sites in terms of suitability and cost estimates during the feasibility study. The detailed investigation and testing scheme commonly focus on but not restricted to problematic areas identified in the preceding phases. This phase is mostly site-specific and largely depends on the scale, complexity, and budget allocated for the project. The project design is generally based on findings and resulting design parameters from the detailed investigation and testing scheme. Monitoring quality compliance and construction management are the main scopes of geotechnical studies during project implementation phase. Although, changes and design amendments can be made during the construction phase, due to encountering expansive soils, addressing such problems at that stage often incur high costs (Chen, 1988; Omotosho and Ogboin, 2009).

2.3 Active clay minerals

Swelling and shrinkage potential of expansive soils depend on several factors, such as type and amount of soil constituent clay minerals; initial moisture content, and the soil water chemistry contained within voids; initial density or voids ratio; grain size, structure and soil fabric; the state of stress, which is the applied stress level and stress history (Al-Rawas, 1999; Bell, 2000; Chen, 1988; Mitchell, 1993; Nelson and Miller, 1992; Ramana, 1993; Seed et al., 1962; Skempton, 1984; Thomas et al., 2000). The presence of active clay minerals is the principal cause of intrinsic soil swelling and shrinkage characteristics. The magnitude of swelling and shrinkage vary considerably with clay mineralogical compositions and clay fractions within soils (Pandian and Nagaraj, 1990; Pascal et al., 2004; Ramana, 1993; Seco et al., 2011; Skempton, 1984).

Active clay minerals are prominently sensitive to moisture content fluctuation (Mitchell, 1993; Pandian and Nagaraj, 1990; Seed et al., 1962). The overall geotechnical characteristics such as volume, strength and stability of soils containing these minerals show extreme variation upon wetting and drying (Al-Rawas and Qamaruddin, 1998; Morin and Parry, 1971; Omotosho and Ogboin, 2009). Three clay mineral species, smectite (montmorillonite, nontronite), illite, and kaolinite (in decreasing order of activity) (Skempton, 1984) are established to be fundamental indicators of soil swelling and shrinkage potential (Seed et al., 1962; Thomas et al., 2000; Yong and Warkentin, 1975). These three clay mineral species are structurally and

compositionally different and exhibit distinctive physicochemical characteristics (Brigatti et al., 2006; Yong and Warkentin, 1975).

Primary structural unit of montmorillonite is a layer composed of two silica tetrahedral sheets with a central alumina octahedral sheet. Such a structure is referred to as a 2:1 structure. Although the layers are continuous, bonds between layers provided by van der Waals forces and interlayer cations (Brigatti et al., 2006; Farmer, 1974) are exceptionally weak, permitting water molecules to occupy the space between layers (Gillot, 1987). Montmorillonite often occurs in a remarkably small platy film like forms. This clay mineral has a large specific surface area (Al-Rawas, 1999; Ross, 1978), which adds to its high affinity to water molecules (Gillot, 1987). Thus, it is susceptible to considerable swelling upon wetting (McCormack and Wilding, 1975; Ross, 1978). On the other hand, loss of moisture (drying) causes proportionately substantial volumetric shrinkage (Bowles, 1984; Karathanasis and Hajek, 1985). The other smectite group clay mineral, nontronite, is compositionally iron-rich and has a similar structural arrangement and characteristics as montmorillonite.

Illite has a structure where single sheets of alumina octahedrons are sandwiched between single sheets of silica tetrahedrons (Brigatti et al., 2006; Hower and Mowat, 1966; Yong and Warkentin, 1975), which is similar to the smectite clay mineral varieties. Bonding provided by Potassium ions is weak, allowing water molecules to be absorbed between layers. Illites expand more than those of kaolinite clay mineral types; but much less than smectite clay mineral varieties (Gillot, 1987). Illite commonly occurs in flaky forms. It has much smaller specific surface area and affinity to water molecules than montmorillonite (Chen, 1988; Gillot, 1987; Nelson and Miller, 1992; Skempton, 1984). Illite often occurs as a mixed smectite-illite (interstratified) variety (Brigatti et al., 2006; Hower and Mowat, 1966), exhibiting properties between the two clay minerals including moderate swelling and shrinkage potential (Yong and Warkentin, 1975).

Kaolinite has a basic structural unit consisting of single sheets of silica tetrahedrons bonded with single sheets of alumina octahedrons stacking together (Yong and Warkentin, 1975). This structure is referred to as a 1:1 structure. Bonding provided by hydrogen molecule is strong, which minimizes interlayer space for absorption of water molecules. Two varieties, kaolinite and halloysite, are of importance with respect to soil swelling and shrinkage potential (Bell, 2000). The kaolinite variety often occurs as plates. The halloysite variety, which has a single layer of water, weakly adsorbed between its sheets (mainly held on surface particles) usually occur in tabular forms. Kaolinite clay minerals are characterized by a smaller specific surface area than montmorillonitic and illitic clay mineral varieties. As a result,

kaolinites exhibit little water affinity (Al-Rawas, 1999; Yong and Warkentin, 1975) and are characterized by minimal expansion rates (Chen, 1988; Ramana, 1993; Thomas et al., 2000). Occurrences of the mixed layer (interstratified) smectite-kaolinite and illite-kaolinite clay minerals are common in soils (Fitzpatrick, 1980; Yerima et al., 1985; Yong and Warkentin, 1975). Soils containing these interstratified clay minerals show a higher expansion and shrinkage potential than the pure kaolinite species (Yerima et al., 1985).

All three clay mineral varieties exhibit additional, unique physicochemical properties, which facilitate their discrimination. Montmorillonite ($(Ca, Na)_{0.33}$ $(Al, Mg)_2$ (Si_4, O_{10}) $(OH)_2 \cdot nH_2O$) has an open structure that allows an abundant cationic substitution (Brigatti et al., 2006; Yong and Warkentin, 1975) and results in a net negative layer charge. Additionally, this clay mineral is characterized by the presence of strongly adsorbed water molecules in its internal structure, which are trapped between the silicate sheets (Gillot, 1987; Yong and Warkentin, 1975). The structure in illite ($(K, H_3O)(Al, Mg, Fe)_2$ $(Al, Si)_4$ $O_{10}[(OH)_2(H_2O)]$) is similar to that of montmorillonite; although with stronger bonds among the silicate sheets and interlayer non-exchangeable cations that compensate for layer charge deficiencies. Isomorphous substitutions, such as, Al for Si in the tetrahedral sheets, and Mg or Fe for Al in the octahedral sheets are sources of layer charge deficiencies (Farmer, 1974; Yong and Warkentin, 1975). Illite is also a water bearing clay mineral. Kaolinite ($Al_2Si_2O_5$ $(OH)_4$), on the other hand, has a structure that characteristically provides minor cationic substitution (Ma and Eggleton, 1999; Yong and Warkentin, 1975). Thus, the layer is neutral. This clay mineral typically contains none (kaolinite) to little (halloysite, $Al_2Si_2O_5(OH)_4 \cdot 4H_2O$) adsorbed water molecules in its structure (Gillot, 1987; Yong and Warkentin, 1975).

Differences in soil geotechnical characteristics show dependency on clay mineralogical compositions among different clay mineral varieties such as montmorillonite, illite, and kaolinite (Gourley et al., 1993; Pascal et al., 2004; Ross, 1978; Thomas et al., 2000; Yitagesu et al., 2009a; Yong and Warkentin, 1975). In soils that are dominated by similar clay mineralogical compositions, the clay fraction appear to control soil behavior (McCormack and Wilding, 1975; Ross, 1978; Schafer and Singer, 1976; Seed et al., 1962; Skempton, 1984; Vaught et al., 2006). The fact that clay mineralogical composition is a crucial factor governing a number of soil geotechnical properties (swelling and shrinkage potential, permeability, and strength parameters etc.) determine the importance of soil clay mineralogical assemblage analysis.

Clay minerals, among other soil constituent minerals, also determine the variation in soil spectral characteristics. Spectral signatures of soils are reflections of constituents of soils and differ as per the compositions of soils. Active clay minerals, which are responsible for soil swelling and shrinkage characteristics, show distinct spectral signatures (Clark, 1999; Farmer, 1974; Hunt, 1977; Van der Meer, 1999). Therefore, it is possible to distinguish expansive soils (qualitatively) by analyzing their reflectance spectra. It is also possible to quantify geotechnical parameters, as the presence and abundance of clay minerals determines soil spectral characteristics (Chabrillat et al., 2002; Goetz et al., 2001; Kariuki et al., 2003). Based on this paradigm, a great deal of effort from the remote sensing society has gone into investigating methods that can be supporting or alternate tools of identifying expansive soils and estimating their geotechnical characteristics. Several researchers have demonstrated that remote sensing techniques can provide with inexpensive, rapid and nondestructive way of analyzing soil mineral compositions. For example, carbonates and oxides (SiO_2, Fe_2O_3,K_2O, Al_2O_3 etc.) in soils (Bendor and Banin, 1990, 1995); exchangeable Mg, Ca, clay content, and organic carbon etc. (Shepherd and Walsh, 2002; Stenberg et al., 2010). Thus, remote sensing methods can be potentially applicable for routine soil geotechnical analyses in order to compliment traditional techniques.

2.4 The study Sites

The study summarized in this dissertation was carried out in two study sites. One of the study sites is located in the city of Addis Ababa. The other is along the newly proposed Addis Ababa-Nazret expressway alignment.

2.4.1 The Addis Ababa study site

This study site is located in the eastern part of the city of Addis Ababa (Figure 2-4). Within this study area, three localities (Kotebe, Bole and CMC) were selected based on the combination of information on the topography, geology, soil types, previous studies and reports on damages to lightweight infrastructure, and site observations.

Addis Ababa is witnessing a large population growth in the past decades and rapid expansion in all directions, engulfing much farmsteads and woodland into urbanized areas. Much construction activities are taking place in the study area (particularly CMC and Bole localities), and problems due to expansive soils are frequently reported.

Topography ranges from rugged, hilly and mountainous at the northeastern (Kotebe) parts to flat towards the south and southwestern parts (Bole and CMC) of the study site. Elevation ranges from 2700 m (northeastern parts) to 2300 m (southern parts) above mean sea level. Climate is cool to temperate

with a mean annual temperature of 16 °C, and an annual rainfall of 1200-1600 mm. According to the geological survey of Ethiopia GSE (1990), the geology of the city is dominated by alkaline basalt with inter-bedded pyroclastic, ignimbrite, trachyte and rhyolite formations (Tertiary volcanics of Trap series).

A generalized soil map of the city indicates three main soil types; luvisols, vertisols and nitosols occurring in the study site (Figure 2-4). Reddish color soils dominate in the northeastern (Kotebe) area. While, in the Bole and CMC areas, dark colored commonly known as black cotton soils (ERA, 2002) and grey colored soils are dominant. The black cotton soils belong to the vertisols family. Apart from Ethiopia, the occurrence of black cotton soils is reported from different parts of the world, e.g., USA, Australia, India, China, Sudan, South Africa, Niger, Chad, Nigeria, Tanzania (Babu et al., 2005; Chen, 1988; Gadre and Chandrasekaran, 1994; Morin, 1971) etc. In between the Kotebe and CMC areas, reddish brown to dark brown soils dominate. According to GSE (1990), soils of the CMC and Bole areas are of lacustrine origin. GSE (1990) described that, during the Pleistocene, these flat low-lying parts of the city were covered with a water body that was supplied by sediments brought by rivers coming from higher altitudes.

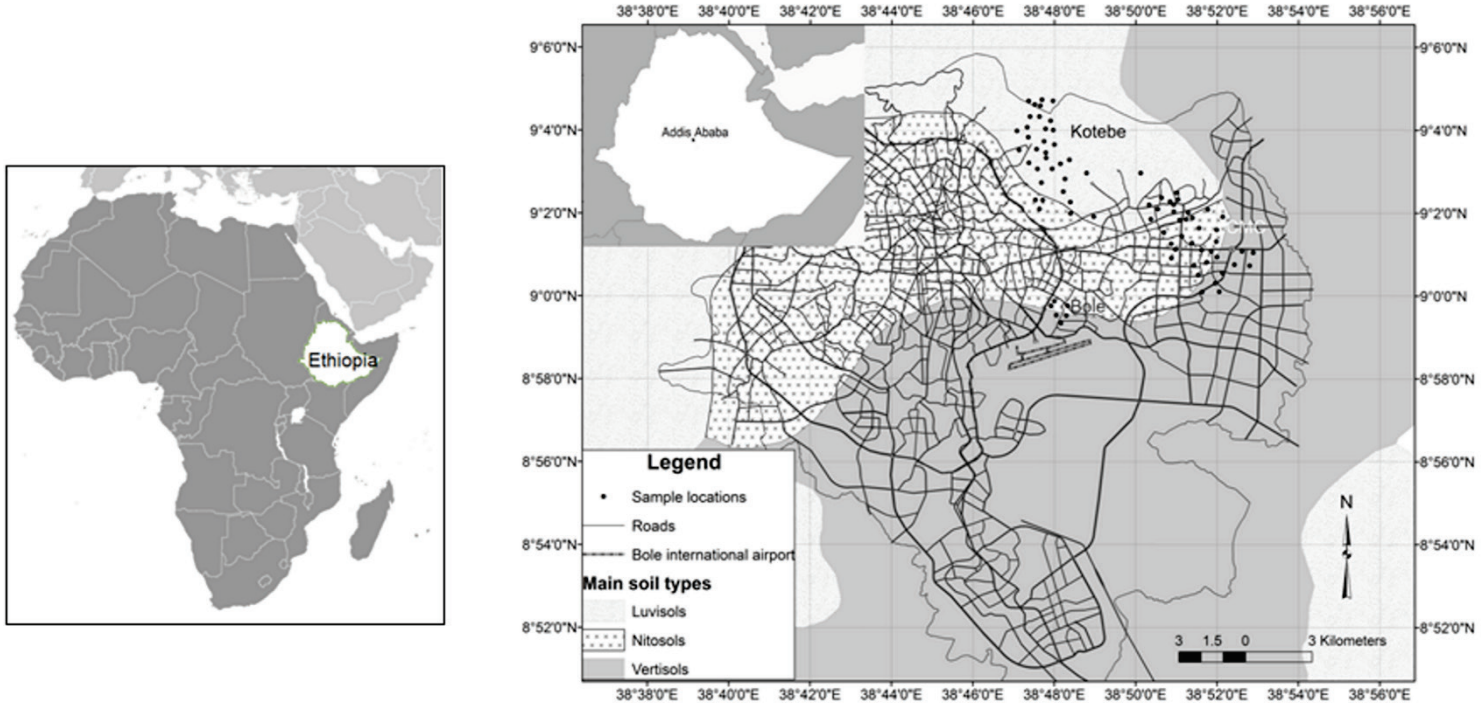

Figure 2-4 Location map of the Addis Ababa study site with names of places and location of sampling points overlaid on a soil map of the city that shows the spatial distribution of main soil types.

2.4.2 The Addis Ababa-Nazret study site

This study site is also located in the central part of Ethiopia (Figure 2-5). Topography ranges from a relatively flat to hilly, undulating and steep mountainous terrain. Elevation ranges from 1500 m to 2500 m above mean sea level. Conical-shaped isolated hills of scoria formed during the late stages of volcanism are common in this study site. Climate is moderate to wet with mean annual rainfall of 1200 mm in Addis Ababa and areas close by, which gradually decreases to 870 mm around the town of Nazret. Temperature ranges from 8 °C to 25 °C with maximum temperature in the vicinity of Nazret town. While topography controls the ease with which the soils are drained, heavy rain periods followed by prolonged dry periods leading to substantial moisture changes in the soils contribute towards the susceptibility of soils to pronounced volume changes.

The geology (Abebe et al., 1999) around TuluDimtu (names of main towns along the existing highway connecting Addis Ababa with the town of Nazret are indicated in Figure 2-5) consists of Tertiary to Quaternary volcanic formations. These formations include alkaline basalt, spatter and cinder cones, ignimbrite, rhyolitic flows and domes, and trachyte. Near DebreZeyt, alluvial and lacustrine deposits dominate which include sand, silt and clay. From DebreZeyt to Modjo town, there are lacustrine deposits. Past Modjo town, fall and poorly welded pyroclastic deposits dominate with rhyolitic and trachytic formation intercalations. The geology of the study area indicates the availability of a wide range of parent materials, from alkaline to intermediate and siliceous varieties from which the soils could be derived.

Soils in the study area can be classified into vertisols, luvisols, leptosols, phaeozems, andosols, cambisols, fluvisols and nitosols (Figure 2-5). According to the FAO (1998) definition, vertisols are smectite-rich highly expanding soils that swell and shrink with changes in moisture content. Luvisols are common soil types in flat or gently sloping land, and often derived from a variety of unconsolidated parent material including alluvial, colluvial and eolian deposits. Luvisols usually exhibit a high cation exchange capacity (CEC) and water retention potential that is associated with the accumulation of active clay minerals (Gray and Murphy, 2002). Leptosols are particularly shallow soils over hard rock or unconsolidated gravely material, and are common in mountainous areas. Phaeozems are soils that are predominantly derived from basic parent material, and are rich in organic matter. Andosols are young soils in volcanic regions and are usually associated with pyroclastic parent materials (FAO, 1998). Andosols show a low CEC and water retention capacity (Gray and Murphy, 2002) unless allophane or immogolite is present (Gray and Allbrook, 2002; Parfitt and Hemni, 1980; Wan et al., 2002). Andosols containing allophane and immogolite, on the other hand, exhibit high water retention capacity, CEC

and activity, low cohesion, shear strength and bulk density (Gray and Allbrook, 2002; Wan et al., 2002; Zehetner et al., 2003). Cambisols are moderately developed soils derived from a wide range of parent material, and are common in areas where there is active erosion. Fluvisols are young soils common in alluvial deposits; they also occur in lacustrine deposits. Nitosols are deeply weathered soils. These soils are mostly gravelly, and they are characterized by low CEC. The hilly and mountainous terrains of the study area are mainly covered with fresh to partially weathered basalt. From an engineering perspective, soils that are mostly black and contain highly expansive clay minerals (black cotton soils) are found between Addis Ababa and Modjo town, and covered an extensive area. According to Abebe et al. (1999), the black cotton soils are of alluvial, lacustrine and colluvial origin.

2.5 Conclusions

Expansive soils are serious obstacles to infrastructure development, particularly lightly loaded and shallowly founded structures. Thus, in comprehensive land-use planning activities, it is imperative to put emphasis on the presence and geotechnical characteristics of these soils.

Expansive soils occur in Ethiopia and cause a wide range of geotechnical problems. Geology, climate and topographic variability of the two study sites are convenient for the formation of soils that are rich in active clay minerals such as smectities (e.g., vertisols). In addition, the strongly seasonal climatic variation between wet and dry periods is an exacerbating factor for the susceptibility these soils to substantial swelling and shrinkage characteristics.

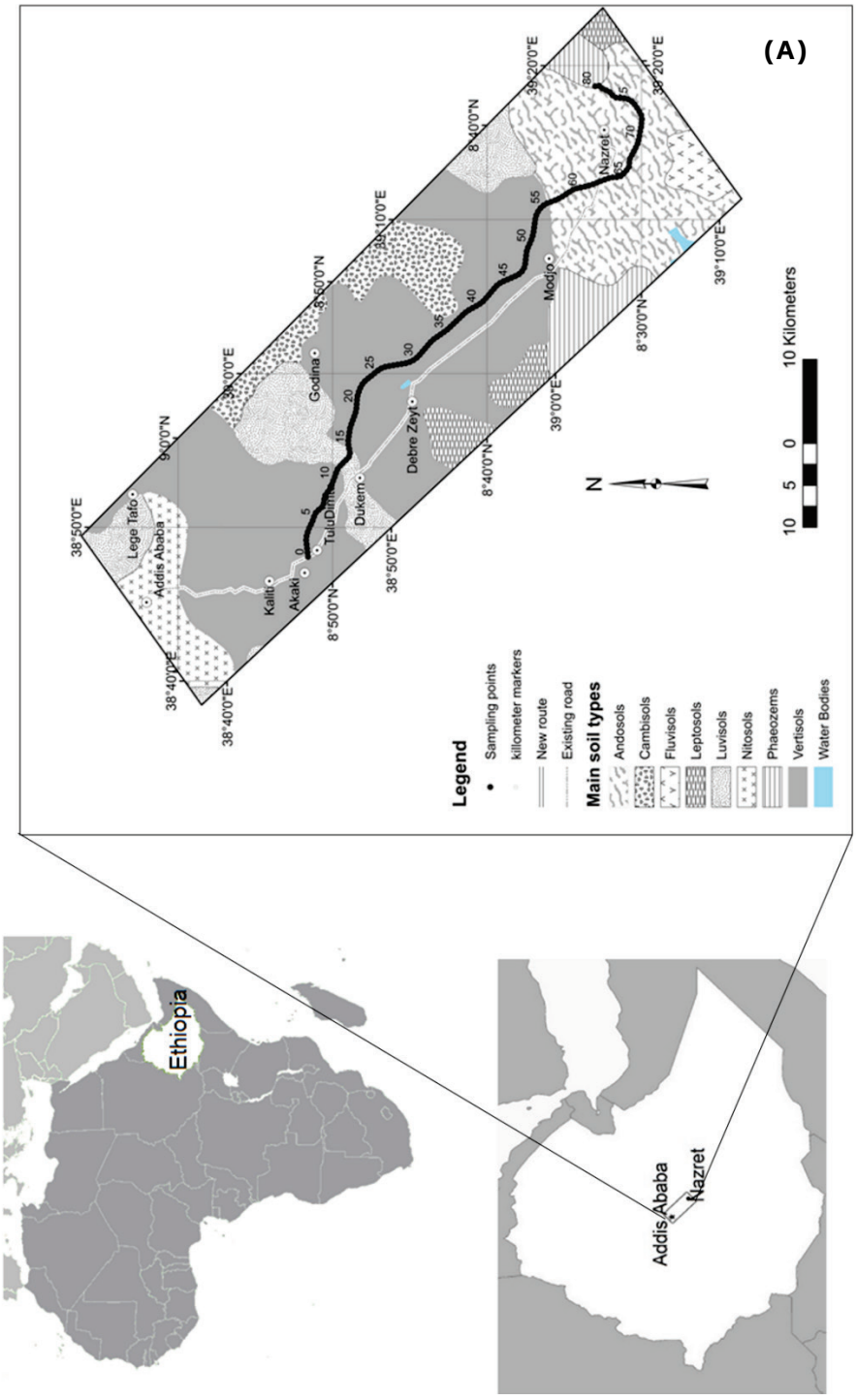
(A)
Legend
Sampling points
kilometer markers
New route
Existing road
Main soil types
Andosols
Cambisols
Fluvisols
Leptosols
Luvisols
Nitosols
Phaeozems
Vertisols
Water Bodies
N
10 Kilometers
Lege Tafo
Addis Ababa
Kaliti
Akaki
TuluDimtu
Dukem
Debre Zeyt
Godina
Modjo
Nazret
38°50'0"E
38°40'0"E
38°40'0"N
8°50'0"N
8°40'0"N
8°30'0"N
39°0'0"E
39°10'0"E
39°20'0"E
Ethiopia
Addis Ababa
Nazret

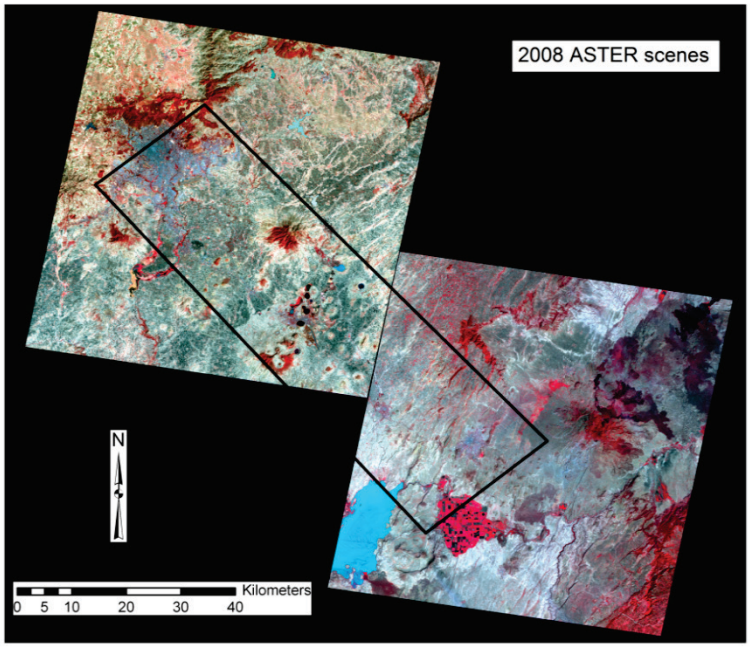

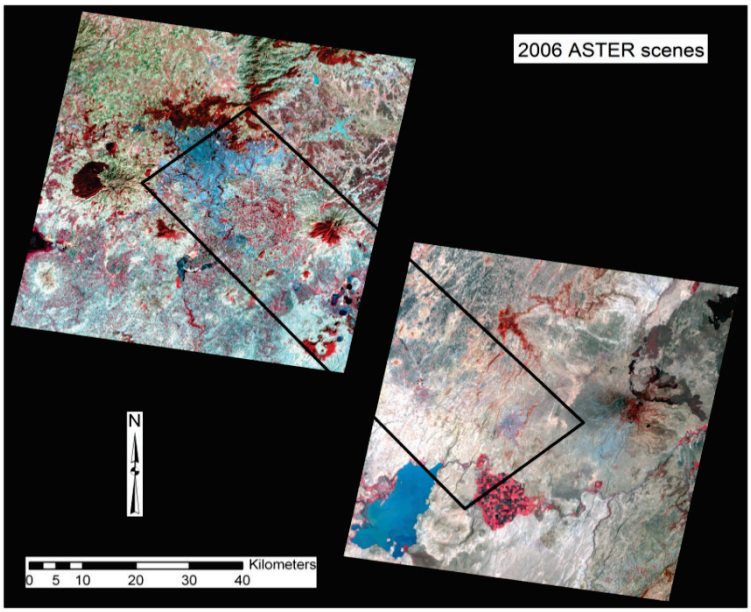

(B)

Figure 2-5 Location map of the Addis Ababa-Nazret study site with kilometer markers on the newly proposed expressway alignment showing its length in five kilometer intervals (A). Names of main towns are indicated along the existing highway. Spatial distributions of sampling points along the proposed expressway alignment are also overlaid on a soil map of the area that shows the main soil types. ASTER images (false color composite bands 3, 2, 1) acquired in the year 2008 and 2006 are shown with outline of the study site superimposed (B).

Chapter 3*

Empirical relationships among geotechnical parameters: soil geotechnical classification

Abstract: Correlations are essential to obtain information on soil geotechnical parameters, which are costly and time consuming to measure directly, such as expansion potential. A common procedure for evaluating and rating soil expansion potential is the expansion index (EI) test. The purpose in this chapter was to establish a multivariate regression model for estimating soil expansion index, thereby classify and rate soil expansiveness. Soil samples were collected from the newly planned expressway connecting the city of Addis Ababa with the town of Nazret in Ethiopia. A regression equation was established from liquid limit, plasticity index and soil fine fraction (percentage of material passing the ASTM 0.075 mm sieve aperture), using a partial least squares multivariate calibration method. A coefficient of determination (R^2) of 0.92 accompanied with a root mean square error of prediction of 9.87, standard error of performance of 9.91, offset of 5.31 and bias of 0.04 was obtained. Response surface models showing three-way relationships among the predictors (Atterberg limits and fine fraction) and response variable (EI) may serve as classification systems for evaluating soil expansion potential. Apart from its basic scientific value as a simple method for estimating and rating soil expansiveness, the approach has the advantage of employing easily and routinely determined soil properties, to get information on soil expansion potential at minimal cost and time requirements.

Keywords: Expansive soil, expansion index, Atterberg limits, fine fraction, response surface, PLS.

* This chapter is based on:

Yitagesu, Fekerte Arega, Van der Meer, F.D, Van der Werff, H., and Seged, H., 2011, Evaluation of Soil Expansion Index from routinely determined geotechnical parameters: Soil Science Society of America v. 75 (5), p. 1640-1651.

3.1 Introduction

Geotechnical characteristics of expansive soils, with respect to bearing potential, stress and deformation are highly sensitive to variation in moisture regime. Such soils exhibit substantial volume change upon alteration of their moisture content. The change in volume is often associated with loss of shear strength and deformation. These phenomena can pose a significant hazard to infrastructures, in particular lightweight structures, founded on such soils. The damage because of expansive soils worldwide was greater than damage caused by all other natural hazards (Jones and Holtz, 1973; Chen, 1988; Nelson and Miller, 1992). Hence, expansive soils are considered hidden hazards.

Identification and quantitative characterization of expansive soils are of critical importance in geotechnical investigations. The purpose is to ensure proper site selection, environmental compatibility and economic feasibility in designing, construction as well as subsequent performance of infrastructure. Expansive soils can be characterized and classified based on their expansion and shrinkage potential, measured by standard methods such as oedometer and triaxial swelling tests (%S, SP), suction, potential volume change (PVC), expansion index (EI), and coefficient of linear extensibility (COLE). Since several factors should be considered while measuring soil expansion and shrinkage potential, these methods require sophisticated sampling and laboratory procedures. As a result, they are costly and time consuming. Hence, identification and characterization of expansive soils often involve the use of correlations and established classification techniques. The bases of these correlations are the dependence of soil expansion and shrinkage potential on soil compositions, mainly clay mineral compositions and content. Soil expansion and shrinkage characteristics are unique to soils containing active crystalline clay minerals, such as smectite, interstratified smectite-illite, illite, and interstratified smectite-kaolinite (Chen, 1988; Karathanasis and Hajek, 1985; Mitchell, 1993; Nelson and Miller, 1992; Thomas et al., 2000; Yerima et al., 1985). Active non-crystalline clay particles such as allophane and imogolite are also responsible for soil swell-shrink susceptibility (Allbrook, 1985; Gray and Allbrook, 2002; Wan et al., 2002; Zehetner et al., 2003). Several indirect relationships and classifications were proposed, mainly based on oedometer, triaxial, suction, potential volume change (PVC), and coefficient of linear extensibility (COLE) methods (Dakshanamurty and Raman, 1973; Erguler and Ulusay, 2003; Erzin and Erol, 2007; Gray and Allbrook, 2002; Kariuki and Van der Meer, 2004; McCormack and Wilding, 1975; Seed et al., 1962; Skempton, 1984; Thomas et al., 2000; Yilmaz, 2006).

Anderson and Lade (1981) proposed the expansion index (EI) test for identifying potentially expansive soils and quantifying the magnitude of

volume changes in these soils. Zapata et al. (2006) presented one to one correlations among soil expansion index and plasticity index, fine fraction (percentage of material passing the ASTM 0.075 mm sieve aperture), and weighted plasticity index (a product of plasticity index and fine fraction). However, the use of a single index property for estimating and rating potential expansion in soils suffered from overlapping ranges for different magnitudes of expansiveness. Moreover, established thresholds of each index property for a likely extent of volume change differed from one researcher to another adding to the uncertainty as to which class of expansiveness to assign a given soil (Carter and Bentley, 1991; Kariuki and Van der Meer, 2004; Reddy et al., 2009; Thomas et al., 2000). Use of multiple geotechnical parameters might improve prediction ability of models, and better model the non-crisp nature of relationship among routinely determined geotechnical parameters and soil expansion index.

The objectives in this chapter were: (1) to determine geotechnical characteristics of soils and quantify their expansion potential in terms of expansion index; (2) to establish a relationship among soil expansion index and routinely determined geotechnical parameters, such as Atterberg (consistency) limits (liquid limit, plasticity index) and soil fine fraction for indirect estimation of expansion potential; and (3) to develop a classification technique for rating soil expansion index, based on these three routinely determined soil geotechnical parameters.

A relationship was established, among expansion index and three routinely determined soil geotechnical parameters. A multivariate calibration method, partial least squares (PLS) regression (Martens and Naes, 1989; Wold et al., 2001), was used to link explanatory variables to the response variable. Response surface models were also used, to illustrate the three-way relationships, among Atterberg limits and soil fine fractions with expansion index.

3.2 Materials and Methods

3.2.1 Soil sampling

A large part of the newly planned Addis Ababa-Nazret expressway route traverses through vertisols (Figure 3-1). Therefore, it was essential to evaluate the expansion and shrinkage potential of the soils to eliminate or minimize detrimental influences of soil volume change on the highway subgrade and the associated adverse impacts on the adjoining environment.

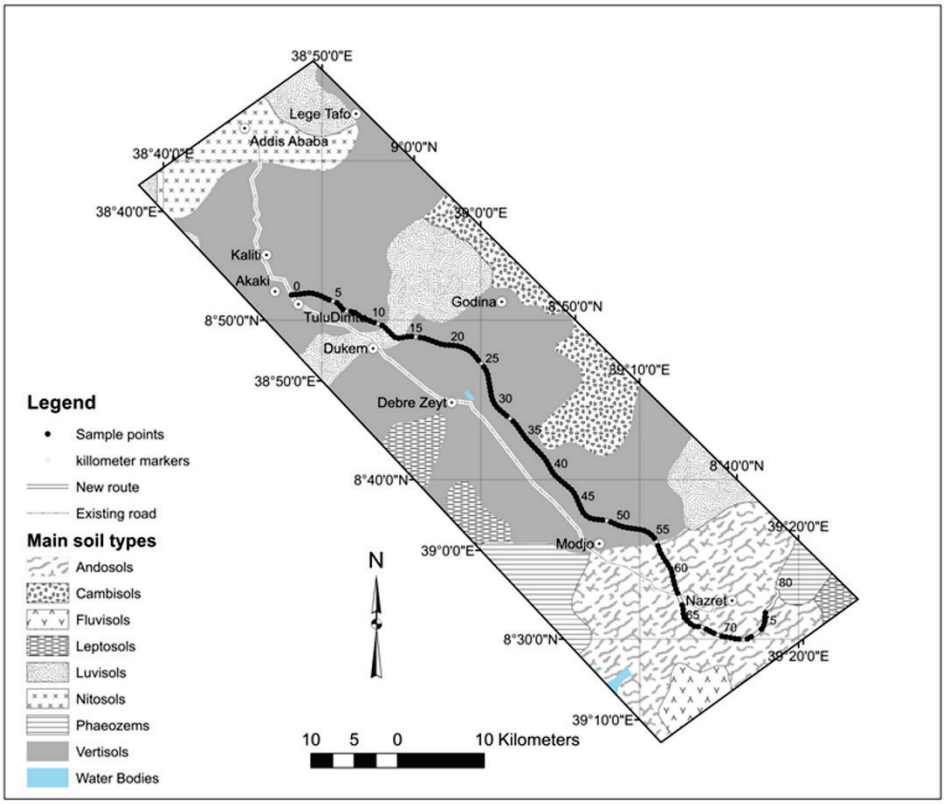

Figure 3-1 Location map of the study site, showing the spatial distribution of soil samples analyzed for expansion index (EI).

Soil samples were collected along this newly planned route from its starting point near TuluDimtu to its ending point at the town of Nazret (Figure 2-5). The sampling was part of a comprehensive geotechnical investigation scheme for assessing the suitability and quality of subgrade materials. This detailed investigation was an essential component of the engineering survey for determining the location and design of the expressway. A dense sampling scheme was planned (ERA, 2002), to gather pertinent information on the geotechnical characteristics of the soils to account for optimal location of the route, appropriate foundation and earthworks designs, environmental effect and remedial works. The samples (in total 161) were recovered at every 500 m interval from shallow trial pits of 1 m depth, which is commonly the depth at which shallowly founded structures are laid.

3.2.2 Geotechnical testing

Consistency limits: liquid limits (LL), plasticity limits (PL) and plasticity indices (PI) were determined in accordance with procedures and requirements of the ASTM D4318-05 standard method.

Particle size distribution tests were conducted in accordance with the ASTM D6913-04e1 standard test method, using sieve analysis (for the fraction passing through the ASTM 2 mm, 0.425 mm and 0.075 mm sieve openings). Grading of soils finer than the ASTM 0.075 mm sieve was determined by hydrometer analysis, in accordance with the ASTM D422-63 standard test method.

Expansion indices of the soils were determined in accordance with the ASTM D4829-07 standard test method. The expansion index test was carried out on 139 soil samples. Soils that are either non-plastic or those exhibiting very low plasticity were not tested for EI. The locations of these samples are shown in Figure 3-1.

3.2.3 Mineralogical analysis

The mineralogical composition of selected soil samples were examined using X-ray diffraction (XRD) analysis. XRD analysis is a most commonly used and well documented method for mineralogical analysis of soils, particularly clay mineral speciation (Moore and Reynolds, 1997). The Siemens D5000 X-ray diffractometer was used. The overall constituents of the soils were determined by analyzing the bulk soil samples. Clay fractions of the soil samples were analyzed to quantify major, minor and trace composition of clay species. The Rietveld refinement method (Young, 1995) was used for quantifying the clay mineral abundances. For this semi-quantitative determination of clay minerals, the soil samples were initially treated to remove organic matter, iron oxides and carbonates. The silt and clay fractions were separated by centrifugation. Then, oriented slides were prepared in four different ways: untreated, treated with ethylene glycol vapor, treated with ethylene glycol vapor plus heated at 400 °C and 550 °C respectively. X-ray florescence (XRF) analysis was used for determining the oxides in the soil samples, and organic matter content on loss on ignition (LOI).

3.2.4 Multivariate regression analysis

Regression analysis is a fundamental statistical tool for exploring possible relationships among explanatory and response variables. In multiple linear regressions (MLR), explanatory variables are assumed to be linearly independent. If explanatory variables are significantly interdependent, the problem of collinearity will arise, which may lead to numerically unstable and

spurious estimates of regression coefficients and over fitting (Brereton, 2000; Hair et al., 1987). Two other multivariate regression analyses techniques, principal component and partial least squares regression analyses are widely used to deal with highly collinear variables.

Principal component regression (PCR) analysis decomposes a set of explanatory variables into eigen vectors and scores that are orthogonal to one another. Therefore, it overcomes collinearity problems. After achieving an optimal projection of explanatory variables in a few principal components, regressing them against the response variable will be followed in a separate step. Choice of the relevant number of principal components can be a complex process when relevant underlying systematic data structure is small in comparison with noise (Brereton, 2000; Martens and Naes, 1989).

Partial least squares (PLS) regression analysis, on the other hand, decomposes both explanatory and response variables simultaneously to capture their common structure. Then, project this common structure into a small number of mutually independent factors. In PLS, explanatory variables are decomposed into new coordinates called 'T-scores'. These T-scores are computed in such a way that they also capture part of the structure in the explanatory variables that are relevant to the response. 'U-scores', on the other hand, summarize part of the structure in the response that is explained by the explanatory variables with a given set of principal components. The decomposition and regression are in a single step, through fewer principal components than is required by PCR (Brereton, 2000; Martens and Naes, 1989; Wold et al., 2001; Yeniay and Goktas, 2002). In PLS, principal components (PLS factors) are extracted in decreasing order of relevance. Hence choice of an optimal number of principal components is not a problem.

The extent and trend of relationships among the soil geotechnical characteristics were examined using a pair-wise correlation analysis. A partial least squares regression analysis was conducted to establish a relationship among the soil expansion index, Consistency limits (liquid limit and plasticity index) and fine fraction (material passing the ASTM 0.075 mm sieve aperture). The PLS regression was preferred as it handles collinearity and find components (PLS factors) from predictors that are also relevant to the response variable. Distributions of variables were checked, and appropriate transformations were carried out on those variables that showed a skewed distribution. As described by Martens and Naes (1989) and Wold et al. (2001), data were mean centered and scaled to unit variance before the regression analysis to ensure equal influence on the model. According to Wold et al. (2001), in the absence of knowledge about the relative importance of variables, the standard multivariate approach is (1) scaling each variable to unit variance by dividing them by their standard deviations,

and (2) centering them by subtracting their averages, so-called auto-scaling. This corresponds to giving each variable (column) the same weight, and hence similar priority in the analysis. A full cross validation procedure was used to calibrate and validate the prediction model. This full cross validation method uses a leave one out principle. One sample will be left out at a time, and the model is calibrated on the remaining samples. There will be N times repeat until every sample is left out once and the model is computed on the remaining samples, and the left out sample is predicted. As in multiple linear and principal component regressions, the R^2 served to evaluate the goodness of fit. The expected prediction error was assessed by the standard error of performance, and root mean square error of the prediction. Bias showed interference error, and was computed as an average value of the variation that was not taken into account by the model. Offset showed the point where the regression line crossed the ordinate in the scatter plot summarizing the relationship between measured and predicted values of the response. Thus, it showed deviation from the ideal one to one correspondence.

3.3 Results

3.3.1 Geotechnical Characteristics

The soils exhibited a wide range of plasticity character: a liquid limit of 27-110%, and plasticity indices of 5-70% (Table 3-1). A majority of soils along the expressway alignment was fine grained (note the mean value of fine fraction in Table 3-1). Percentage by weight passing the ASTM 0.075 mm sieve aperture ranged from 8% in coarser soils to a 100% in most black cotton soils. Hydrometer analysis conducted on 40 randomly selected soil samples showed a high amount of clay fraction. Clay content in these tested soil samples, ranged from 10-60% by weight, with higher proportions recorded in black cotton soils. The clay fraction was higher in those samples obtained from the 0-60 km stretch of the expressway route. Figure 3-2 shows typical particle size distribution curves of soil samples.

The expansion index of the soil samples, ranged from 1-152%, covering the classes of expansiveness very low to very high (ASTM, 2007). The ranges in geotechnical properties of the soil samples appeared larger. However, the variability was narrow, which tend towards the highly plastic and fine grained geotechnical characteristics.

Table 3-1 Summary of descriptive statistics: minimum, maximum, mean and standard deviation values of the soils geotechnical parameters, showing that the soil samples exhibited a wide range of properties.

Descriptive statistics	EI	LL	PI	Fine fraction (% passing ASTM 0.075 mm sieve aperture)
			-%-	
Minimum	1	27	5	8
Maximum	152	110	70	100
Mean	70.8	68.3	34.1	76.7
Standard Deviation	35.2	22.7	17	22.4

The plasticity chart of the soil samples (Figure 3-3) shows that the soil samples are highly plastic, particularly those obtained from the 0-60 km of the route. In addition, the majority of the samples (75%) plotted above the 'A' line, indicating that they belong to the inorganic clay varieties "Fat clay". On the other hand, the soil samples originated from 60 km up to the end of the route at Nazret town mainly fall within the medium and lower plasticity portions of the plasticity chart. Thus, the susceptibility of the soils to pronounced volume changes is high for those from the 0-60 km of the route, while it is low for those from the 60-80 km.

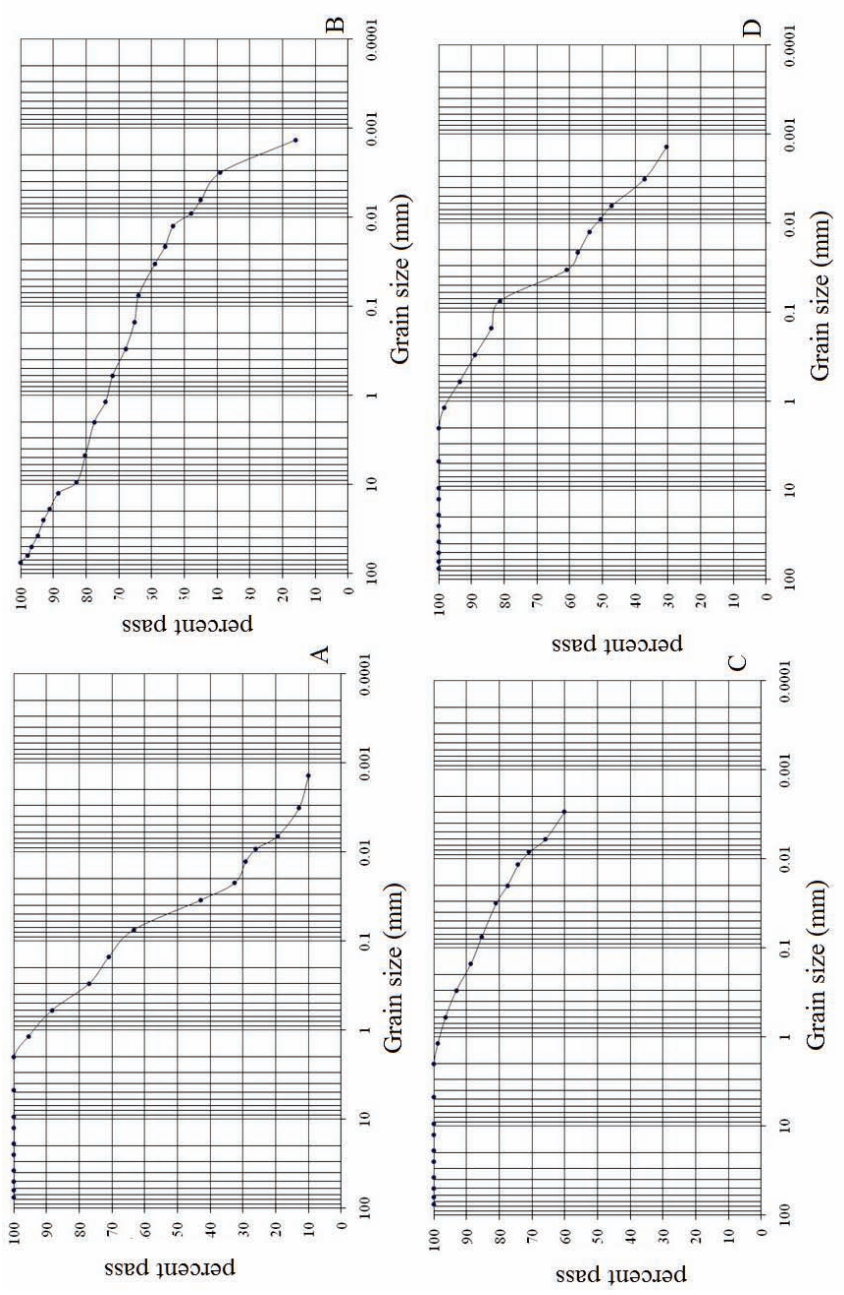

Figure 3-2 Particle size distribution curves of selected soil samples, showing grading of soil samples from kilometer (A) 8.5, (B) 28, (C) 57.5 and (D) 71.

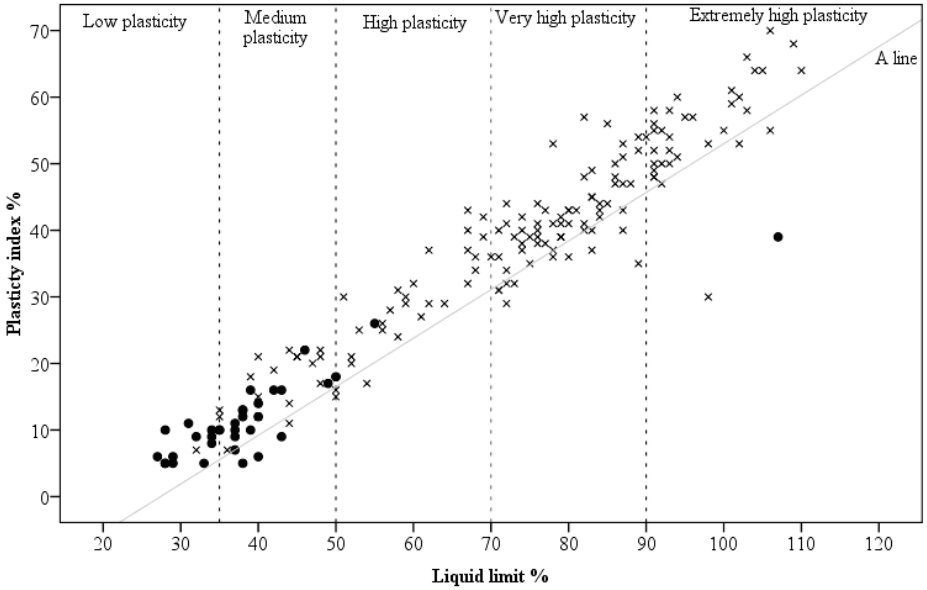

Figure 3-3 Plasticity chart of the soil samples with samples divided by their origin: label 'X' showing samples obtained from the 0 to 60 km stretch of the newly proposed alignment, and dark circles indicating samples obtained from the 60 to 80 km stretch of the route.

3.3.2 Mineralogical assemblage

The XRD analyses results showed the dominance of 2:1 clay minerals in the tested soil samples. XRD and XRF results are presented in Tables 3-2A and 3-2B, showing the mineralogical assemblages and oxides present in the soils respectively. XRD patterns of the clay fractions are presented in Figure 3-4. Smectite (montmorillonite and nontronite) is a major constituent, comprising more than 30% by weight in most of the soil samples. Illite-montmorillonite interstratified clay minerals, illite, and kaolinite were also found in the soils ranging from major (>30%) to moderate (10-30%), minor (2-10%) and trace (<2%) amounts. Apart from the clay minerals, which significantly influence the geotechnical behavior of expansive soils, associated minerals such as quartz, feldspar and goethite were identified in the mineralogical assemblage analysis. These associated minerals are common constituents of soils (Fitzpatrick, 1980; Yong and Warkentin, 1975) but do not contribute to soil expansiveness due to their low activity. In addition, calcite was found as a minor constituent. Presence of oxides such as SiO_2, Al_2O_3, Fe_2O_3, MgO, CaO, Na_2O, K_2O, TiO_2, P_2O_5, MnO, and Cr_2O_3 were identified from the XRF analysis result (Table 3-2B).

Montmorillonite $((Ca, Na)_{0.33} (Al, Mg)_2 (Si_4, O_{10}) (OH)_2 nH_2O)$ is a product of weathering of calcium and magnesium rich parent materials. It is one of the

most common smectite minerals found in soils (Galan, 2006). It also forms from weathering of volcanic ashes and primary silicate minerals, such as feldspars, pyroxenes, or amphiboles, under conditions of insufficient leaching of the soil profile due to low permeability and excessive evaporation (Chen, 1988; Fitzpatrick, 1980). As indicated in the summary of its geology, the study area is covered with rocks of volcanic origin. Volcanic debris and alkaline rocks such as basalt is common and abundant. The rainfall is seasonally moderate, where evaporation exceeds precipitation. The geology accompanied with this seasonally moderate rainfall, under poorly drained conditions that can allow retention of magnesium and calcium in the soils, can favor the formation of montmorillonite. Nontronite ($(Ca, Na)_{0.66}\ Fe^{3+}{}_4(Si, Al)_8\ O_{20}(OH)_4\ nH_2O$) is also a common smectite clay mineral found in soils and weathered bedrock. Its formation is similarly favored by alkaline to neutral pH environments, as well as availability of iron and calcium rich parent materials. Thus, formation of nontronite can also be favored by the geology, climatic conditions and topographic setting of the study area.

Illite ($(K, H_3O)\ (Al, Mg, Fe)_2\ (Al, Si)_4\ O_{10}\ [(OH)_2\ (H_2O)]$) commonly occurs in soils. It can be formed by weathering of silicates, primarily feldspars and micaceous rock forming minerals such as biotite and muscovite (Galan, 2006). Illite formation is favored in silicic to intermediate geologic environment, where there are high concentrations of Aluminum and Potassium (Fitzpatrick, 1980). These conditions are fulfilled in the study area. Illite regularly appears with smectite (Hower and Mowat, 1966; Mitchell, 1993) forming interstratified smectite-illite clay minerals such as interstratified illite-montmorillonite. This is shown in the XRD analysis result (Table 3-2A and Figure 3-4).

Table 3-2 Summary of results of (A) X-ray diffraction (XRD) analysis showing 2:1 clay minerals dominated in the soil samples in both bulk and clay fractions; and (B) X-ray fluorescence (XRF) analysis showing oxides in the soil samples.

(A)XRD results

	Mineralogical assemblage			
ID	Major	Moderate	Minor	Trace
Km 8.5				
Bulk	Montmorillonite	Quartz, calcite, nontronite	kaolinite, plagioclase, potassium feldspar, illite	brookite, rutile, goethite
Clay fraction	Montmorillonite	-	illite, kaolinite, calcite, quartz, potassium feldspar	-
Km 28				
Bulk	Montmorillonite	Quartz, nontronite	kaolinite, plagioclase, potassium feldspar, illite, calcite	brookite, rutile, goethite
Clay fraction	Montmorillonite	-	illite, kaolinite, calcite, quartz, potassium feldspar	-
Km 57.5				
Bulk	Montmorillonite	Quartz, nontronite	kaolinite, plagioclase, potassium feldspar, illite	brookite, rutile, goethite
Clay fraction	Illite-Montmorillonite (interstratified)	-	illite, kaolinite, quartz	-
Km 60				
Bulk	Montmorillonite	Quartz, nontronite	kaolinite, plagioclase, potassium feldspar, illite	brookite, rutile, goethite
Clay fraction	Illite-montmorillonite (interstratified)	-	illite, kaolinite, potassium feldspar	-

(B)XRF results

ID	SiO_2	Al_2O_3	Fe_2O_3	MgO	CaO	Na_2O	K_2O	TiO_2	P_2O_5	MnO	Cr_2O_3	V_2O_5	LOI^+
	-%-												
Km 8.5	46	13.8	7.14	2.29	5.66	0.79	1.46	1.14	0.08	0.18	0.02	0.02	21.4
km 28	50.1	19	7.95	1.63	0.3	0.77	1.86	1.22	0.15	0.17	0.01	0.02	13.2
km 57.5	50.8	15.9	8.46	1.5	1.33	2.16	2.53	1.03	0.04	0.24	0.02	0.02	14.5
km 60	62.9	13.2	6.82	0.58	0.97	4.53	3.42	0.6	0.06	0.24	<0.01	<0.01	6.86

$^+$LOI= loss on ignition

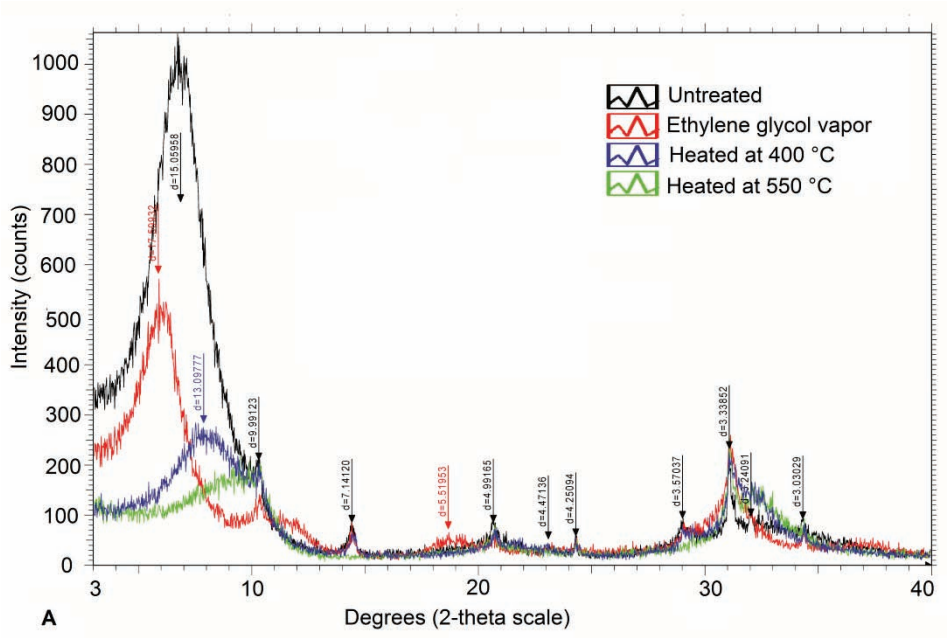

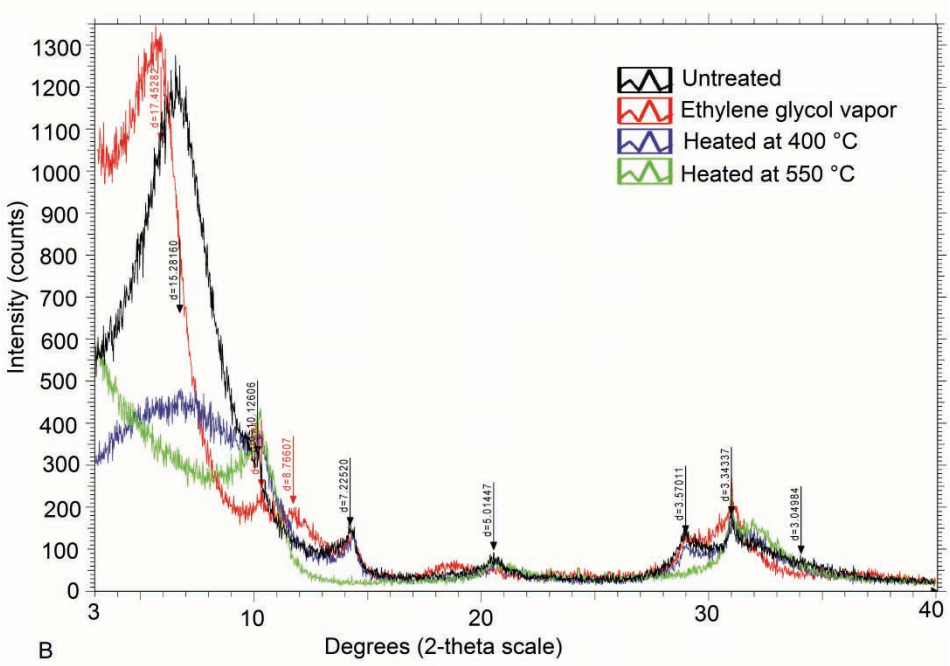
Untreated
Ethylene glycol vapor
Heated at 400 °C
Heated at 550 °C
Intensity (counts)
Degrees (2-theta scale)
d=15.28160
d=10.12606
d=8.76607
d=7.22520
d=5.01447
d=3.57011
d=3.34337
d=3.04984

B

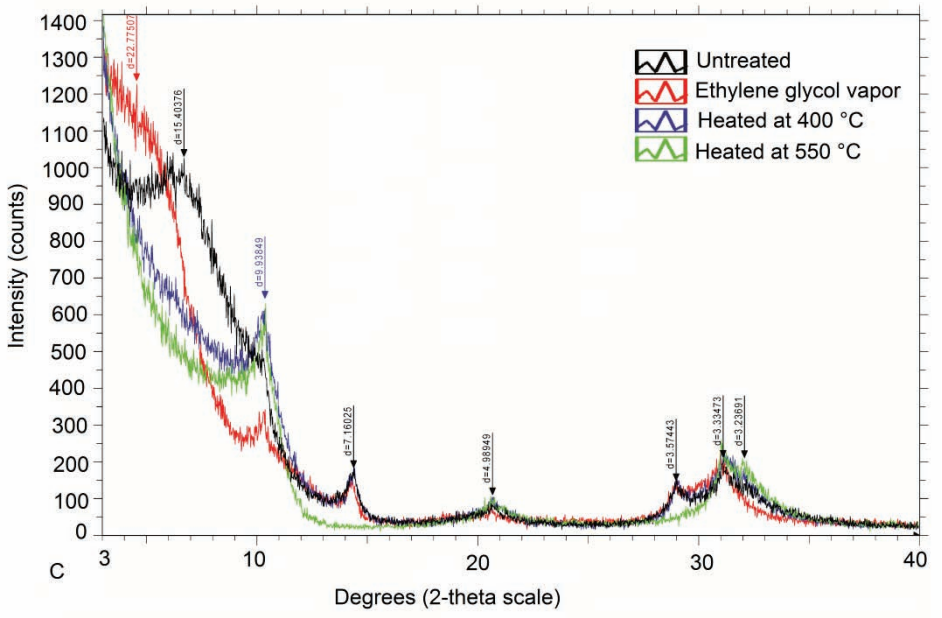
Untreated
Ethylene glycol vapor
Heated at 400 °C
Heated at 550 °C
Intensity (counts)
Degrees (2-theta scale)
d=22.77507
d=15.40376
d=9.93849
d=7.16025
d=4.98949
d=3.57443
d=3.33473
d=3.23691

C

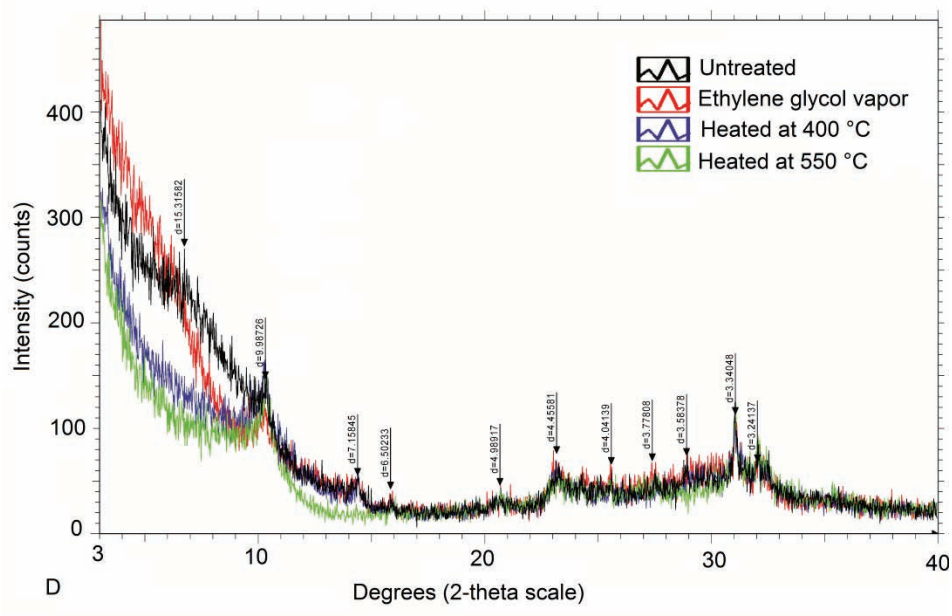

Figure 3-4 X-ray diffraction (XRD) patterns of the clay fractions of four soil samples from kilometer (A) 8.5, (B) 28, (C) 57.5 and (D) 60, indicating the presence of expansive clay minerals in the soil samples.

Kaolinite ($Al_2Si_2O_5$ $(OH)_4$) is another commonly occurring clay mineral in soils (Fitzpatrick, 1980; Yong and Warkentin, 1975). It can be derived from almost all silicate minerals. Hence, its formation in the study area can be favored by the environmental conditions. Halloysite ($Al_2Si_2O_5$ $(OH)_4$ $4H_2O$) occurs in soils and the uppermost weathered part of the bedrock. Halloysite is a common constituent of various volcanic soils (Takahashi et al., 2001). It can be formed as a result of weathering of aluminum rich minerals that are also abundant in the study area and its surroundings. Interstratified kaolinite-illite and kaolinite-montmorillonite clay minerals are also common in soils (Yerima et al., 1985).

The feldspar groups, calcium and sodium-rich (plagioclase) and potassium feldspar, are igneous rock-forming silicate minerals. Goethite can be formed from any iron bearing parent material and is a most common iron oxide in soils (Fitzpatrick, 1980). Calcite can be derived from calcium bearing rock-forming minerals such as plagioclase, pyroxene and amphibole. Rutile and brookite (TiO_2) are common in soils derived from igneous rocks (Fitzpatrick, 1980). Therefore, the formation of these minerals can be favored by the geology of the study area, accompanied with the highly seasonal tropical climatic conditions and topographic setting.

3.3.3 Estimating Expansion index

The soil geotechnical parameters were strongly positively correlated at p-value of 0.01 significance levels (Table 3-3). Therefore, collinearity was evident among the explanatory variables. The magnitudes of relationships were higher among the Consistency limits (Liquid limit and Plasticity index) and expansion index. The fine fraction showed lower correlations with Atterberg (Consistency) limits and expansion index. The fine fraction of the soils was likely to contain a large amount of clay minerals. The Consistency limits reflected high activity (Figure 3-3). The XRD results in Figure 3-4 and Table 3-2A, on the other hand, showed that compositions of the soil samples are dominated by 2:1 clay mineral species. This explains the reason why most of the soil samples plotted above the 'A' line, and that they belong to the highly plastic clayey soil varieties. According to Thomas et al. (2000), strong correlations among Consistency limits are due to the presence of active clay minerals. Thus, the overall strong relationships among the geotechnical parameters were ascribed to the influence of clay minerals in the presence of 2:1 clay minerals and high soil fine fraction content.

Table 3-4 summarized explained variances in the explanatory (X) and response (Y) spaces. The PLS model accounted for a large percentage of the original variance in the data. Two PLS factors were used. The accompanying root mean square error of prediction (RMSEP) reached a minimum at the second PLS factor. Thus, the variation in the X-space was directly relevant to the variation in the Y-space. This direct correlation was attributed to common factors i.e., clay mineralogical composition and content, dictating the soil geotechnical parameters.

Table 3-3 Pair-wise correlation matrix among the soils geotechnical parameters, showing significant correlation among the explanatory variables (liquid limit, plasticity index and fine fraction).

	Fine fraction	Liquid limit (LL)	Plasticity index (PI)	Expansion index (EI)
Fine fraction	1			
Liquid limit (LL)	0.636**	1		
Plasticity index (PI)	0.643**	0.958**	1	
Expansion index (EI)	0.604**	0.844**	0.930**	1

** Correlation is significant at the 0.01 (1%) probability levels.

Table 3-4 Total amount of variation in the explanatory (X) variables used to explain the response (Y) variable in each PLS factor used in the analysis, accompanied with root mean square error of prediction (RMSEP) after incorporating each component.

PLS factor	X-explained variance	Y-explained variance	RMSEP
		-%-	
PLS factor _1	54.9	86.4	13.24
PLS factor_2	94.3	92.4	9.87

A regression overview of the actual (measured) versus predicted expansion index is presented in Figure 3-5. The accompanying summary of model performance indices is also shown. The final equation for estimating the expansion index (EI) from Consistency limits and fine fraction is given in Equation [3-1].

$$EI = -73.52 + (0.392 * fine\ fraction) + (1.015 * LL) + (0.976 * PI) \quad [3\text{-}1]$$

All model terms were statistically significant at a P-value of less than 0.05 significance levels. This again indicated that the variation in the explanatory variables explained the variation in the response than could be expected due to chance, or that the effect is significant at a 5% level.

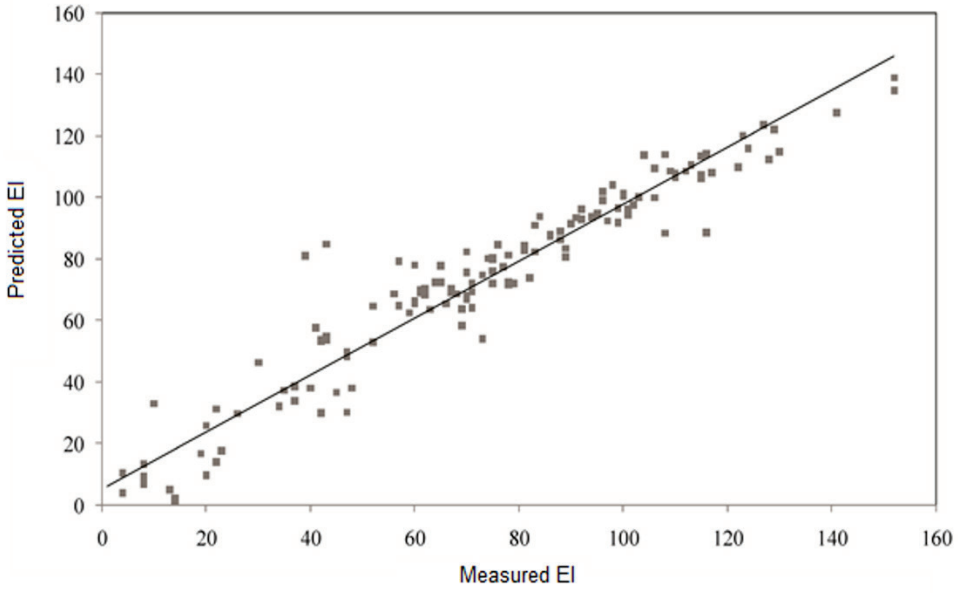

Model performance indices	
Root mean square error of prediction (RMSEP)	9.87
Standard error of performance (SEP)	9.91
Offset	5.31
Bias	0.04
Coefficient of determination (R^2)	0.92

Figure 3-5 Scatter plot showing the relationship between measured and predicted expansion index values, with a summary of model performance indices indicating that the model fitted the data well and explained a large portion of the variance in expansion index of the soil samples.

The coefficient of determination (R^2), which is a measure of the amount of variation about the mean explained by the model, was large. This showed that the model predicted the response variable well. Besides the large R^2, the RMSEP, SEP, offset and bias were low. These model performance indices also showed that the PLS regression model fitted the data appropriately.

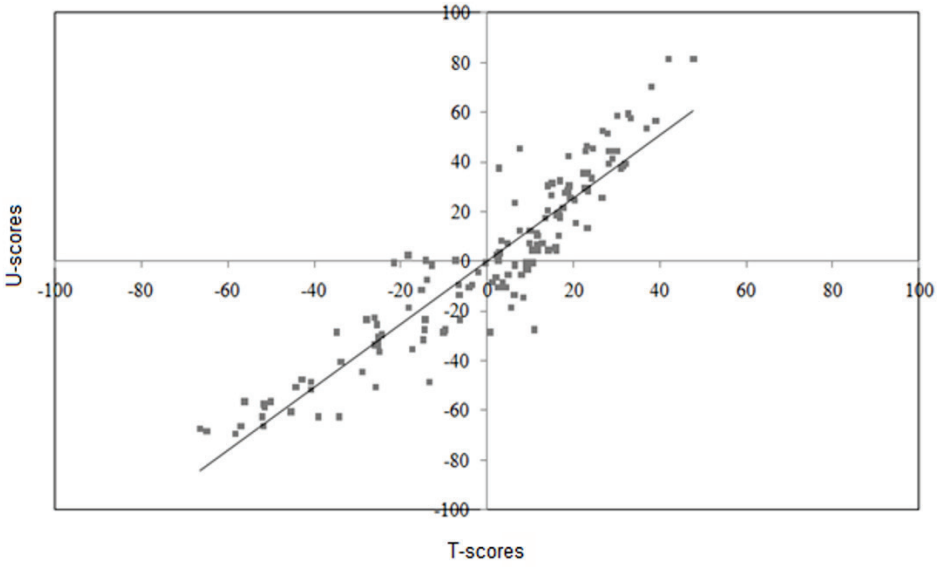

Figure 3-6 Scatter plot showing relationship between T-scores and U-scores from the PLS modeling, indicating no systematic curvature (nonlinearity) in the data hence suggesting that the PLS linear model best approximated the relationship between the explanatory and response variables.

There was no apparent deviation from linearity, detected in the PLS analysis result. Examining various plots such as the plot of U-score versus T-score

and residual plots, did not show any nonlinearity. These plots are powerful tools for detecting systematic curvatures. A scatter showing the relationship between the U-score and T-scores is presented in Figure 3-6. In addition, the scatter showing the relationship between measured and predicted expansion index values (Figure 3-5), showed no nonlinear pattern in the PLS analysis result. A lack of fit test, which is important for assessing the functional part of the model, was found to be not significant; again indicating that the linear PLS model fitted the data well.

The response surfaces in Figure 3-7 illustrated the general trend of relationship among Consistency limits (axes Plasticity index and Liquid limit) and fine fraction with expansion index. It appeared that there are no sharply defined boundaries (or numerical ranges) of plasticity index, liquid limit or fine fraction alone for classifying soils into different expansion index classes.

3.4 Discussion

Plasticity is an intrinsic property caused by the presence of active clay minerals in soils (Gourley et al., 1993; Mitchell, 1993; Seed et al., 1962; Snethen, 1975; Thomas et al., 2000; Yong and Warkentin, 1975). Thus, Consistency limits are indicators of the mineralogical compositions of fine particles in soils (Al-Rawas, 1999; Chen, 1988; Dakshanamurty and Raman, 1973; McCormack and Wilding, 1975; Ross, 1978; Seed et al., 1962; Skempton, 1984; Snethen, 1975; Thomas et al., 2000). Previous research established the importance of Consistency limits in indicating soil expansion potential. While high plasticity indicates the presence of active clay minerals (Al-Mukhtar et al., 2010; Al-Rawas, 1999; Carter and Bentley, 1991; Chen, 1988; Dakshanamurty and Raman, 1973; Kariuki and Van der Meer, 2004; McCormack and Wilding, 1975; Mitchell, 1993; Nelson and Miller, 1992; Perloff and Baron, 1976; Seed et al., 1962; Snethen, 1975; Thomas et al., 2000), non-plasticity often indicates an absence of such clay minerals in soils.

The fine fraction indicates the specific surface area of clay particles within soils (Carter and Bentley, 1991; Chen, 1988; Kariuki and Van der Meer, 2004). The material passing the ASTM 0.075 mm sieve contain fine sand, silt and clay fractions of the soil samples. The fine sand and silt fractions may have little effect on soil expansion potential, depending on their mineralogical composition. Clay content is as significant as Atterberg limits for assessing soil expansiveness (Carter and Bentley, 1991; Chen, 1988; McCormack and Wilding, 1975; Seed et al., 1962; Vaught et al., 2006; Wan et al., 2002). The more clay fraction a soil contains the larger is its expansion and shrinkage potential. This is due to increasing specific surface area, and thereby the water affinity (Bohn et al., 1985; Carter and Bentley, 1991; Chen, 1988; Perloff and Baron, 1976; Seed et al., 1962; Skempton, 1984).

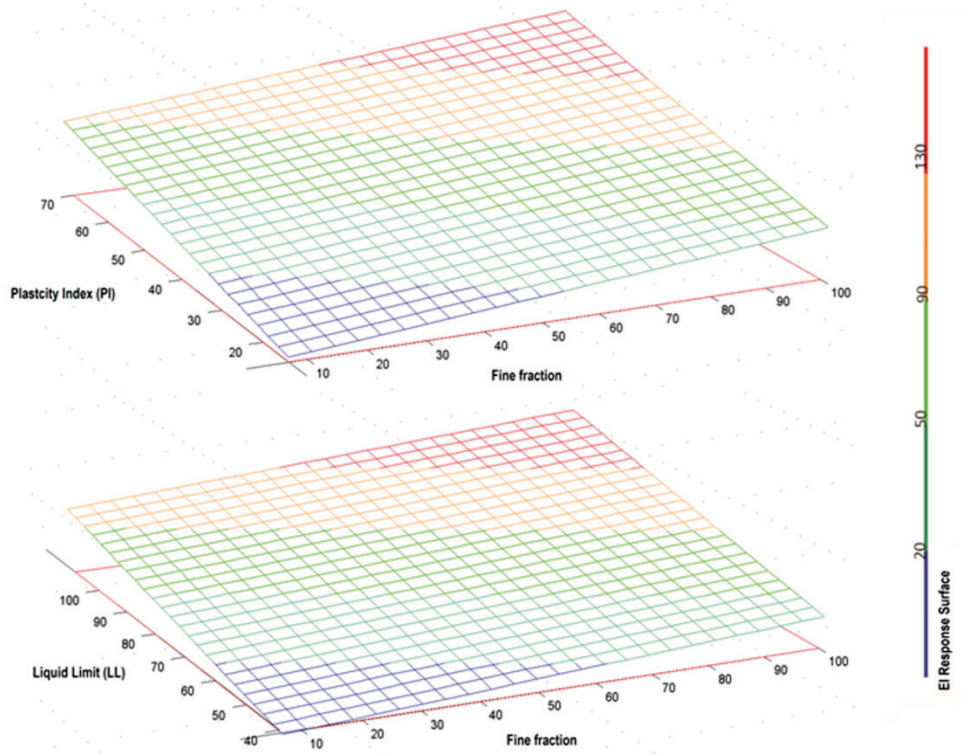

Figure 3-7 Response surfaces showing relationships among the percentage of material passing the ASTM 0.075 mm sieve aperture (axis Fine fraction), Plasticity index and liquid limit with Expansion index represented in varying colors.

Clay mineral composition is much more influential than clay content in dictating soil expansiveness. Several researchers (Al-Mukhtar et al., 2010; Al-Rawas, 1999; Karathanasis and Hajek, 1985; Kariuki and Van der Meer, 2004; Schafer and Singer, 1976; Thomas et al., 2000) demonstrated that soil expansion and shrinkage potential are primarily correlated to smectite content. Compared to their equivalent illite and kaolinite varieties, smectites can cause much more expansion in soils. Smectites have a larger specific surface area (Carter and Bentley, 1991; Ross, 1978) than illite and kaolinite. They also have an open structure, which typically accommodates abundant cationic substitution (Farmer, 1974; Yong and Warkentin, 1975). Hence, the dependence of soil expansiveness on clay mineral composition is partly due to the size of the clay mineral, particularly to its specific surface area. Kaolinite, illite and smectite, in increasing order of activity, are significant with respect to soil expansion potential (Carter and Bentley, 1991; Chen, 1988; Yong and Warkentin, 1975). The ranges of particle thickness, diameter and specific surface area of these three crystalline clay minerals are summarized in Table 3-5. Non-crystalline clay minerals, allophane and imogolite, are characterized by smaller particle thickness and diameter.

These non-crystalline clay minerals have a larger specific surface area (Wada, 1977) than the crystalline clay minerals. Yerima et al. (1985) and Yerima et al. (1987) demonstrated that soil expansiveness depends on mineralogy and clay content. Higher concentration of low to moderately expandable clay minerals behaved similarly as those of the highly expanding clay minerals. They justified this behavior to be a function of specific surface area. Therefore, control of clay fraction on soil expansion and shrinkage potential seems to hold true within the same clay mineral varieties. However, naturally occurring soils are heterogeneous and can be mixtures of more than one clay mineral. Thus, the increase or decrease in soil expansion potential with clay fraction may not be in direct proportion. Higher correlations among the Consistency limits and expansion index (Table 3-3), and lower (though statistically significant) correlations of those with the fine fraction are considered indicators of the strong influence of clay mineralogical compositions on soil geotechnical characteristics in the presence of active clay minerals.

In the response surface models (Figure 3-7), as the Consistency limits (axes Plasticity index and Liquid limit) increased for the same amount of material passing the ASTM 0.075 mm sieve (axis Fine fraction), the expansion index also increased. A gradual increase was manifested for smaller fractions of material passing the ASTM 0.075 mm sieve. The increase in expansion index was pronounced with increasing percentage of material passing the ASTM 0.075 mm sieve. As the amount of material passing the ASTM 0.075 mm sieve increased, while the plasticity index or liquid limit terms were fixed, the increase in expansion index was faint, particularly for lower plasticity index and liquid limit. On the other hand, when both the amount of material passing the ASTM 0.075 mm sieve and Consistency limits increased (for instance diagonal to axes plasticity index or liquid limit, and fine fraction) the expansion index showed a prominent increase. The increase in expansion index along the plasticity index or liquid limit axes can be attributed to possible changes in compositions of clay minerals from low to moderate and highly expanding varieties. The faint increase in expansion index of soils along the fine fraction axis, when the plasticity index and liquid limit terms were fixed, can be a result of increasing specific surface area of clay particles probably within the same clay mineral species. The prominent increase in expansion index, diagonal to both axes can be ascribed to changes in mineralogical composition as well as associated increase in specific surface area of clay particles in the soil samples. The response surfaces also illustrated the fuzziness of the soil geotechnical properties, and fuzzy membership of the combinations of these properties with respect to expansion potential. Boundaries for the ranges of each property were fuzzy, and there was a significant overlap of all terms (plasticity index, liquid limit and fine fraction). It was difficult to assign exact numeric ranges of

Consistency limits and fine fraction with respect to the expansion index, due to these overlaps. This conforms to earlier observations by Kariuki and Van der Meer, (2004), Reddy et al. (2009), Thomas et al. (2000) who discussed uncertainties of assigning exact numeric thresholds of a single soil property for rating soil expansion potential.

Overall, the findings in this study are in agreement with those of (Kariuki and Van der Meer, 2004; Nelson and Miller, 1992; Reddy et al., 2009; Ross, 1978; Schafer and Singer, 1976; Seed et al., 1962; Thomas et al., 2000; Zapata et al., 2006), who concluded that soil expansion potential can be estimated from liquid limit, plasticity index and soil fine fraction mainly clay fraction. In this study, fine fraction passing the ASTM 0.075 mm sieve aperture was used, as it is a routinely carried out parameter in geotechnical investigations, and easier to determine than clay content. The proposed multivariate regression model showed an improved prediction ability compared to previously proposed univariate regression models e.g., Zapata et al. (2006). In addition, the use of multiple geotechnical parameters enabled modeling the fuzzy interrelationship among the explanatory variables with respect to expansion index. Both the empirical relationship and response surfaces can provide a reliable estimate of expansion potential of soils. Thus, it can serve as guides for reliable analysis of design parameters of structures. The presented results can also be extrapolated to soils of a similar nature that exist in different parts of the world, e.g., soils containing expanding clay minerals derived from similar ranges of parent materials, described in chapter two, section 2.4.2.

Table 3-5 Ranges of particle thickness, diameter and Specific surface area of kaolinite, illite and smectite (after Chen 1988); other sources (Yong and Warkentin, 1975) roughly indicate that illite is five times less than the size of kaolinite, and montmorillonite is fifty times less than the size of illite.

Typical properties	Kaolinite	Illite	Smectite (Montmorillonite)
Particle thickness (μ)	0.5- 2	0.003-0.1	<9.5 Å
Particle diameter (μ)	0.5-4	0.5-10	0.05-10
Specific surface area (m^2 g^{-1})	10- 20	65-180	50-840

3.5 Conclusions

The purpose in this chapter was to characterize soils; establish a relationship among expansion index, Consistency limits and fine fraction passing the ASTM 0.075 mm sieve aperture; thereby develop an empirical method for

evaluating expansion index of soils. The soils were mostly fine grained, with 2:1 clay minerals dominating their composition. Thus, they were characterized by high plasticity and large susceptibility to pronounced volume changes. The expansion index ranged from very low to very high. A strong and statistically significant correlation was obtained from the PLS regression analysis. The high coefficient of determination (R^2 of 0.92), low root mean square error of prediction (±9.87%), narrow standard error of performance and negligible bias, showed significant model prediction ability. The fuzziness of soil geotechnical characteristics with respect to expansion potential were modeled by the response surface models, which is attributable to the use of multiple geotechnical parameters in establishing the relationship.

The established equation and presented relationships (response surfaces) can serve as classification techniques for identifying, classifying and evaluating expansion potential of soils. This can be particularly useful for preliminary assessment of soil expansion potential at an early stage of a geotechnical investigation, where availability of site information and laboratory test results are limited. The proposed multivariate relation and response surface models can be reasonably valid for other soils of a similar nature. The relations were developed from soils characterized by high liquid limit and plasticity indices, high percentage of material finer than the ASTM 0.075 mm sieve (up to a 100% with mean value of 76.7%), with most samples characterized by high clay and organic matter content. For wider applications, the established relationship should be tested on soils with a wider range of liquid limit, plasticity indices, particle size distribution and organic matter content. In general, the approach has an advantage of employing easily and routinely determined geotechnical parameters to derive information on soil expansion potential at minimal cost and time requirements.

Chapter 4*

Geotechnical characteristics of expansive soils and the VNIR and SWIR spectroscopy

Abstract: Occurrence of expansive soils in construction sites has serious cost and safety implications in the planning, design, construction, maintenance, and overall performance especially of lightweight engineering infrastructures. Thus, identifying expansive soils and determining their geotechnical characteristics is crucial. For this study, soil samples were collected from the eastern part of Addis Ababa. Geotechnical parameters were determined in a soil mechanics laboratory. Reflectance spectra of the soils were acquired in a remote sensing laboratory. The ASD FieldSpec full range spectrometer was used for spectral data acquisition. Expansive soils were identified and categorized, based on the unique spectral characteristics that soil constituent active clay minerals exhibited. A multivariate calibration method, partial least squares (PLS) regression analysis, through simple wavelength approach, was used to establish relationships among the geotechnical and spectral characteristics of the soils. Significant correlations were obtained, showing that a large portion of the variation in geotechnical parameters of expansive soils can be accounted for by spectral characteristics. Apart from high correlation coefficients, small root mean square error of calibration and prediction, standard error of calibration and prediction, and minimum bias and offset were achieved. Overall, the results signified the potential of spectroscopy for deriving geotechnical parameters of expansive soils from their respective spectra; and thus, its potential applicability in supporting geotechnical investigations of such soils.

Keywords: spectroscopy, expansive soil, active clay minerals, VNIR and SWIR, absorption features, PLS.

* This chapter is based on:

Yitagesu, Fekerte Arega, Van der Meer, F.D., and Van der Werff, H., 2009, Quantifying engineering parameters of expansive soils from their reflectance spectra: Engineering Geology, v. 105, p. 151 - 160.

Yitagesu Fekerte Arega., Van der Meer, F.D, Van der Werff, H., and Zigterman, W., 2008, Assessing expansive soil engineering parameters using spectroscopy, Geoscience and Remote Sensing Symposium, 2008. IGARSS 2008. IEEE International: Boston, MA, p. II-1255 - II-1258.

4.1 Introduction

Identifying expansive soils and quantifying their potential to swelling and shrinkage is a crucial concern in geotechnical investigations. However, traditional geotechnical practices of characterizing expansive soils require dense sampling, thus are costly, labor intensive and time consuming. It is also impossible to obtain continuous representation of soil masses in space. These constraints can force engineers to take as few samples as possible and depend on interpreting the results as representative of the whole project site. In the meantime, presence of expansive soils can be overlooked, and their swelling and shrinkage potential can be underestimated. Generally, low expenditure in geotechnical investigation, very often, results in large ground uncertainties (Stravern and Seters, 2004). Therefore, it is important to design a cost effective investigation technique that can support conventional geotechnical investigation and testing methods.

In this respect, the potential of spectroscopic techniques, as tools, for assessing soil expansiveness have been reported (Chabrillat et al., 2002; Goetz et al., 2001; Kariuki et al., 2003; Kariuki et al., 2004; Van der Meer, 1999). Spectroscopic techniques rely on detecting and analyzing distinct spectral signatures of active clay minerals in expansive soils. Spectroscopy is study of light as a function of wavelength reflected, absorbed, emitted or scattered from materials (Clark, 1999). The processes responsible for reflection, absorption, and emission are wavelength dependent and distinct for different materials. That is, spectral response of materials depends on particular crystal structure of materials and chemical structures of minerals within (Van der Meer, 1999). Thus, gives an opportunity to derive compositional information of materials from their spectra. In the visible-near infrared (VNIR) wavelength region, electronic and vibrational processes are responsible for the prevalence of absorption features in the spectra of minerals (Clark, 1999; Hunt, 1977). In this wavelength region, reflectance spectra of minerals are dominated by the presence or absence of transition metal ions (e.g., iron). In the short wave infrared (SWIR) wavelength region, spectra of minerals are mainly dominated, among other molecules, by the presence or absence of water and hydroxyl molecules (Baumgardner et al., 1985; Farmer and Russell, 1964; Hunt and Salisbury, 1970; Van der Meer, 1999). Active clay minerals exhibit diagnostic spectral characteristics that can be used for detecting their presence and identification purposes, due to differences in mineralogical compositions, structure, and associated physicochemical properties. Figure 4-1 shows spectra of clay minerals (USGS spectral library of minerals embedded in ENVI software (ITT Visual Information Solutions, 2009)) and differences in spectral characteristics among clay minerals. Van der Meer (1999) outlined the possibility of discriminating and mapping clay soils from remotely sensed data based on the dependence of spectral signatures on soil constituent minerals. Goetz et

al. (2001) established relationships between the SWIR (short wave infrared), 1.8–2.4 µm spectral bands and soil expansion potential classes of Seed et al. (1962). Chabrillat et al. (2002) identified and mapped exposed clay minerals (the three key clay minerals with respect of soil expansion and shrinkage: montmorillonite, illite, kaolinite) from airborne remote sensing images based on diagnostic absorption bands in the SWIR wavelength region. Kariuki et al. (2004) proposed models that made use of spectral parameters from selected wavelength regions. They established a one-to-one link between geotechnical parameters and absorption feature parameters (position, depth, width, asymmetry and area of the absorption band) at 1.4 µm, 1.9 µm and 2.2 µm wavelengths. Absorption feature parameters are schematically illustrated in Figure 4-2.

The purpose in this chapter was to establish empirical models for predicting specific geotechnical parameters of expansive soils from their respective reflectance spectra. A multivariate calibration method, partial least squares regression (PLS) analysis, through simple wavelength approach (Viscarra Rossel et al., 2006), was used to link geotechnical parameters and spectral characteristics. The models provide numerical estimates of geotechnical parameters that can be directly used in practical engineering applications. Though atmospheric absorption bands in the SWIR were reported to be significant for predicting soil geotechnical parameters (Chabrillat et al., 2002; Goetz et al., 2001; Kariuki et al., 2003; Kariuki et al., 2004), these bands were excluded in this analysis. The aim of doing so was to identify wavelength regions for providing an outlook in considering an extension of the approach to multispectral remote sensing image data. Geotechnical parameters that are commonly used to infer swelling and shrinkage potential (cation exchange capacity, CEC), and strength (California bearing ratio, CBR and accompanying CBR-swell) of materials (such as subgrade, sub-base and base-course) were related to soil spectral characteristics. Since these parameters are often used as direct inputs for designing thickness of pavements such as road and airfield pavements (Divinsky et al., 1998), their simple estimation is important.

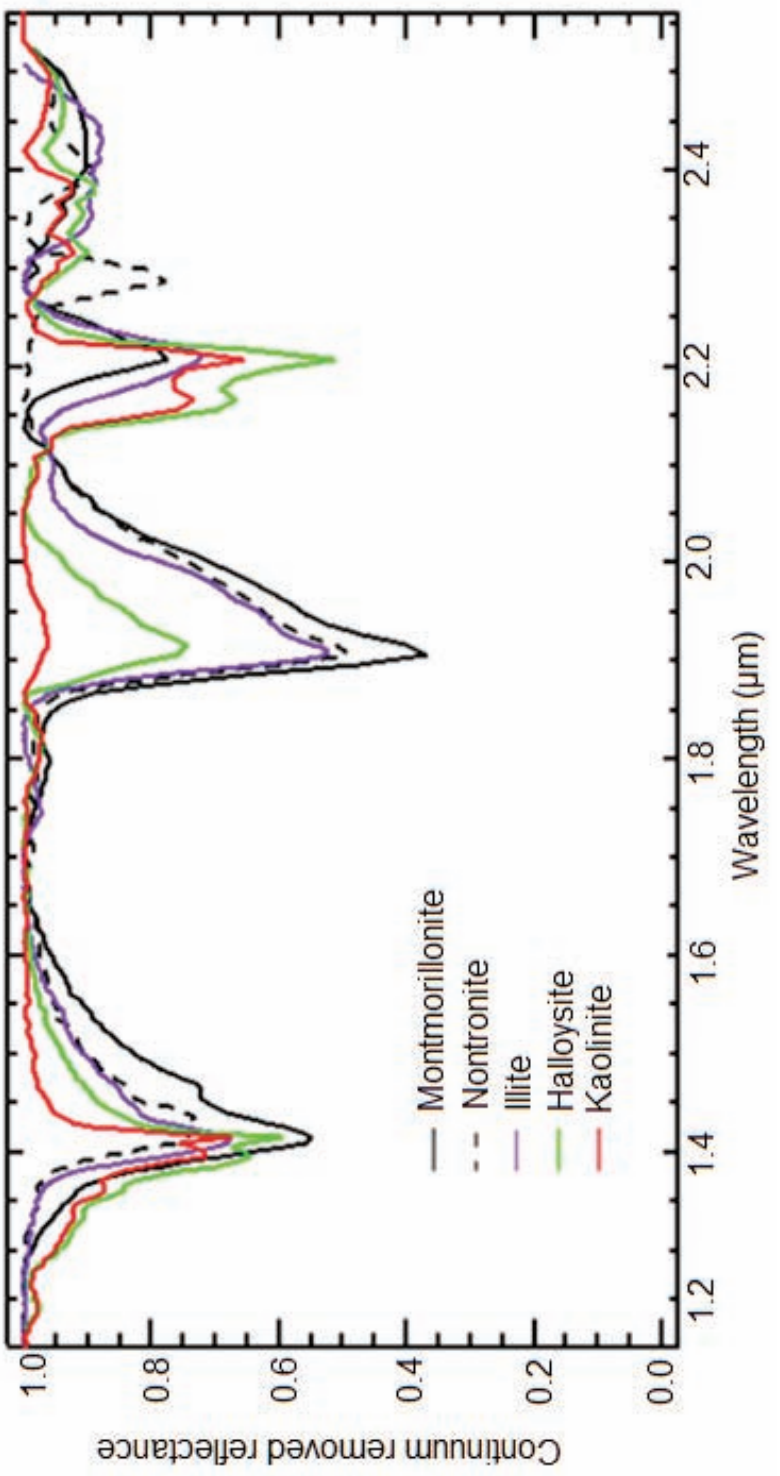

Figure 4-1 Spectra of clay minerals showing characteristic spectral differences. Note the changes in the absorption feature parameters such as depth, position and asymmetry of the features at ~1.4 µm, ~1.9 µm and ~2.2 µm.

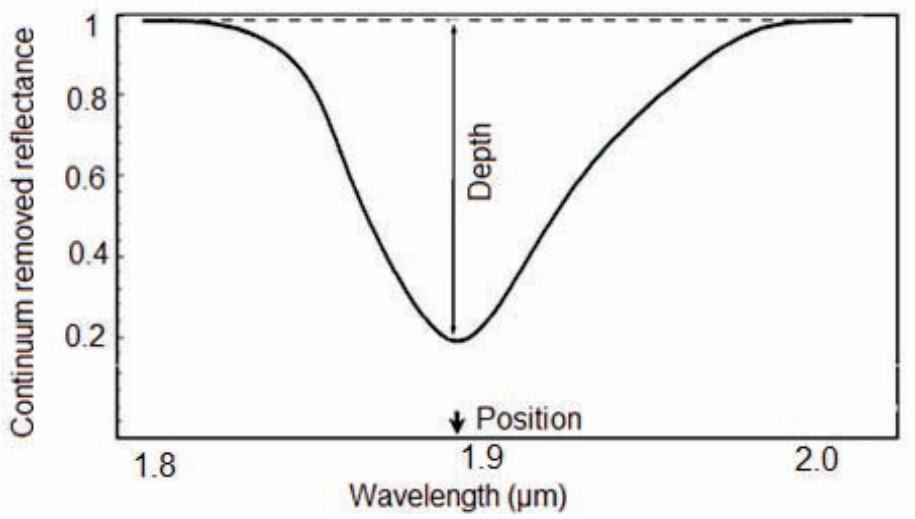

Figure 4-2 Schematic illustration of absorption feature parameters (Van der Meer, 2004a). Width is represented by the broken line at the top of the absorption feature. Area of an absorption band is calculated as triangles left and right side of the position. Dividing area at the left side of position by area at the right side of position gives asymmetry of the absorption feature.

4.2 Materials and Methods

4.2.1. Sampling and laboratory testing procedures

Disturbed soil samples were collected (from the Addis Ababa study area) from open pits of depth of 1m, a depth at which foundations of lightweight structures are commonly constructed. Based on site information and soil characteristics summarized in chapter two, section 2.4.1, a stratified random sampling strategy was followed.

Soil geotechnical parameters that are commonly used for identification of expansive soils and indirect estimation of their swelling and shrinkage potential such as cation exchange capacity (CEC) were measured in a soil mechanics laboratory. The CEC of soil samples were determined using the methylene blue adsorption test 'spot' method (Verhoef, 1992). Strength of the soil samples was determined by measuring their California bearing ratio (CBR). Accompanying CBR-swell of the soil samples were also measured. The CBR test was carried out in accordance with the ASTM D1883-05 standard test method for determining CBR and CBR-swell of laboratory-compacted soils. CBR and CBR-swell are commonly used geotechnical parameters to evaluate subgrade characteristics for pavement design (Cross and Gregory, 2007; Divinsky et al., 1998). It gives estimates of the load-bearing value and swelling characteristics of subgrade and bases, thereby their suitability for

use as road construction materials. Expansive soils commonly exhibit low CBR values and are characterized by high CBR-swell (percentage swell upon soaking for four days) when saturated.

Mineralogical compositions, oxides and organic matter content of the soil samples were determined using X-ray diffraction (XRD) and X-ray florescence (XRF) analyses. Protocols are described in chapter three, section 3.2.3.

4.2.2 Spectral analysis

Soil reflectance spectra were acquired using the ASD FieldSpec full range spectrometer (http://www.asdi.com), which measures reflectance in the wavelength region from 0.35-2.5 µm. Spectral resolution of the ASD FieldSpec full range spectrometer is 3 nm for the 0.35–1 µm and 10 nm for the 1–2.5 µm wavelength region (ASD, 1995). The spectrometer has three separate detectors, one in the visible-near infrared region (VNIR) and two in the short wave infrared (SWIR) region. Measurements were performed (in a contact probe mode) on small portions of air-dried soil samples, quartered from the whole sample, to ensure representativeness. An average of ten spectral measurements was taken (each taking about one second), for a good signal to noise ratio. Calibration of the spectrometer against a white reference was done after each sample measurement. The spectra were splice corrected for the three detectors junctions. The time spent to acquire the reflectance spectra of soil samples was on the order of hours, which saved a lot of time as compared to the traditional geotechnical testing methods that took several weeks.

Visual interpretation in combination with automated approaches was carried out to identify clay mineral species dominating the soils compositions. The automated approaches employ various statistical correlation techniques to relate each spectrum with a built-in or imported reference spectrum. These techniques include correlations via correspondence of wavelength positions and banded correlations. Spectral analyses were performed using the PIMA view (Spectronics, 1999), The Spectral Geologist (TSG) (Mason et al., 2011; Pontual et al., 1997) and ENVI software's (ITT Visual Information Solutions, 2009).

4.2.3 Multivariate regression analysis

Partial least squares (PLS) regression analysis is a fundamental statistical tool for estimating soil properties from reflectance spectra (Cloutis, 1996; Shepherd et al., 2005; Viscarra Rossel et al., 2006; Waiser et al., 2007). The technique is particularly important when dealing with a large number of variables that express common information to avoid collinearity (Martens and Naes, 1989; Viscarra Rossel et al., 2006). PLS1 regression analysis (Martens and Naes, 1989), built in The Unscrambler software (CAMO Process AS.,

2005) was used to determine the relationships between geotechnical parameters (CEC, CBR and CBR-swell) and spectral characteristics of the soil samples.

All wavelengths of the ASD Fieldspec full range spectrometer acquired soil spectra that also fall within the nine ASTER (Advanced Spaceborne Thermal Emission and Reflection Radiometer) band sets in the VNIR and SWIR were used. Hence, atmospheric absorption bands were excluded. Distributions of spectral variables were examined. Appropriate transformations (in this case logarithmic) were carried out on variables that showed skewed distributions to make their distribution fairly symmetrical (Wold et al., 2001). Various spectral data preprocessing techniques (Martens and Naes, 1989; Selige et al., 2006) were applied on the soil spectra prior to performing PLS analysis. Spectral data normalization was done through dividing each variable by the maximum value for better account of the spectral range. Martens and Naes (1989) mentioned the need to normalize spectral input data in order to remove uncontrollable scale variations. Multiplicative scatter correction, MSC (in this case common amplification) was done to avoid scatter effects from the soils texture, grain size and porosity. The aim of MSC is to prevent effects of scattering from being imposed on the phenomena of interest that one need to model (Dhanoa et al., 1994; Martens and Naes, 1989). To achieve this, an average or mean spectrum, $\overline{X}$ was calculated from the set of spectra constituting the calibration samples. For each individual spectrum, X_i, the parameters a_i and b_i were estimated by regression onto $\overline{X}$. The estimated parameters a_i and b_i representing the offset or additive parameter and the slope or multiplicative parameter of the regression line were then used for correction of the spectrum according to equation 4-1.

$$Mnew(i,k) = \frac{M(i.k)}{bi} \text{ ... [Common amplification]}$$

$$Mnew(i,k) = \frac{M(i.k) - ai}{bi} \text{ ... [Full MSC]} \qquad [4\text{-}1]$$

Then each spectrum was corrected so that all the spectra appear to have the same scatter level as the reference (Martens and Naes, 1989). The spectral data were mean centered and scaled to unit variance before calibration, for enhancing variance in the explanatory data and removing any systematic bias (Martens and Naes, 1989). Full cross validation, leave one out at a time method was used to validate the models.

4.3 Results and Discussion

4.3.1 Soil geotechnical and spectral characteristics

As for the spatial variability of the soil samples, a wide range of variability in their geotechnical characteristics was also represented. Soils obtained from the flat, low lying Bole area (located near to Bole international airport), and similar soil samples obtained from CMC area showed high CEC and CBR-swell; while their CBR was low. Whereas soils from the hilly areas of Kotebe exhibited low CEC and CBR-swell values, while their CBR values were highest of all the other localities. Other soils from the area in between Kotebe and CMC showed intermediate characteristics.

Differences in spectral characteristics among the spectra of soil samples were used in discriminating various clay mineral types that are present in the soil samples. Position of absorption features, their shapes, types and number, depth intensity and asymmetry; shape of spectral curves, differences in slopes of spectral curves and variations in reflectance intensity were some of the important qualitative parameters that helped to identify spectrally dominant clay mineral from the soil reflectance spectra (Figure 4-3). Some spectra showed a sharp rise in slopes and variable reflectance intensity throughout the whole wavelength region of the electromagnetic spectrum. Other spectra are characterized by lower reflectance intensity throughout the entire wavelength range; and were on overall dark. The latter also exhibited monotonously rising convex slopes in the visible-near infrared (VNIR) wavelength region and minor variability in reflectance intensity in the shortwave infrared (SWIR). Some spectra showed moderate rise in slopes with a moderate increase of reflectance intensity from the VNIR to the SWIR wavelength regions.

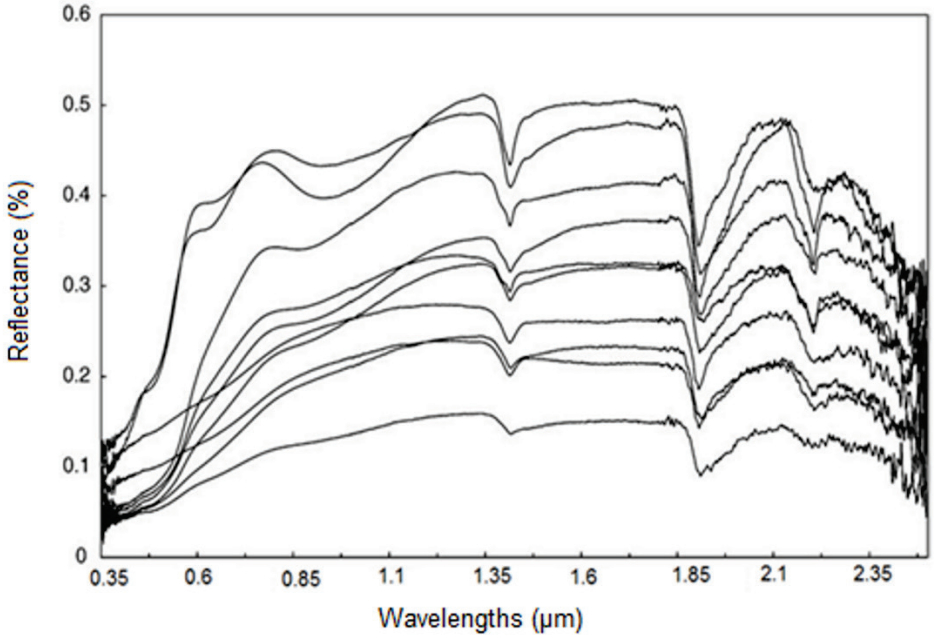

Figure 4-3 Variability in spectral characteristics of selected soil samples (no offset). Note the differences in shapes of spectral curves; overall reflectance intensity, shape, depth, position and number of absorption features among the spectra.

Up on spectral interpretation, the spectra of the soil samples were grouped into three main categories of clay mineralogical compositions; smectites, mixtures and kaolinites. Among the smectites were montmorillonite and nontronite; and of the kaolinite groups were halloysite and kaolinites. Those that were grouped under mixtures are a mixture of smectites, kaolinites and probably others such as illite.

Montmorillonite showed strong absorption features at ~1.4 µm, ~1.9 µm and ~2.2 µm. The depths of the features are intense at ~1.9 µm and ~1.4 µm accompanied with sharp minima and asymmetric shape. The absorption features at ~1.4 µm and ~1.9 µm, in nontronite show similar depth intensity and asymmetric shape as montmorillonite. Additionally, nontronite has diagnostic absorption features at ~2.27 µm to ~2.296 µm. The XRD mineralogical assemblage analysis results (Table 4-1A) verified the presence of montmorillonite and nontronite that were spectrally discriminated as well. XRD patterns of three representative samples are also shown in Figure 4-4.

Kaolinite clay mineral varieties showed doublet features at ~1.4 µm and ~2.2 µm, which are diagnostic (Clark, 1999; Hunt, 1977; Mustard et al., 2008). While the doublets for kaolinite appeared at ~1.4 µm and ~1.45 µm, and

~2.17 µm and ~2.21 µm respectively; they appeared at ~1.39 µm and 1.41 µm, and 2.18 µm and 2.21 µm for halloysite. Farmer (1974) and Hunt (1977) related these doublet features in kaolinite clay mineral species to the vibrations of structural hydroxyl groups (particularly to the Al-OH stretching and bending modes). In addition, the hydrated form of kaolinite, halloysite, shows an absorption feature ~1.9 µm. The presence of kaolinite is also attested from the XRD analysis result (Table 4-1A).

Features of illite did not appear strongly in the soils spectra. According to literature, illite exhibits absorption features at ~1.4 µm, ~1.9 µm and ~2.2 µm (note also the features in Figure 4-1). Furthermore, it has features at ~2.34 µm and ~2.45 µm, which are absent in the spectra of smectite clay minerals (Van der Meer, 1999). As compared to the spectra of smectite clay minerals, all features at ~1.4 µm, ~1.9 µm and ~2.2 µm tend to be slightly shallower while their positions shifted towards longer wavelengths in illite spectrum (Kariuki et al., 2004). Illite, due to abundant Al for Si substitution (Farmer and Russell, 1964; Yong and Warkentin, 1975), commonly exhibited broad and not well-resolved absorption features (Van der Meer, 1999).

Hunt and Salisbury (1970) assigned absorption features at ~1.4 µm, ~1.9 µm to the overtone and combination tones of fundamental modes of water molecules. Accordingly they attributed the feature at ~1.4 µm to the asymmetric stretching of OH groups, while the feature at ~1.9 µm is due to the combination tones of bending of H-O-H and asymmetric stretching of OH groups. The presence of both features at ~1.4 µm and ~1.9 µm is diagnostic of minerals bearing water molecules in their structures (Farmer, 1974). The OH groups (structural hydroxyl) other than in water molecules are noted to produce strong feature at ~1.4 µm (Hunt and Salisbury, 1970). In these minerals, such as kaolinite, the feature at ~1.9 µm is almost absent. The combination tones of OH groups stretching and bending in metal-OH (such as Al-OH, Mg-OH, Fe-OH) appeared in the ~2.1 µm to 2.5 µm wavelength region (Chabrillat and Goetz, 2000; Chabrillat et al., 2002; Clark, 1999; Farmer and Russell, 1964; Hunt and Salisbury, 1970; Kariuki and Van der Meer, 2003; Kariuki et al., 2004). The soils spectra exhibited absorption features in the 2.1-2.5 µm spectral region (Figure 4-3), which can be assigned to the metal-OH stretching and bending tones.

Table 4-1 (A) Summary of XRD analysis results showing abundance of major (>30%), moderate (10–30%), minor (2–10%) and trace (<2%) mineral constituent of soil samples; and (B) XRF analysis results showing the oxides in the soils.

(A)

		Mineralogical assemblage			
ID		Major	Moderate	Minor	Trace
1	Bulk	-	montmorillonite Kaolinite Nontronite	quartz, illite, potassium feldspar, goethite	Brookite
	Clay fraction	kaolinite	Quartz, illite	illite, montmorillonite	Potassium feldspar
2	Bulk	montmorillonite	Quartz, nontronite	Kaolinite, potassium feldspar, plagioclase	Illmenite, goethite, brookite
	Clay fraction	montmorillonite	-	Illite, kaolinite, quartz	
3	Bulk	-	Quartz, kaolinite	potassium feldspar, plagioclase, montmorillonite, nontronite	goethite, brookite, pyrite
	Clay fraction	kaolinite	-	quartz, illite	Potassium feldspar

(B)

ID	SiO_2	Al_2O_3	Fe_2O_3	MgO	CaO	Na_2O	K_2O	TiO_2	P_2O_5	MnO	Cr_2O_3	V_2O_5	LOI$^+$
	-%-												
1	53.4	19.6	6.28	0.69	1.11	0.52	1.17	0.77	0.07	0.03	<0.01	0.02	15.1
2	51.1	14.4	8.47	1.73	2.84	0.54	1.24	1.37	0.07	0.27	0.02	0.03	17.8
3	53.9	19	7.95	0.63	0.3	0.77	1.86	1.22	0.15	0.17	0.01	0.02	13.2

$^+$LOI = loss on ignition

In the VNIR, some soils showed features at ~0.478 µm, ~.493 µm, ~0.675 µm, ~0.765 µm, ~0.93 µm and ~0.967 µm. These features are related to the presence of iron oxides (Bendor and Banin, 1994; Hunt and Salisbury, 1970), and are common in soils for instance due to goethite (Baumgardner et al., 1985), which is the most commonly occurring iron oxide in soils (Fitzpatrick, 1980). The appearances of iron features in the visible wavelength region may also be related to substitution of Fe for Al and Mg in the octahedral sites (Farmer, 1974) (for instance in soils dominated by nontronite clay mineral varieties). The XRD analyses results (Table 4-1A) indicated the presence of iron-oxides such as goethite and pyrite in the soil samples. Note also the XRF analyses results showing presence of iron oxide (Table 4-1B). Furthermore, in the VNIR, slope differences were apparent (Figure 4-3). The overall dark spectra and strongly convex shapes exhibited by some soil spectra, as demonstrated by Bendor and Banin (1994), are attributed to the influence of

organic matter that is present within the soil samples (Table 4-1B loss on ignition, LOI).

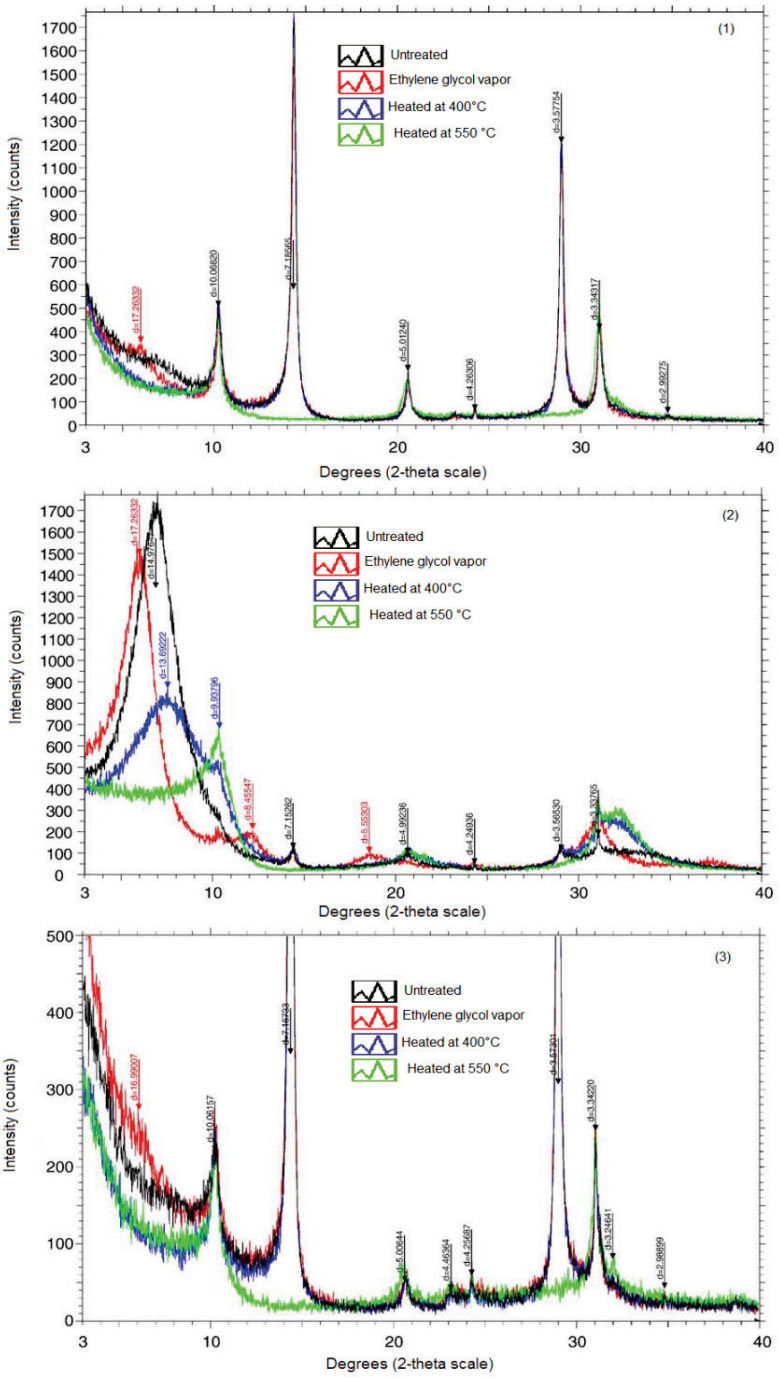

Figure 4-4 X-ray diffraction patterns of the clay fractions of representative soil samples from the three localities: (1) mixtures (CMC); (2) smectite (Bole, black cotton soil) and (3) kaolinite (Kotebe) categories of spectral analysis results.

4.3.2 Relationships among soil geotechnical and spectral characteristics

The relation in Figure 4-5 depicted that soils with high CBR-swell in general showed lower CBR values. However, soils with low CBR-swell values may not necessarily exhibit high CBR values. The latter is attributable to factors that affect the strength of soils such as mineralogical composition, particle size distribution and degree of interlocking, extent of weathering and organic matter content.

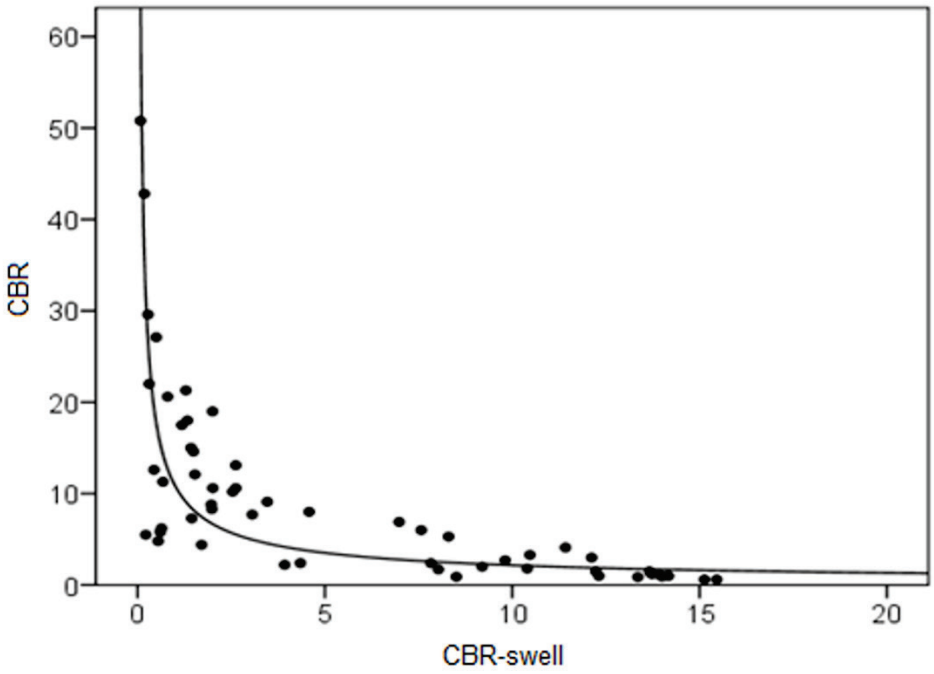

Figure 4-5 Relationship between CBR and CBR swell, showing soil samples with high CBR-swell generally exhibiting low CBR values.

Figure 4-6 illustrates relationships among geotechnical parameters, mineralogical compositions of the soils as spectrally interpreted, and depth and position of the absorption feature at ~1.9 µm. The observed correlation conforms to the expected trend, which is an opposite nature of percentage swell and bearing capacity of soils (Figure 4-5). Again CBR and CBR-swell of the soils revealed opposite trend of relationships among the assigned mineralogical classes and absorption feature parameters at ~1.9 µm. CBR-swell is negatively correlated with the position of the absorption feature at ~1.9 µm while it relates positively with soil mineralogical composition (Figure 4-6A). Highly expanding clay mineral (smectite) dominated soils exhibited large CBR-swell values, while the position of the absorption feature at ~1.9

µm shifted towards shorter wavelengths. On the contrary, the position at ~ 1.9 µm shifted to longer wavelengths in kaolinite dominated soil samples, which exhibited low CBR-swell values.

CBR-swell is positively correlated with the depth of the absorption feature at ~1.9 µm and soil mineralogical composition (Figure 4-6B). The highly expanding clay mineral (smectite) dominated soils exhibited large CBR-swell values, while their spectra were characterized by deeper absorption (as is also illustrated in Figure 4-1). Soil samples dominated by non-expanding clay minerals such as kaolinite showed low-CBR-swell values; and their spectra exhibited shallower depth at the ~1.9 µm absorption feature.

CBR is negatively correlated with the soils mineralogical compositions. Smectite dominate soils exhibited low CBR values. CBR showed positive correlation with the position of the absorption feature at ~1.9 µm (Figure 4-6C). Position of the ~1.9 µm absorption feature shifted to longer wavelengths with increasing CBR values. On the other hand, CBR is negatively correlated to the depth of the absorption feature at ~1.9 µm (Figure 4-6D). Soil samples dominated by smectite, which is responsible for substantial swelling and shrinkage characteristics in soils (Thomas et al., 2000) exhibited low-CBR values, while their spectra are typically characterized by deeper absorptions at ~1.9 µm (as is also illustrated in Figure 4-1). Soil samples dominated by non-expanding clay minerals (kaolinite) showed higher CBR values, while their spectra exhibited shallower depth at ~1.9 µm.

The above observations are in agreement with previous findings; e.g., Kariuki et al. (2003 and 2004), that they published relationships among absorption feature parameters at ~1.9 µm and soil swelling and shrinkage characteristics determined by Coefficient of linear extensibility (COLE) and linear extensibility ($LE_{(rod)}$) tests.

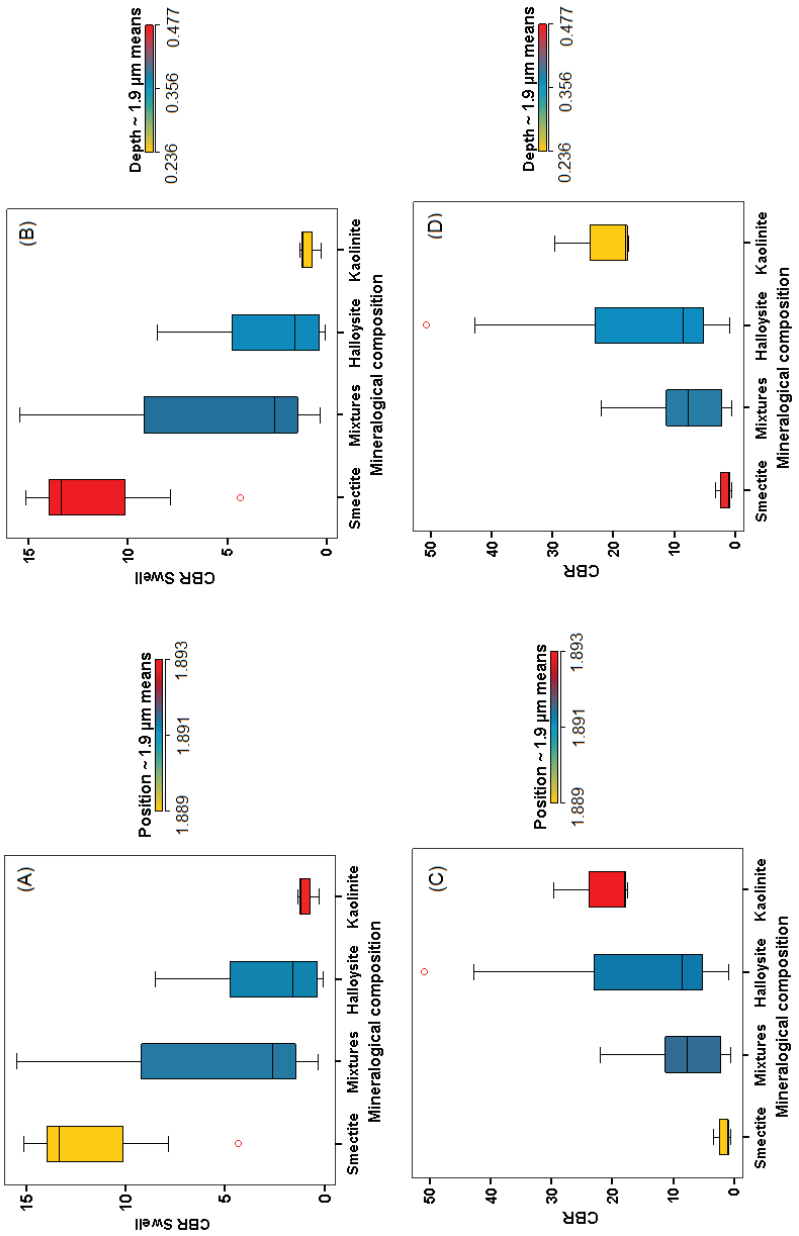

Figure 4-6 Box plots showing relationships among CBR-swell (A and B) and CBR (C and D) with mineralogical composition of the soil samples interpreted from their reflectance spectra, and position and depth of the absorption feature at ~1.9 µm.

Although large sample variability was evidenced (note the spread of the boxes of each mineralogical class), centers (mean) in each mineralogical category suggested strong correlations among geotechnical parameters and

mineralogical classes. In general, for CBR-swell, as the mineralogical composition changes towards the highly expansive clay minerals (from kaolinites to smectites), the values of the CBR-swell of the soils also increased. For the strength parameter (CBR), as mineralogical compositions change towards highly expansive clay minerals (from kaolinites to smectites), the CBR values of the soils decreased. The observed large variability of samples in each mineralogical class can be attributed to the inhomogeneous nature of the soil samples. That is, difference in content of clay minerals, the presence of other clay minerals apart from the dominant ones in each category, and probably interference from other soil constituents on both geotechnical and spectral characteristics of the soils.

PLS regression analyses results showed that geotechnical parameters (CEC, CBR and CBR-swell) of soils can be predicted from spectral data. The models (Figures 4-7 and 4-8) showed good prediction performance as evidenced by high correlation coefficients and low errors in terms of RMSEC & RMSEP, SEC & SEP and Bias. Significant predictors showed slight differences, but fall within similar spectral regions. Figure 4-7 presents results of the PLS regression analysis for CEC. It can be noted that less than 5 % of the samples fall outside the 95% confidence ellipse (Figure 4-7A). Only one sample lies outside the 95% confidence ellipse; under normal situation it is expected that about 5 % of the samples to lie outside the ellipse. Note also that there are no outlying samples lying outside the rest of the cloud. The remaining unexplained variance in CEC by the spectral parameters is small after fitting the third PLS component (Figure 4-7C); CEC values during the calibration and validation stages showed negligible deviations (Figure 4-7D) suggesting the model fitted to the calibration data set described the prediction data set as good as possible for the validation method that is used is this analysis i.e., full cross validation, leave one out at a time method. Hence, it is clear that there exists a strong relationship among geotechnical and spectral characteristics.

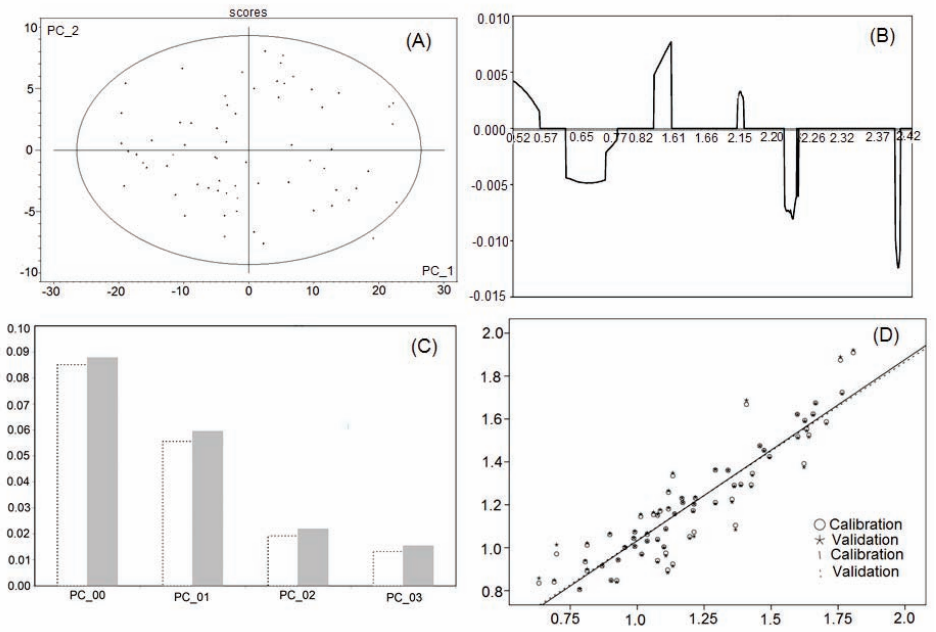

CEC

	Correlation coefficient	RMSEC/P	SEC/P	Bias	Offset
Calibration	0.92	0.12	0.12	0.00	0.19
prediction	0.90	0.12	0.12	0.00	0.21

Figure 4-7: Results of PLS regression analysis and accompanying summary of model performance indices for CEC showing: (A) Scores principal components 1 (x-axis) versus 2 (y-axis) with samples in the 95% confidence ellipse showing that there is no particular grouping of samples, but rather a random pattern (one population) suggesting a single model can fit the data. (B) Regression coefficients (statistically significant wavelength regions) in predicting CEC from the laboratory soil reflectance spectra. X-axis shows wavelength in µm and y-axis shows regression coefficients. These wavelength regions can be used in attempting to extrapolate or use airborne or satellite images for mapping spatial variability in soil expansiveness. (C) Residual variance (white during calibration and grey during prediction stages) showing the remaining variation that is not taken in to account by the model is minimum after fitting three PLS components, and depicting much of the variability in CEC is explained by the model. (D) Regression overview showing the relation between measured (x-axis) and predicted (y-axis) CEC. Calibration and prediction points lie close to each other, suggesting that the model fitted to the calibration data set described the prediction data set as good as possible. NB. Full cross validation, leave one out at a time method was used.

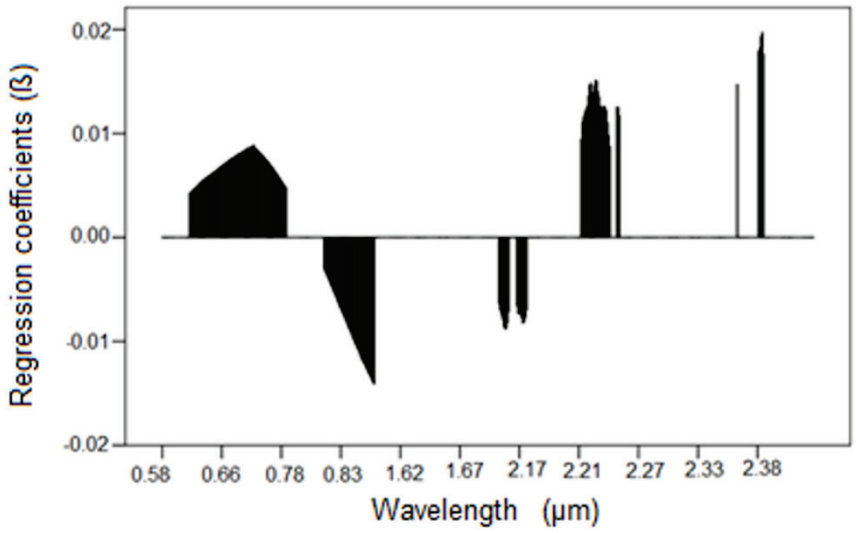

CBR

	Correlation coefficient	RMSEC/P	SEC/P	Bias	Offset
Calibration	0.87	0.187	0.190	0.000	0.216
prediction	0.85	0.206	0.209	0.001	0.252

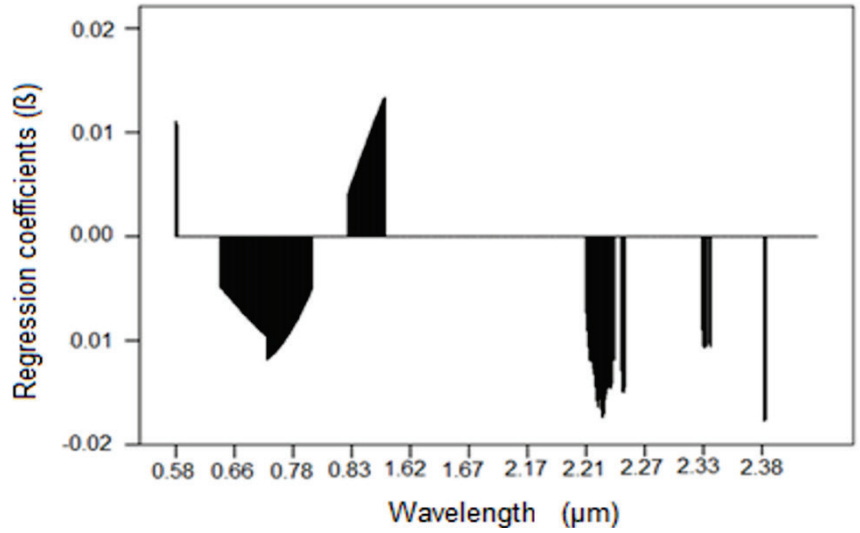

CBR-swell

	Correlation coefficient	RMSEC/P	SEC/P	Bias	Offset
Calibration	0.87	0.188	0.190	0.001	0.146
prediction	0.84	0.204	0.206	0.002	0.167

Figure 4-8 PLS regression coefficients for CBR and CBR-swell with accompanying summary of model performance indices, where RMSEC/P is root mean square error of calibration/prediction and SEC/P is standard error of calibration/prediction.

The resulting spectrally active wavelength regions (Figure 4-7B and Figure 4-8) in the VNIR can be attributed to slope differences among the spectra of soil samples, which seemed to vary with mineralogical compositions, and features related to organic matter and iron oxides. Those in the SWIR wavelength region can be ascribed to diagnostic clay mineral features associated with the combinations of stretching and bending vibrations of the OH group bonds with metal (Al, Mg, Fe) (Clark, 1999; Hunt, 1977; Kariuki et al., 2004). Overall, the results signified the possibility that laboratory spectroscopic experiments can be extrapolated to image data for a large scale (covering a wide area) mapping of expansive soil geotechnical parameters.

4.4 Conclusions

The soils showed variability in their geotechnical and spectral characteristics that appeared to be related to differences in their mineralogical compositions. The presence of clay minerals such as montmorillonite, nontronite, halloysite and kaolinite were distinguished based on characteristic absorption features that they exhibited. As a result, it was possible to identify expansive soils from their respective spectra, and derive information regarding their geotechnical characteristics. There exist a strong correlation among the spectra, mineralogical compositions and geotechnical parameters of expansive soils. Absorption feature parameters were useful in estimating geotechnical parameters such as CRB, which are direct design inputs (e.g., in highway pavement design). In addition, excluding atmospheric absorption bands seem to have little effect on the wealth of information content of soil spectra with respect to estimating geotechnical parameters of soils. A great deal of information can be obtained over a short time. Potentially, dense sampling can be achieved since a small amount material is required per sample. Thus, under-sampling can be avoided. Overall, spectroscopy can play a significant role particularly in identifying sites that might need due attention and further detailed geotechnical assessment with respect to the presence of potentially expansive soils.

Chapter 5*

Clay minerals in the mid-infrared (MIR) wavelength region: a laboratory experiment

Abstract: Identification and quantification of clay minerals, particularly those that are responsible for susceptibility of soils to expansion and shrinkage, is a constant focus of research in geotechnical engineering. The visible-near infrared and short wave infrared wavelength regions are well explored. However, little is understood about the spectral characteristics of such clay minerals in the wavelength region longer than 2.5 µm. The objective in this study was to determine the potential of laboratory spectroscopy in the 2.5-14 µm wavelength region for characterizing clay minerals. Montmorillonite, illite and kaolinite were investigated for these clay minerals are key indicators of soil swelling and shrinkage potential. Characteristic absorption features and their changes for mixtures of clay minerals were determined. Partial least squares (PLS) regressions in combination with continuum removal analyses were used to determine wavelength regions that best discriminate differences in mineralogical contents. Spectral contrast was high in the 3-5 µm wavelength region but overall low in the 8-14 µm. The clay minerals were characterized by strong diagnostic absorption features. Much of the variation in compositions of the mixtures were explained by the PLS models (coefficients of correlations of >0.90). Thus, spectroscopy in the 2.5-14 µm wavelength region is a useful technique for characterizing clay minerals.

Key words: Clay minerals, montmorillonite, illite, kaolinite, spectral characteristics, PLS.

* This chapter is based on:

Yitagesu, Fekerte Arega, Van der Meer, F.D, Van der Werff, H., and Hecker, C., 2011, Spectral characteristics of clay minerals in the 2.5-14 µm wavelength region: Applied Clay Science, v. 53 (4), p. 581-591.

5.1 Introduction

Montmorillonite, illite and kaolinite are the most common soil forming clay minerals (Fitzpatrick, 1980; Galan, 2006; Gray and Murphy, 2002). In geotechnical engineering, they are key indicators of soil swelling and shrinkage potential (Al-Rawas, 1999; Chen, 1988; Fall and Sarr, 2007; Karathanasis and Hajek, 1985; Mitchell, 1993; Seed et al., 1962; Thomas et al., 2000; Yong and Warkentin, 1975). These clay minerals are distinct in composition, structural arrangements and physicochemical characteristics (Brigatti et al., 2006; Yong and Warkentin, 1975). Montmorillonite can be formed from parent materials with high levels of calcium, ferro-magnesium oxides in low content of silica under favorable environmental conditions; poorly drained environment and seasonally moderate rainfall where evaporation exceeds precipitation (Fitzpatrick, 1980; Galan, 2006; Gray and Murphy, 2002). Primary illitization can be favored by an abundance of feldspars and mica (biotite, muscovite) such as in silicic to intermediate geologic environment (Fitzpatrick, 1980; Galan, 2006), at high levels of aluminum and potassium at the expense of calcium and sodium. Illite often occurs as mixed smectite-illite interstratified minerals, exhibiting properties between the two clay minerals (Brigatti et al., 2006; Yong and Warkentin, 1975). Low concentrations of basic cations, high feldspar and silica contents, accompanied with high rainfall and temperature easing extensive leaching, favor kaolinite formation (Galan, 2006). All the three clay minerals can also be found in a variety of sedimentary rocks such as mudstones, claystone and shale (Galan, 2006).

Soil expansiveness constitutes a significant challenge in geotechnical engineering (Al-Mukhtar et al., 2010; Al-Rawas, 1999; Bell, 1999; Kariuki et al., 2004; Morin, 1971; Seco et al., 2011; Shi et al., 2002; Snethen, 1975; Sridharan and Gurtug, 2004; Thomas et al., 2000). It is an intrinsic property caused by the presence of active clay minerals in soils (Fityus and Buzzi, 2009; Seed et al., 1962; Skempton, 1984; Snethen, 1975). Detection of the presence of such clay mineral is a key factor for differentiating potentially expansive soils. Identification and quantification of their abundance is essential for rating soil expansiveness. Conventional mineralogical analysis involves X-ray diffraction (XRD) analysis, scanning electron microscopy (SEM), transmission electron microscopy (TEM), differential thermal analysis (DTA), thermogravimetric analysis (TGA), and various chemical analysis methods. These methods are vital in research laboratories for exploring the basic properties of clay minerals. However, they are costly and require sophisticated laboratory procedures. Thus, they are not commonly used in soil mechanics laboratories for routine analysis of soil geotechnical characteristics. An easier alternate identification and quantification of expanding clay minerals is thus a constant focus of research in geotechnical engineering, including the application of remote sensing techniques.

Reflectance spectra of clay minerals were subjected to intensive research in the visible-near infrared (VNIR) and short wave infrared (SWIR) wavelength regions (Bourguignon et al., 2007; Chabrillat et al., 2002; Clark, 1999; Kariuki and Van der Meer, 2003; Kariuki et al., 2003; Kruse, 1991; Kruse et al., 1990; Rowan et al., 1977; Rowan et al., 2003; Van der Meer, 1995; Viscarra Rossel et al., 2009; Yitagesu et al., 2009b). Particularly in the SWIR, clay minerals exhibit diagnostic absorption features (Clark, 1999; Kariuki et al., 2004; Mustard et al., 2008; Van der Meer, 1999) resulting from vibrational processes related to their structural water molecules and hydroxyl groups (Farmer, 1974). Spectral responses of clay minerals result from vibrations of structural water molecules, hydroxyl groups, the silicate framework, and the octahedral, tetrahedral and interlayer cations (Farmer and Russell, 1964). Spectral characteristics differ, depending on the chemical composition, structural arrangement and bonding characteristics (Clark, 1999; Van der Meer, 2004a) and provide a significant potential for discriminating clay minerals (Bourguignon et al., 2007; Chabrillat et al., 2002; Frost et al., 2001; Kariuki and Van der Meer, 2004; Mustard et al., 2008; Roush et al., 1987; Yitagesu et al., 2009b).

Absorption feature analysis (Clark and Roush, 1984; Goetz et al., 2001; Kariuki et al., 2003; Kariuki et al., 2004; Van der Meer, 2004a) and multivariate regression analysis (Martens and Naes, 1989; Wold et al., 2001) were extensively used for estimating soil properties (Cloutis, 1996; Gomez et al., 2008; Rainey et al., 2003; Selige et al., 2006; Shepherd et al., 2005; Viscarra Rossel et al., 2009; Viscarra Rossel et al., 2006; Waiser et al., 2007), including geotechnical characteristics (Yitagesu et al., 2009b). However, research in this respect is limited in the wavelength region longer than 2.5 µm. In this wavelength region, molecules exhibit strong, fundamental vibrations of high frequency (Arnold, 1991; Clark, 1999; Farmer and Russell, 1964; Ludwig et al., 2008). Therefore, this wavelength region is often termed a fingerprint region (Griffiths and de Haseth, 2007). The spectral sensitivity of clay minerals in this wavelength region is associated to their structural and compositional variations (Farmer and Russell, 1964). Furthermore, Famer et al. (1974) presented infrared transmission spectra and assigned wavelengths with vibrations of clay mineral constituent molecules. Frost et al. (2001) studied absorbance spectra of sepiolites and palygorskites. They reported that the spectral changes of these minerals were related to differences in their structural arrangements and compositions. Although, transmission and absorbance spectra contain similar spectral information (Michalski et al., 2006); they are not directly applicable to remote sensing, for emission or reflectance than transmittance and absorbance are detected. Roush et al. (1987) discussed reflectance spectra of kaolinite, montmorillonite and palagonite in the 2.5-4.6 µm wavelength region; and spectrally discriminated these minerals based on characteristic

absorption features at ~3 µm. Michalski et al. (2006) linked spectral emission bands of clay minerals and clay mineral bearing rocks to crystal chemical properties. They also reported detection of poorly crystalline clay minerals in the 6-25 µm wavelength region with the thermal emission spectrometer (TES) on Mars that were previously not easily detectable in the VNIR and SWIR wavelength regions. Other researchers (Cooper and Mustard, 1999; Hecker et al., 2010; Johnson et al., 1998; Salisbury and D'Aria, 1992a, 1994; Salisbury et al., 1994) published spectral behavior of different minerals and discussed various issues related to spectral data acquisitions and interpretations. Among the clay science society, there is a growing interest in Fourier transform infrared (FTIR) spectroscopy, as it allows a rapid, economical and nondestructive method for investigating clay minerals (Petit, 2006).

The objectives in this chapter were to determine the potential of laboratory spectroscopy in the 2.5-14 µm wavelength region for detection, identification and quantification of clay minerals, thereby determining characteristic absorption features and their variation in clay mineral mixtures. Experimental investigations were carried out with the three clay minerals that were established to be crucial with respect to soil swelling and shrinkage characteristics. This study on pure clay minerals, and known mixtures of these clay minerals, aimed at an understanding of the manifestations of such clay minerals in natural soils. Emphasis was given to the 3-5 µm and 8-14 µm wavelength regions, to provide an outlook for a remote sensing implication.

5.2 Materials and Methods

5.2.1 Sample preparation

Experiments were conducted on pure clay minerals: montmorillonite, illite, kaolinite and their proportioned mixtures. The clay mineral specimens were commercially supplied by VWR international (https://www.vwrsp.com), as powders (particle size <2 µm). Mixtures were prepared at 20% by mass increments composing totals of 100 g. The specimens were weighted on a top loading precision balance (of ±1 g precision, model: Mattler PE 360), then poured into a porcelain mortar bowl and stirred by a spatula for about five minutes to homogenize the mixtures.

Spectral measurements were done on loosely packed, randomly oriented specimens. The spectra were acquired in the 2.5-14 µm wavelength region, using a Bruker Vertex 70 Fourier transform infrared spectrometer (http://www.brukeroptics.com). The spectrometer was equipped with an accessory mode integrating sphere, coated inside with a diffusely reflecting gold surface, which was attached to its external port. This enabled directional

hemispherical spectral reflectance measurements. With such a setup, Kirchhoff's law can be used to derive the directional spectral emissivity (Johnson et al., 1998; Salisbury and D'Aria, 1994). The spectrometer was configured to provide spectral reflectance with 4 cm^{-1} spectral resolution at 512 scans per each measurement and eight measurements per specimen, which were later averaged for a better signal to noise ratio. Referencing was done before each sample measurement against a gold-coated plate having the same surface as the inside wall of the integrating sphere. The spectrometer was continuously purged with nitrogen gas, to remove any water vapor and carbon dioxide from the system. Liquid nitrogen was used for cooling the detector. The OPUS spectroscopy software version 6.5 (Bruker Optik GmbH, 2007) in a desktop system which is integrated with the spectrometer was used for parameter setting and visualization of the acquired spectra.

5.2.2 Spectral analysis

Two approaches were followed to analyze the spectra of clay minerals. The first was an evaluation of the shape and intensity of the spectra, absorption features and the changes in absorption feature parameters such as the depth, position, width and area (Gaffey, 1986; Van der Meer, 1995, 2004a) relative to compositions of the mixtures. Second, a quantitative estimation of the compositions of mixtures from the spectra using a multivariate calibration technique, partial least squares (PLS) regression analysis (Shepherd et al., 2005; Viscarra Rossel et al., 2006; Waiser et al., 2007; Yitagesu et al., 2009b). The multivariate quantitative analyses were limited to the 3-5 µm and 8-14 µm wavelength regions.

The analyses were conducted on continuum removed spectra. A continuum is a mathematical function used to isolate specific absorption features (Clark and Roush, 1984). It corresponds to the background or overall albedo of the reflectance curve (Van der Meer, 2004a). The continuum can be calculated using straight lines, Gaussians and modified Gaussians, polynomials and splines (Clark and Roush, 1984; Fu et al., 2007; Sunshine et al., 1990; Van der Meer, 2004a). A classical continuum removal modeled by straight line segments tangential to the spectra (Clark et al., 1987; Clark and Roush, 1984; Van der Meer, 2004a) built in the ENVI software (ITT Visual Information Solutions, 2009) was used. ENVI uses an automated algorithm described by Clark et al. (1987) to find maximum tie points for fitting straight line segments and establish the continuum line, then remove the continuum by dividing it into the original spectrum. Van der Meer (2004) reported that continuum removal enhances all absorption bands including noise. Hence, careful selection of wavelength regions is essential. The continuum removal was done independently for the 3-5 µm and 8-14 µm wavelength regions, due to differences in spectral contrast.

5.2.3 Partial least squares regression analysis

PLS1 (Martens and Naes, 1989), built in The Unscrambler software (CAMO Process AS., 2005) was used to establish relationships among the spectra and clay mineral contents. The 3-5 µm and 8-14 µm wavelength regions were analyzed separately. Before the PLS regression analyses, the distributions of variables were checked, and appropriate transformations were carried out on variables that showed skewed distribution. As described by Martens and Naes (1989) and Wold et al. (2001), the data were mean centered and scaled to unit variance before calibration, for enhancing variance in the explanatory data and removing any systematic bias. A full cross validation method based on a leave one out principle was used to calibrate and validate the prediction models. PLS component selections were based on evaluation of residual and explained variances, and corresponding root mean square errors. Thus, factors with low residual variances accompanied with low root mean square errors were selected. The models performance was assessed by various statistics and graphical outputs, as outlined by Martens and Naes (1989). Coefficients of correlations (R) and coefficients of determinations (R^2) served to evaluate the goodness of fits. Expected prediction errors were assessed using the root mean square errors of predictions (RMSEP). Standard errors of performance (SEP), which were computed as the standard deviation of the residuals indicated the precision of the predictions over the whole samples. Bias showed interference errors and was computed as an average value of the variations that were not taken into account by the models. Offset showed the point where regression lines crossed the ordinate in the scatter plots, summarizing the relationship between measured and predicted values of the response variables, thus showed possible deviations from ideal one to one correspondences. Graphical outputs such as score plots, stability plots, scatter plots of X-Y relation outliers, and scatter plots of the measured versus predicted responses were also examined. These graphs were used to check sample distributions, identify samples causing perturbation, detect outliers and assess the nature of relationships among the predictors and responses such as deviation from linearity, and the quality of the regression models in terms of fitting the data respectively. Plots of B-coefficients were used to visualize significant wavelengths for predicting clay mineral contents. These coefficients were used to build model equations. Weighted coefficients B_{ow} and raw coefficients B were identical, because no weighting was applied on the variables.

5.3 Results

5.3.1 Spectral characteristics of the clay minerals

5.3.1.1 Montmorillonite, Illite, Kaolinite

The spectra of montmorillonite (Figure 5-1A), illite (Figure 5-1B), and kaolinite (Figure 5-1C) were well resolved in the 2.5-14 µm wavelength region. All spectra exhibited strong, broad absorption features in the 2.5-3.7 µm wavelength region, with absorption minima at ~2.75 µm and ~3.1 µm for montmorillonite and illite, being generally broader in the illite spectrum. The kaolinite spectrum showed asymmetric and sharply defined absorption minimum centered at ~2.75 µm.

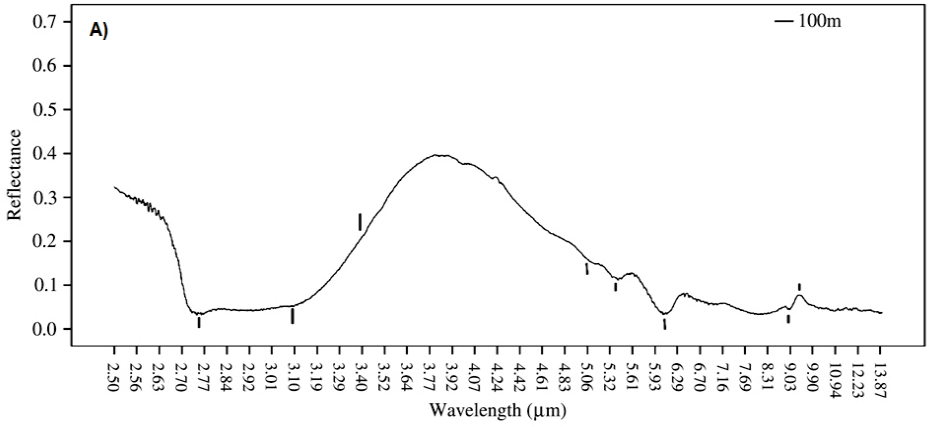

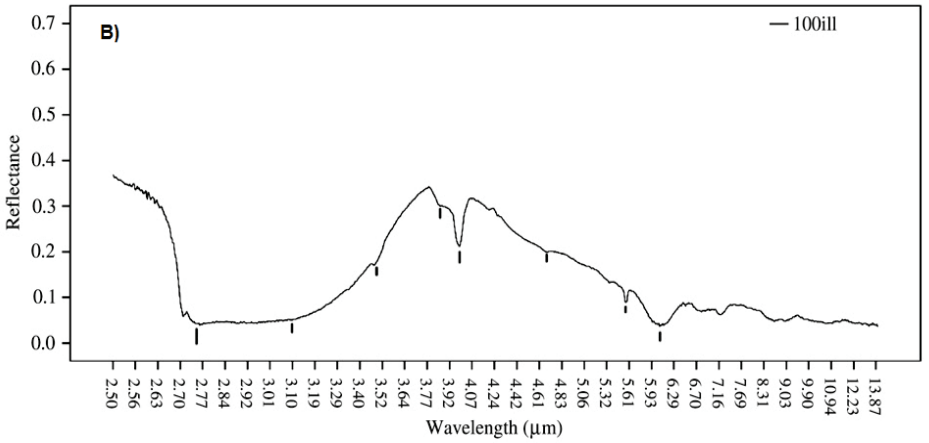

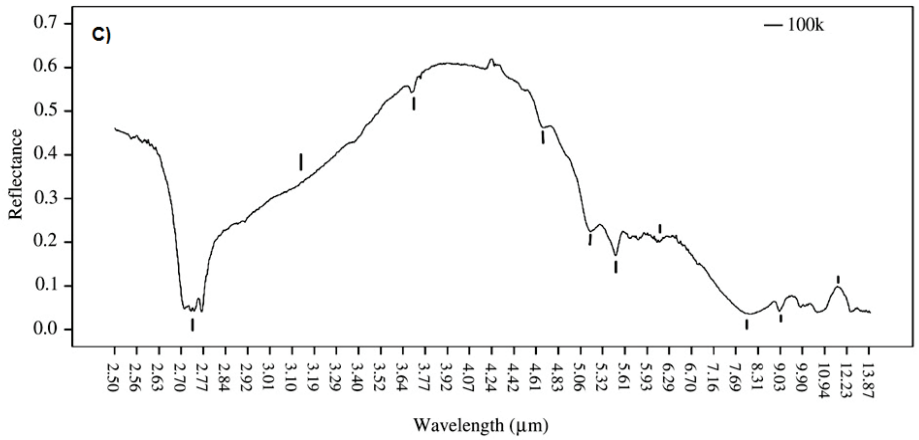

Figure 5-1 Spectrum of (A) montmorillonite, (B) illite and (C) kaolinite in the 2.5-14 µm wavelength region with characteristic spectral features annotated with lines.

The montmorillonite spectrum was further characterized by rounded doublet-like absorption features at ~5.1 µm and ~5.4 µm. The prominent absorption feature centered at ~6.1 µm, according to Farmer (1974) is typical of water bearing clay minerals and is associated with the bending vibrations of structural water molecules (Frost et al., 2001). Near 9.4 µm, montmorillonite exhibited reflectance maxima following an absorption feature at ~9 µm.

In the illite spectrum, weak absorption features were seen at ~3.48 µm and ~4.67 µm. The doublet with absorption minima at ~3.84 µm and ~3.98 µm was intense and sharp at the latter. The narrow, intense absorption feature at ~5.56 µm was followed by a broader absorption feature at ~6.1 µm.

A slight deep at ~3.69 µm and a doublet at ~5.2 µm and ~5.5 µm seemed to be diagnostic of kaolinite. In addition, the kaolinite spectrum showed weak absorption features at ~4.7 µm, ~8.6 µm, ~9.8 µm, ~10.6 µm and ~12.4 µm; and reflectance peaks at ~6.3 µm, ~9.4 µm and ~11.7 µm.

5.3.1.2 Mixtures of Montmorillonite and kaolinite

Overall spectral shapes and reflectance intensities of the spectra of montmorillonite, kaolinite and their mixtures exhibited characteristic differences (Figure 5-2). The absorption features at 2.5-3.7 µm varied with the montmorillonite/kaolinite ratio. The sharp, asymmetric absorption feature minimum at ~2.75 µm in kaolinite became poorly defined with increasing montmorillonite content. The absorption feature minimum at ~3.1 µm, which is typical of water bearing clay minerals (Farmer and Russell, 1964; Roush et al., 1987), subtly shifted to shorter wavelengths as kaolinite content increased. The weak absorption feature at ~3.69 µm in kaolinite gradually

disappeared with increasing montmorillonite content. The slopes of the spectra in the ~3-3.5 µm increased with the kaolinite content.

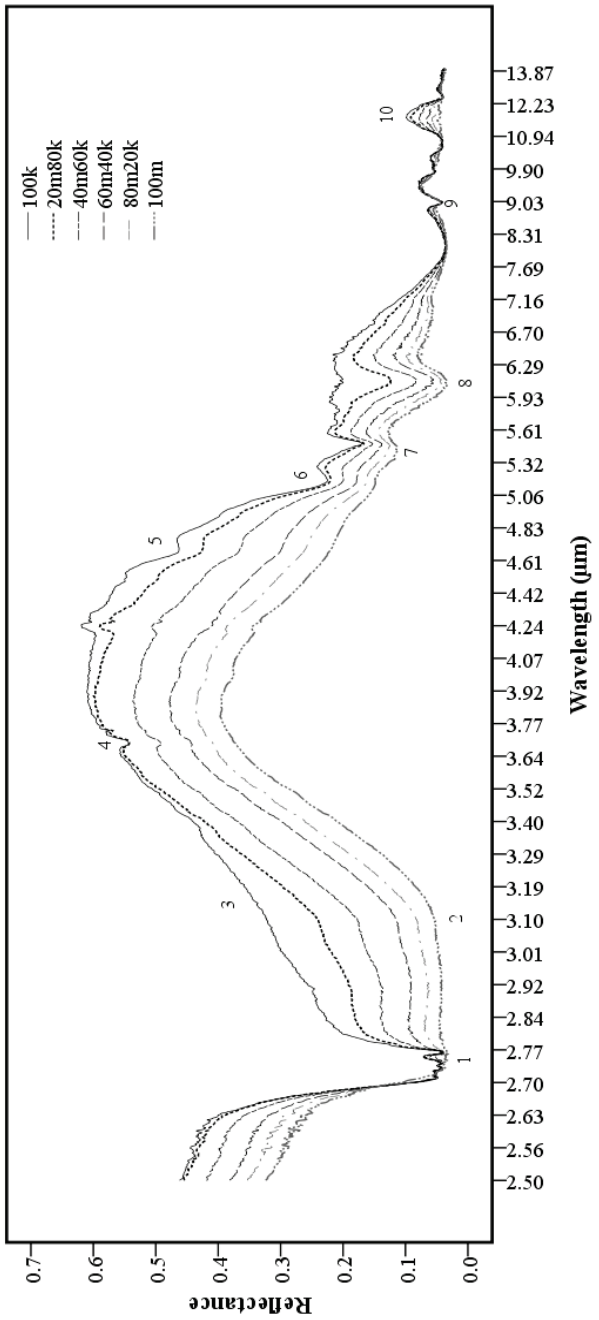

Figure 5-2 Spectra of montmorillonite, kaolinite and their mixtures, annotated with numbers, showing changes in characteristic spectral features among the spectra: (1) changes in absorption minima ~2.75 µm with changing montmorillonite/kaolinite ratio, (2) shifts in position ~3.1 µm, (3) slope differences in the 3-3.5 µm, (4) weak absorption feature ~3.69 µm and (5) ~4.7 µm for kaolinite disappearing with increased montmorillonite content, (6) doublet feature with minima at ~5.2 µm and ~5.5 µm for kaolinite, (7) changes in absorption features at ~5.1 µm and ~5.4 µm for montmorillonite, (8) changes in depth of the absorption feature at ~6.1 µm and (9) ~9 µm with changing montmorillonite/kaolinite ratio, and (10) differences in reflectance intensity at ~11.6 µm with increasing kaolinite content. (k= kaolinite, and m= montmorillonite with prefix numbers showing contents in percent).

Continuum removal enhanced the changes in absorption features in the 3-5 µm (Figure 5-3A) and 8-14 µm (Figure 5-3B) wavelength regions. The changes seemed to correspond to the montmorillonite/kaolinite ratio. While the depth of the absorption feature centered at ~3.1 µm increased with increasing montmorillonite content; its position shifted to the longer wavelengths. Similarly, the depth of the water molecule absorption feature at ~6.1 µm increased with increasing montmorillonite content. In a 100% kaolinite spectrum, the ~6.1 µm absorption feature entirely disappeared. On the other hand, its position slightly shifted towards longer wavelengths with increasing kaolinite content (Figure 5-3C). The doublet with minima at ~5.2 µm and ~5.5 µm in kaolinite became rounded and less pronounced with increasing montmorillonite content; and disappeared at <40% kaolinite. The rounded features in montmorillonite at ~5.1 µm and ~5.4 µm, subtly disappeared in the spectra of samples at high kaolinite contents. Additionally, the sharp absorption feature at ~9 µm slightly varied in depth, and the ~11.6 µm reflectance intensity increased with increasing kaolinite content.

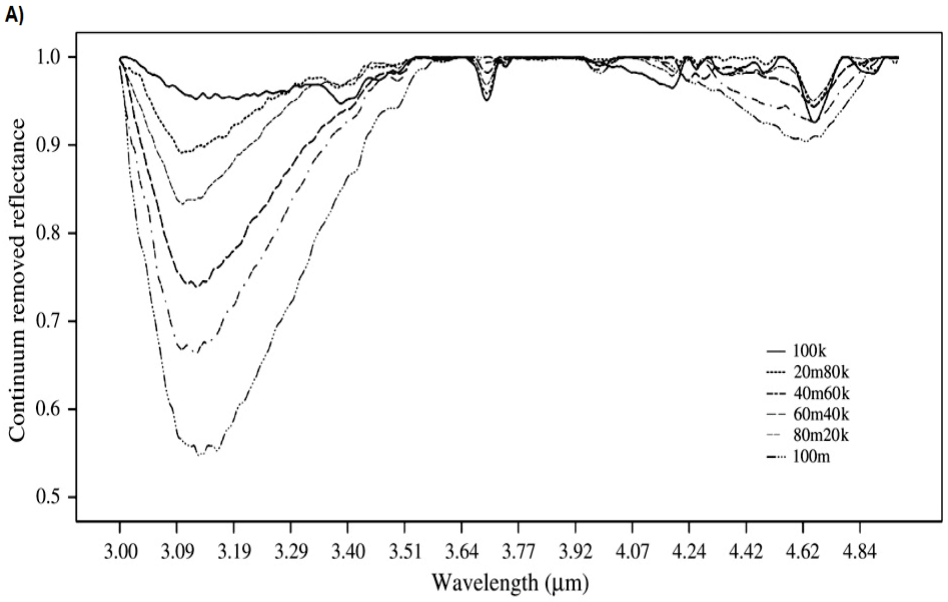

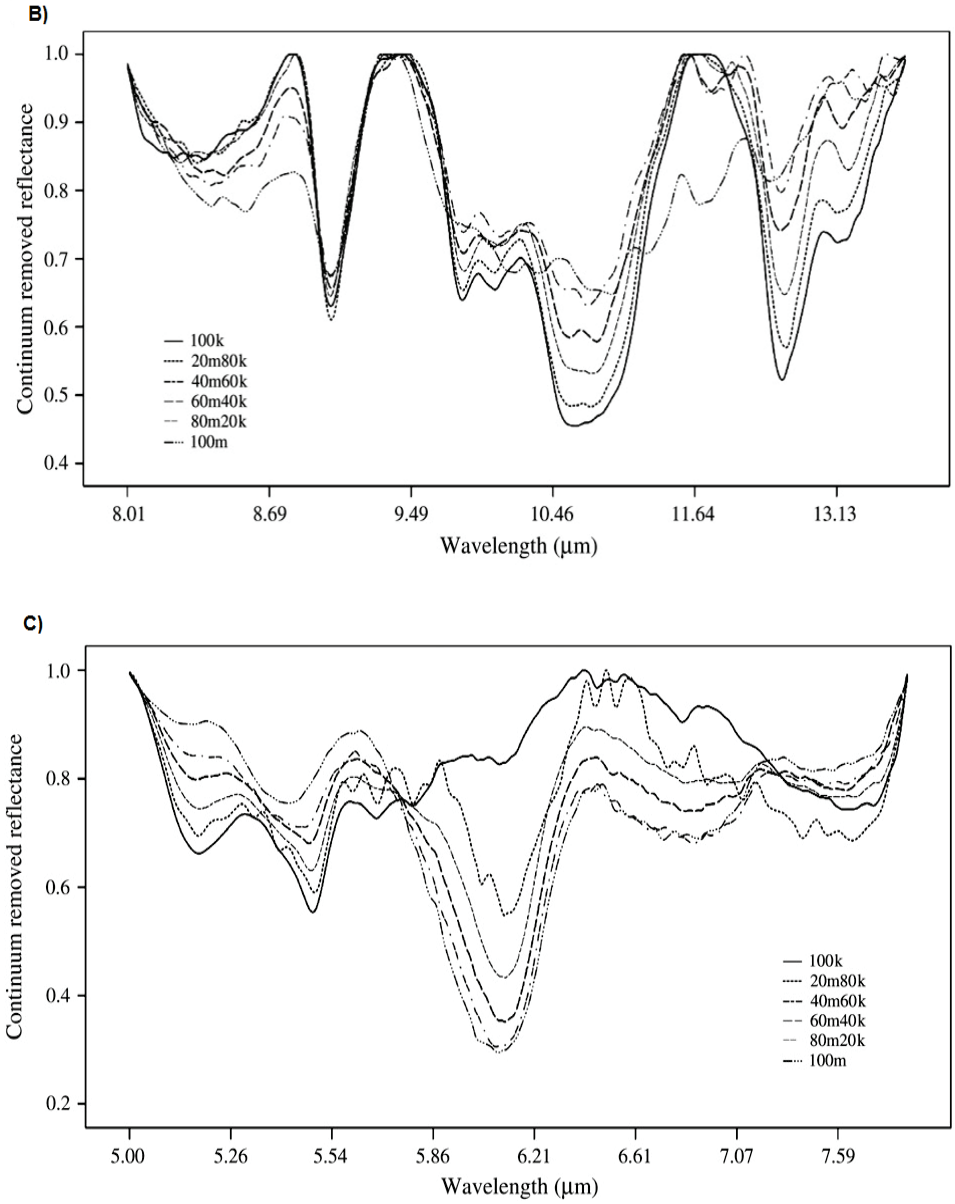

Figure 5-3 Continuum removed spectra of montmorillonite, kaolinite and their mixtures, showing variations in absorption features corresponding to changes in mineral contents: at the (A) 3-5 µm, (B) 8-14 µm and (C) 5-8 µm wavelength regions. Note the changes in absorption features centered at (A) ~3.1 µm, (B) ~8.5 µm, 10.6 µm and ~12.4 µm to ~13.5 µm, (C) ~6.1 µm; also differences in sharpness and depth intensity of doublet feature with minima at ~5.2 µm and ~5.5 µm for kaolinite (k= kaolinite, and m= montmorillonite with prefix numbers showing contents in percent).

5.3.1.3 Mixtures of illite and kaolinite

The spectra of illite, kaolinite and their mixtures differed in overall shapes and reflectance intensities (Figure 5-4). The absorption features at 2.5-3.7 µm varied with changes in the mineralogical compositions. The sharp absorption minimum at ~2.75 µm became poorly defined with increasing illite content. The slopes of the spectra at ~3-3.5 µm progressively increased with increasing kaolinite content.

Continuum removal of the spectra in the 3-5 µm wavelength region (Figure 5-5A) enhanced differences in depth and position of the feature at ~3.1 µm. While the depth of this feature increased with increasing illite content, its position shifted to the longer wavelengths. The weak absorption feature at ~3.48 µm for illite diminished with increasing kaolinite content. The modest feature in the kaolinite spectrum at ~3.69 µm disappeared at <80% kaolinite. Depth of the doublet features at ~3.84 µm and ~3.98 µm in the illite containing samples spectra decreased with increasing kaolinite content. Depth of the narrow absorption feature at ~5.56 µm for illite also lessened with decreasing illite content. The doublet features in the kaolinite spectrum gradually disappeared with increasing illite content and was absent at illite content of >60%. Depth of water molecule absorption feature at ~6.1 µm decreased with increasing kaolinite content (Figure 5-5C). This decrease in depth intensity was accompanied with a shift of the position towards longer wavelengths.

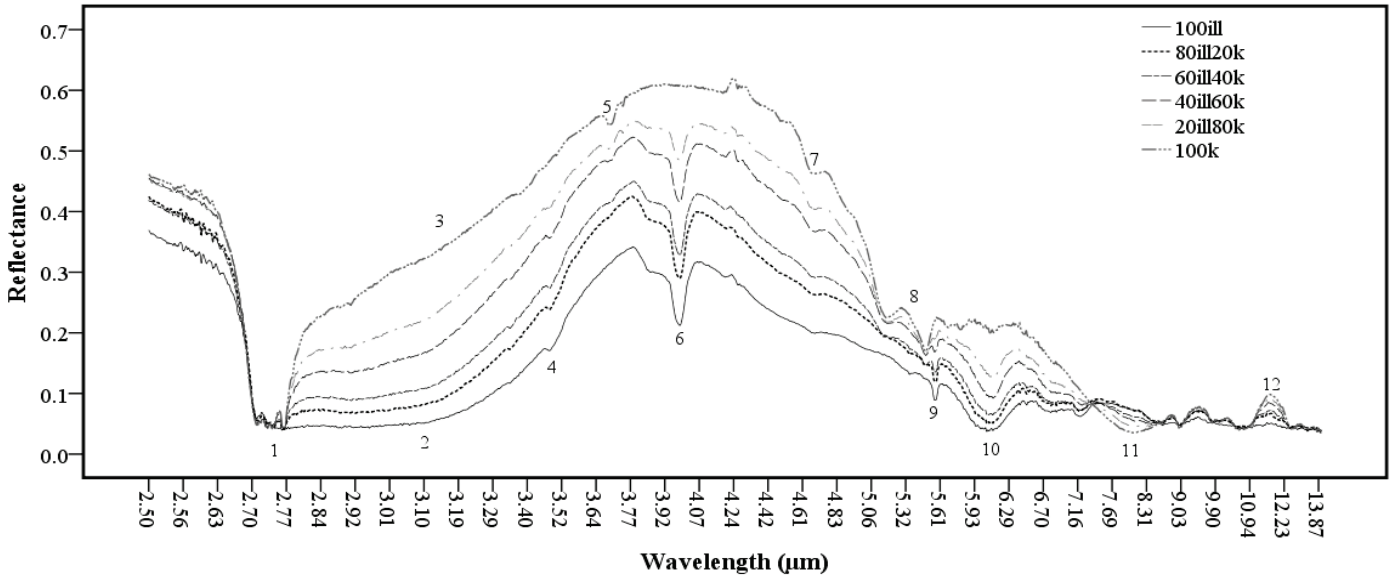

Figure 5-4 Spectra of illite, kaolinite and their mixtures, annotated with numbers, showing characteristic spectral differences: (1) changes in absorption minima at ~2.75 µm, (2) shifts in position at ~3.1 µm, (3) slope differences at 3-3.5 µm, (4) the weak absorption feature at ~3.48 µm for illite that disappeared in the spectra of samples with high kaolinite content, (5) the modest absorption feature at ~3.69 µm for kaolinite that disappeared in the spectra of samples at <80% kaolinite, (6) changes in depth intensity of the doublet feature at ~3.84 µm and ~3.98 µm for illite, (7) the weak absorption feature at ~4.7 µm for kaolinite that disappeared as illite content increased, (8) the doublet for kaolinite that gradually diminished in the spectra of samples with high illite content, (9) changes in depth of the narrow absorption feature at ~5.56 µm for illite, (10) changes in depth of the absorption feature at ~6.1 µm (11) variations in reflectance intensity at ~8.10 µm and (12) ~11.6 µm, with changing illite/kaolinite ratio. (k= kaolinite and ill= illite with prefix numbers showing contents in percent).

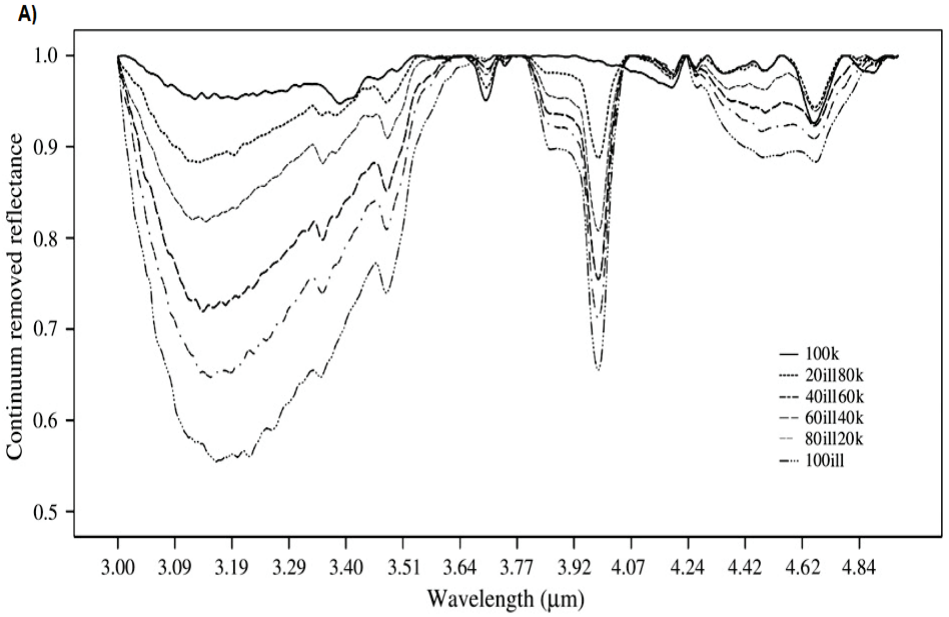
A)
Continuum removed reflectance
1.0
0.9
0.8
0.7
0.6
0.5
3.00 3.09 3.19 3.29 3.40 3.51 3.64 3.77 3.92 4.07 4.24 4.42 4.62 4.84
Wavelength (µm)
100k
20ill80k
40ill60k
60ill40k
80ill20k
100ill

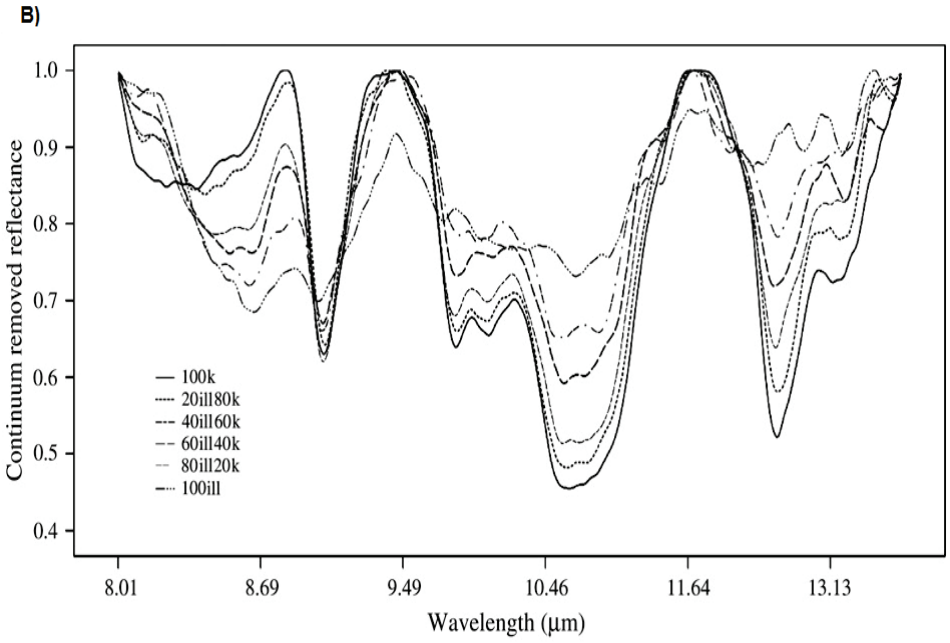
B)
Continuum removed reflectance
1.0
0.9
0.8
0.7
0.6
0.5
0.4
8.01 8.69 9.49 10.46 11.64 13.13
Wavelength (µm)
100k
20ill80k
40ill60k
60ill40k
80ill20k
100ill

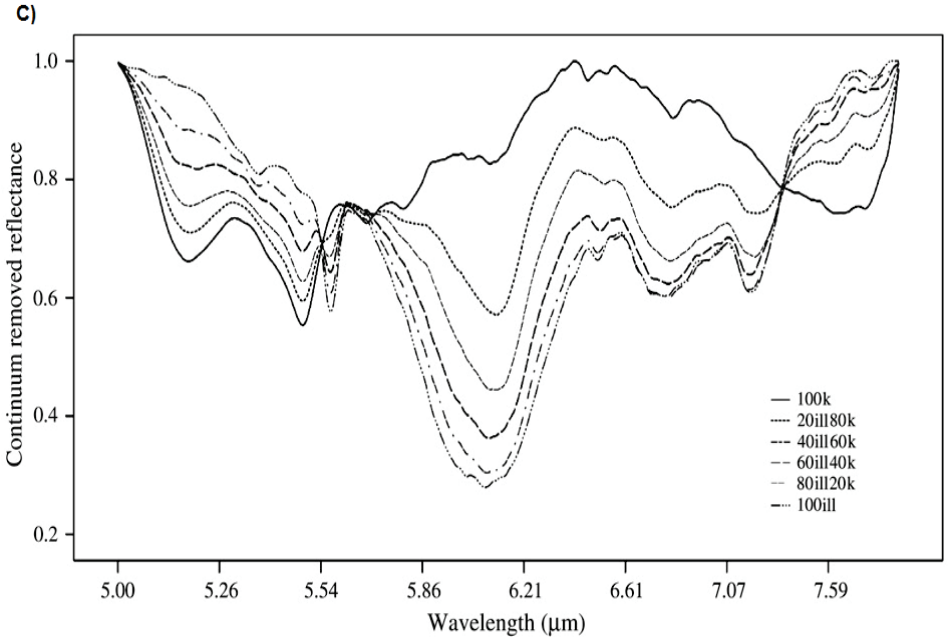

Figure 5-5 Continuum removed spectra of illite, kaolinite, and their mixtures showing variations of absorption features relative to changes in compositions of the mixtures: in the (A) 3-5 µm, (B) 8-14 µm and (C) 5-8 µm wavelength regions. Note the changes at the features centered (A) ~3.1 µm, (B) ~8.5 µm, 10.6 µm, ~12.4 µm to ~13.5 µm, and (C) ~6.1 µm. The doublet for kaolinite became rounded at high illite contents. The narrow, intense absorption feature at ~5.56 µm for illite subtly decreased as kaolinite content increased. (k= kaolinite and ill= illite with prefix numbers showing contents in percent).

5.3.1.4 Mixtures of montmorillonite and illite

The spectra of montmorillonite and illite overlapped at the water absorption features centered at ~3.1 µm and ~6.1 µm. The positions of these absorption features subtly varied with changing montmorillonite/illite ratio. Both features became broad with increasing illite content (Figures 5-6 and 5-7A).

The spectra of montmorillonite containing samples showed rounded doublet-like absorption features at ~5.1 µm and ~5.4 µm. The spectra of illite containing samples showed modest deeps at ~3.48 µm, doublets with absorption minima at ~3.84 µm and ~3.98 µm, and narrow, intense absorption features at ~5.56 µm. Depth intensities of the doublets with absorption minima at ~3.84 µm and ~3.98 µm, and the narrow absorption features at ~5.56 µm decreased with decreasing illite content. Both absorption features consistently appeared in the presence of illite. Therefore, they were prominent features to differentiate illite from montmorillonite.

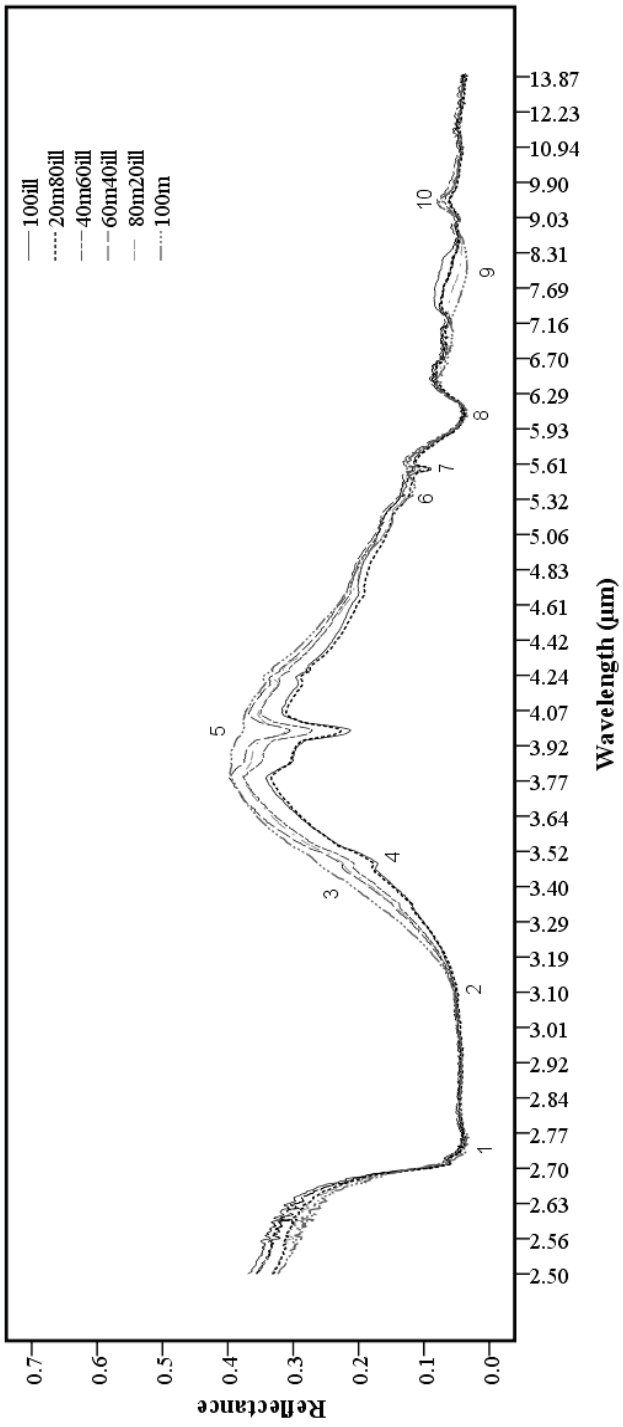

Figure 5-6 Spectra of illite, montmorillonite, and their mixtures, annotated with numbers, showing characteristic spectral differences with changing montmorillonite/illite ratio: (1) changes in absorption minima at ~2.75 µm, (2) subtle shifts in position to longer wavelengths of the ~3.1 µm with increasing illite content, (3) slope differences at 3-3.5 µm, (4) variations in the weak absorption feature at ~3.48 µm for illite, (5) variations in depth of the doublet at ~3.84 µm and ~3.98 µm for illite, (6) changes in the rounded features for montmorillonite at ~5.1 µm and ~5.4 µm, (7) changes in the narrow, intense absorption feature at ~5.56 µm with decreasing illite content, (8) faint variations in position and depth of the absorption band at ~6.1 µm, (9) differences in reflectance intensity at ~8.10 µm and (10) at ~9.4 µm with changing montmorillonite/illite ratio. (m= montmorillonite and ill= illite with prefix numbers showing contents in percent).

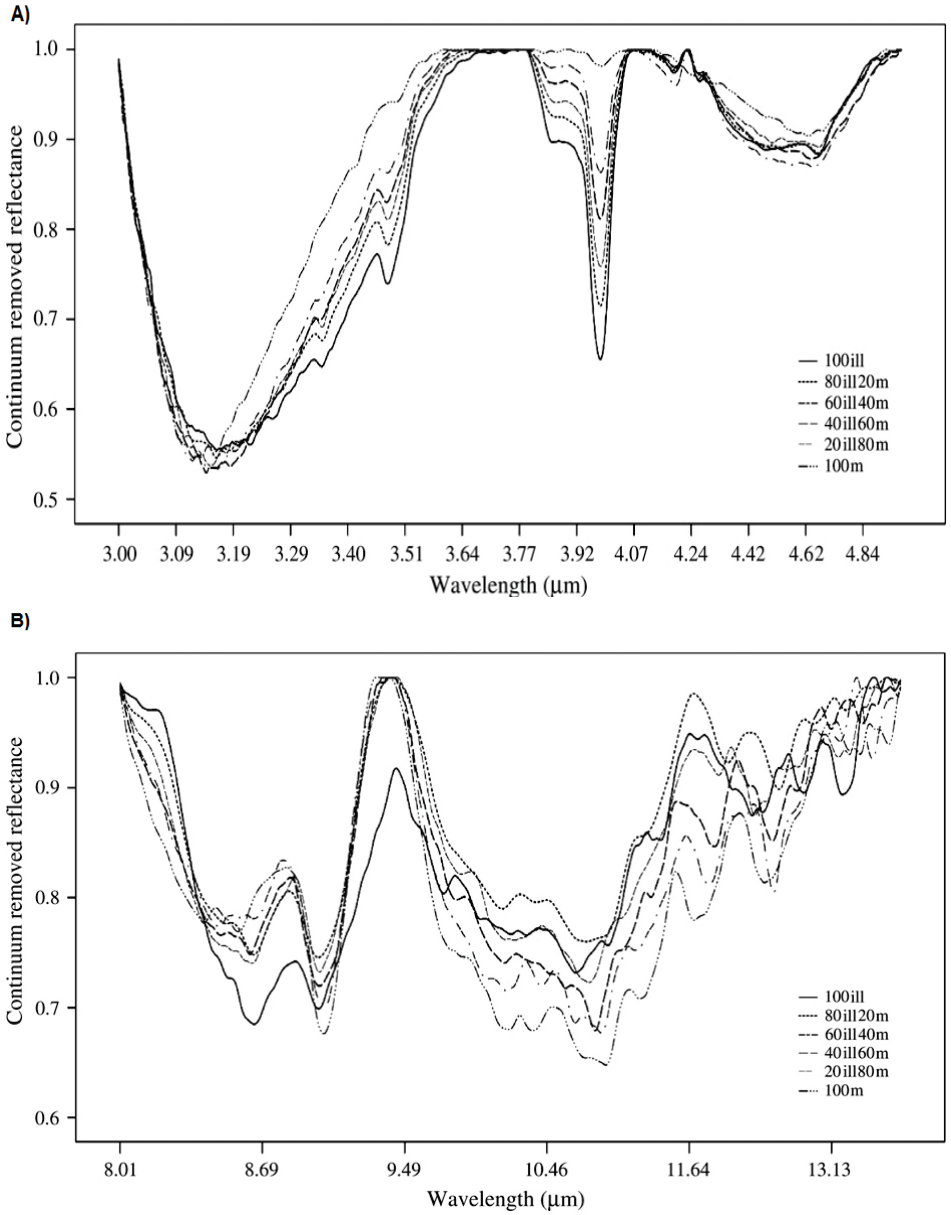

Figure 5-7 Continuum removed spectra of montmorillonite, illite and their mixtures, showing changes in spectral characteristics: in the (A) 3-5 µm and (B) 8-14 µm wavelength regions. The depth of the water absorption feature at ~3.1 µm increased subtly accompanied with slight shifts of positions to shorter wavelengths as montmorillonite content increased. Conversely, as the illite content increased the depth intensity of this band slightly decreased associated with shifts in positions towards longer wavelengths. (m= montmorillonite and ill= illite with prefix numbers showing contents in percent).

5.3.2 Estimation of clay mineral contents

Pair-wise correlation analyses showed that the mean reflectance in the 2.5-14 µm wavelength region were strongly correlated to the clay mineral compositions at 0.01 significance levels. The clay mineral compositions in montmorillonite-kaolinite, illite-kaolinite, and montmorillonite-illite mixtures were negatively related to the mean reflectance at Pearson correlations of -0.99, -0.98 and -0.90, respectively. These correlations indicated that absorption features and clay mineral compositions are linearly related. The correlation in the montmorillonite-illite mixtures was lower than for montmorillonite-kaolinite and illite-kaolinite mixtures. This is probably due to the similar structure of the two water bearing clay minerals, which might in turn, determine their spectral characteristics.

Significant wavelengths for estimating the contents of montmorillonite and illite from the spectra of montmorillonite-kaolinite (Figures 5-8A and 5-8B), illite-kaolinite (Figures 5-8C and 5-8D), and montmorillonite-illite (Figures 6-8E and 6-8F) mixtures are presented for the 3-5 µm and 8-14 µm wavelength regions.

Table 5-1 shows: the correlation coefficients, root mean square error of the predictions (RMSEP), standard error of performances (SEP), biases and offsets. Much of the variation in the clay mineral compositions was explained by the PLS models. A better agreement was achieved at 3-5 µm wavelength region than at 8-14 µm. The relation was weaker, particularly for the montmorillonite-illite mixtures, where the coefficient of correlation was lower, and the model error terms were higher (Table 5-1) than those obtained for montmorillonite-kaolinite and illite-kaolinite mixtures.

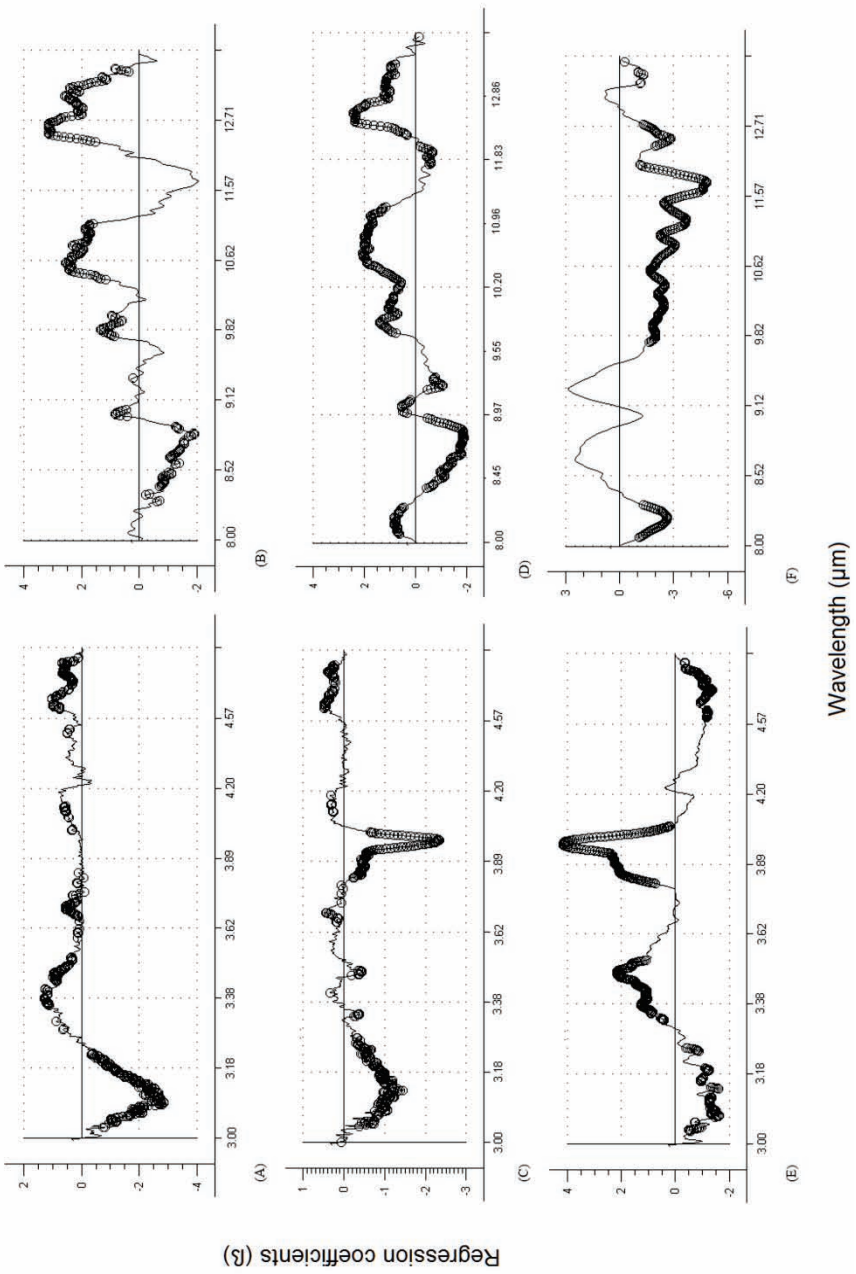

Figure 5-8 PLS regression analyses results for estimating clay mineral contents from spectra of montmorillonite-kaolinite mixtures in the wavelength regions (A) 3-5 µm and (B) 8-14 µm; illite-kaolinite mixtures in the wavelength region (C) 3-5 µm and (D) 8-14 µm; montmorillonite-illite mixtures in the wavelength region (E) 3-5 µm and (F) 8-14 µm. Statistically significant regression coefficients (wavelengths) are highlighted in black circles.

5.4 Discussion

Montmorillonite, illite, kaolinite, and their mixtures showed spectrally distinct characteristics such as absorption features. The overall shape and reflectance intensity of the spectra and absorption features varied with the clay mineral contents. Thus, as described by Clark and Roush (1984), Gaffey (1986) and Van der Meer (1995 and 2004) these spectral changes were effective measures of compositions of the mixtures.

The strong absorption feature in the 2.5-3.7 µm wavelength region, in the spectrum of montmorillonite (Figure 5-1A), exhibited minima at ~2.75 µm and ~3.1 µm. Hunt (1977) assigned the absorption feature at ~2.75 µm to fundamental vibrations of hydroxyl groups, at ~2.9 µm to asymmetric stretching of hydroxyl groups, at ~3 µm to overtone bending vibrations of water molecules, and the feature at ~3.1 µm to asymmetric stretching vibration of H-O of the water molecules. The overlapping vibrations of structural hydroxyl groups and water molecules (Farmer, 1974) broadened absorption features in the illite spectrum (Figure 5-1B). In kaolinite, the asymmetric stretching of hydroxyl groups (Farmer, 1974; Farmer and Russell, 1964) produced a deep and narrow absorption feature centered at ~2.75 µm (Figure 5-1C). Changes took place when montmorillonite and kaolinite were heated (Roush et al., 1987). The ~2.75 µm feature became narrower in montmorillonite due to loss of structurally adsorbed water molecules. Little changes occurred in kaolinite spectrum due to the absence of water molecules. The wide absorption feature exhibited in the illite spectrum can be associated with the substitution of Al for Si (Yong and Warkentin, 1975). The absorption features at ~3.1 µm and ~6.1 µm were prominent in the spectra of montmorillonite and illite containing samples (Figures 5-2, 5-3A, 5-3C, 5-4, 5-5A, 5-5C, 5-6, and 5-7A), due to the similar structure of these clay minerals (Brigatti et al., 2006). The intensity (in depth, width, area etc.) of these absorption features decreased with increasing kaolinite contents in montmorillonite-kaolinite (Figures 5-3A and 5-3C) and illite-kaolinite (Figures 5-5A and 5-5C) mixtures. This strong, negative relationship between the kaolinite content and intensity of these absorption features is attributed to lack of water molecules in kaolinite. In the PLS regression models, the significant, opposite contributions of the wavelength region between 3 and 3.2 µm in montmorillonite-kaolinite (Figure 5-8A), montmorillonite-illite (Figure 5-8E) and illite-kaolinite (Figure 5-8C) mixtures were similarly attributed to differences in structure and water molecules among the clay minerals.

Concerning the structural hydroxyl groups coordinated to the octahedral cations (Brigatti et al., 2006; Gillot, 1987), substitution of cations can shift the position of absorption features (Farmer, 1974). This probably explains the shifts in positions of absorption features in the clay mineral mixtures as

suggested by Van der Meer (1995) as shifts in positions are characteristics of cation substitutions. Therefore, shifts in the absorption feature positions, in the spectra of montmorillonite-illite mixtures (Figure 5-6 and 5-7A) are probably related to reorientation of the hydroxyl groups, due to substitution of Fe and Mg for Al, or Al for Si (Farmer and Russell, 1964; Yong and Warkentin, 1975). The broad absorption feature centered at ~3.1 µm in the spectra of samples with illite might be further associated with distortion in the structure to accommodate longer bonds resulting from replacement of Al for Si (Farmer and Russell, 1964; Yong and Warkentin, 1975). Illite exhibited distinct doublet absorption features at ~3.84 µm and ~3.98 µm. The unique presence of this doublet in all spectra of illite containing samples (Figures 5-4, 5-5A, 5-6 and 5-7A) and the narrow, intense absorption feature at ~5.56 µm, which also appeared in the presence of illite can be considered diagnostic features. These features and the weak absorption feature at ~3.48 µm were significant PLS regression coefficients in estimating illite contents from mixtures of illite-kaolinite (Figure 5-8C) and illite-montmorillonite (Figure 5-8E).

Table 5-1 Summary of the models performance, showing correlation coefficients in the 3-5 µm and 8-14 µm wavelength regions with corresponding RMSEP, SEP, Bias and offsets. Better agreement was achieved at 3-5 µm than in the 8-14 µm wavelength region.

Wavelength regions	Clay mineral mixtures	Correlation coefficients	RMSEP	SEP	Bias	Offset
3-5 µm	Montmorillonite-Kaolinite	0.99	3.46	3.79	-0.12	2.96
8-14 µm	Montmorillonite-Kaolinite	0.96	10.86	11.56	-2.58	9.07
3-5 µm	Illite-Kaolinite	0.99	2.11	2.29	0.26	-0.46
8-14 µm	Illite-Kaolinite	0.99	4.08	4.46	-0.34	3.78
3-5 µm	Montmorillonite-Illite	0.99	2.87	3.13	-0.28	-0.37
8-14µm	Montmorillonite-Illite	0.90	15.33	16.33	3.61	15.05

As established by many experts (Clark, 1999; Farmer and Russell, 1964; Frost et al., 2001; Michalski et al., 2006), the 8-14 µm wavelength region is dominated by absorption features resulting from SiO, hydroxyl and metal-hydroxyl vibrations. Michalski et al. (2006) reported that clay minerals exhibited absorption features centered in the 9-10 µm wavelength region, due to the SiO stretching vibration. They assigned absorption features in the 10-14 µm wavelength region to metal-hydroxyl bending vibrations. Frost et al. (2001) associated the features at ~8-10 µm wavelength region with the SiO stretching and those at ~ 10-14 µm with hydroxyl groups bending vibrations. Farmer and Russell (1964) similarly assigned wavelength regions of 8-10 µm to (Al, Si)-O stretching vibrations in the tetrahedral sheets, and

those of 10-14 µm to the hydroxyl and metal-hydroxyl bending vibrations in the octahedral sheets. The spectra of the clay minerals investigated here showed a sharp absorption feature near 9 µm, which is probably due to the SiO stretching vibration. However, this absorption feature seems to be not a diagnostic feature because it showed overlapping features of kaolinite and montmorillonite, while it appeared shallower, with its shoulder shifted to the longer wavelength in the illite spectrum. The appearance of this feature in illite might also be influenced by distortion in structure caused by substitution of Al for Si that shifts the positions to longer wavelengths (Farmer and Russell, 1964; Michalski et al., 2006). Other absorption features centered at ~8.6 µm, ~10.6 µm and ~12.4 µm showed significant variations that seemed to correspond to changes in mineralogical composition (Figures 5-3B, 5-5B and 5-7B). Thus, they were useful in discriminating the clay minerals as well as in estimating content of the clay minerals in the mixtures (Figures 5-8B, 5-8D and 5-8F). The features at ~10.6 µm and ~12.4 µm appeared strong and well-structured in the presence of kaolinite (Figures 5-3B and 5-5B) probably due to higher contents of aluminum relative to the other cations in the octahedral sites (Brigatti et al., 2006; Farmer and Russell, 1964).

Overall, the variation in spectral characteristics of the clay mineral mixtures was largely due to differences in mineralogical compositions. The absorption features were strong and diagnostic, thus enabled a clear differentiation of the clay minerals. The presented experimental data and results are seen useful to comprehend presence of clay minerals in expansive soils, and thereby making rational spectral-compositional analysis and correlations.

5.5 Conclusions

In this chapter, the potential of laboratory spectroscopy in the 2.5-14 µm wavelength region was investigated for clay mineralogical characterization (detecting, identifying and quantifying abundances). Pure clay minerals and their proportioned mixtures were analyzed to determine characteristic spectral features. The clay minerals and mixtures exhibited distinct spectral characteristics. Reflectance and spectral contrast differed in the 3-5 µm and 8-14 µm wavelength regions being higher in the former, but generally low in the latter. The PLS prediction models showed that much of the variations in clay mineralogical compositions can be accounted for by spectral features. Significant wavelengths that appeared diagnostic in differentiating the clay minerals were identified. For all the mixtures, the 3-5 µm wavelength region was more suited than the 8-14 µm. The 5-8 µm wavelength region also provided valuable spectral differences among the clay minerals and mixtures. In summary, apart from furthering the knowledge and understanding of the spectral characteristics of clay minerals, the approach demonstrated the pragmatic implication that laboratory spectroscopy in the 2.5-14 µm wavelength region is a useful technique for characterizing clay minerals.

Chapter 6*

Soil spectral and geotechnical characteristics in the 3-5 µm wavelength region

Abstract: Soil expansiveness can cause substantial economic loss and increase in cost of constructions, which often exceeds the initial budget estimate or allocated funding for projects. Simple identification of expansive soils and evaluation of their geotechnical characteristics is a constant focus of research in geotechnical engineering, including the application of spectroscopic techniques. The potential of laboratory spectroscopy in the 3-5 µm wavelength region was investigated for compositional analyses and classification of expansive soils into different swelling and shrinkage potential categories. Spectra of bulk and fine fraction (passing through the ASTM 0.075 mm sieve aperture) soil samples were analyzed. Relationships among soil spectra and plasticity classes were examined using various statistical analyses techniques such as cluster analysis, cross tabulation and non-parametric statistical measures of associations. Classification of soils based on their spectral characteristics showed significant correlations with the soils plasticity classes. Significant chi-square test statistics, likelihood ratio, Cramer's V and contingency coefficients were found. Additionally, statistically highly significant lambda, Goodman and Kruskal tau, and uncertainty coefficients were obtained. The correlations varied from bulk to fine soil fraction. A higher level of agreement with plasticity was achieved for spectra of fine fraction soils than for bulk soil samples. Overall, the results ascertained that spectroscopy in the 3-5 µm wavelength region is capable of providing additional useful information for geotechnical Characterization of expansive soils.

Keywords: expansive soils, geotechnical characteristics, plasticity, soil spectra, 3-5 µm.

* This chapter is based on:

Yitagesu, Fekerte Arega, Van der Werff, H., Van der Meer, F.D, and Hecker, C., 2012, On the relationships between plasticity and spectral characteristics of Expansive soils: the 3-5 µm wavelength region: Applied clay science (accepted with minor corrections).

6.1 Introduction

Soil swelling and shrinkage potential largely determines engineering use of soils, either as a foundation or construction material that soils can be used as subgrade, embankment fill, binder for bases etc. This essential geotechnical characteristics of soils is primarily due to the presence of active clay minerals in soils (Al-Rawas, 1999; Allbrook, 1985; Chen, 1988; Skempton, 1984; Wan et al., 2002) that have got a high inherent affinity to water molecules. Thus, clay mineralogical composition analysis is fundamental in soil geotechnical investigation. As mentioned in the previous chapters, conventional soil geotechnical testing requires dense sampling, and sophisticated in-situ and laboratory testing procedures. Consequently, they are time consuming, labor intensive, and often prohibitively expensive. Therefore, despite the variability of soil geotechnical characteristics over short distances, limited numbers of samples are normally utilized. Results from limited number samples, accompanied with expert deduction and simple interpolation will then be used for estimating soil properties in sites where samples were not taken. To provide with a better representation of the variability and thereby reduce design and construction risks associated with changing site conditions, a simple, rapid, inexpensive yet reliable soil geotechnical characterization tool is highly sought for. In this respect, spectroscopic techniques have got wide realization for they allow the aforementioned apart from being non-destructive (Chabrillat et al., 2002; Kariuki et al., 2004; Yitagesu et al., 2011a; Yitagesu et al., 2009b). Furthermore, several soil properties can be estimated from a single soil spectrum (Stenberg et al., 2010; Viscarra Rossel et al., 2006; Yitagesu et al., 2009b).

Researchers in soil science established the potential applicability of spectroscopic techniques for qualitative as well as quantitative characterization of soils and soil properties. The visible-near infrared (VNIR) and short wave infrared (SWIR) wavelength regions were extensively explored for predicting various soil properties including clay content and mineralogical composition analyses (Bendor et al., 2002; Chabrillat et al., 2002; Kariuki et al., 2004; Stenberg et al., 2010; Viscarra Rossel et al., 2006). Clay mineralogical composition is indispensable towards understanding the geotechnical behavior (Chen, 1988; Vaught et al., 2006; Yitagesu et al., 2011b; Yong and Warkentin, 1975) as well as spectral characteristics of expansive soils (Chabrillat et al., 2002; Kariuki et al., 2004; Yitagesu et al., 2008a; Yitagesu et al., 2009a; Yitagesu et al., 2009b, 2011c; Yitagesu et al., 2008b), providing a unique opportunity to derive soil geotechnical information from their respective spectra. Advances in remote sensing techniques enabled discrimination of clay minerals that cause expansion and shrinkage in soils; and mapping their abundance. Again, the VNIR and SWIR wavelength regions were successfully used to identify (Chabrillat et al., 2002; Kariuki et al., 2004), characterize and map

(Bourguignon et al., 2007; Chabrillat et al., 2002; Yitagesu et al., 2009b) expansive soils.

The potential of laboratory spectroscopy for compositional analysis of geologic materials in the mid infrared (MIR) wavelength region has also been demonstrated (Boyd and Petitcolin, 2004; Bras and Erard, 2003; Farmer and Russell, 1964; Salisbury and D'Aria, 1994; Salisbury and Eastes, 1985). Better performance of the MIR over the VNIR and SWIR wavelength regions was reported by Viscarra Rossel et al. (2006). They scrutinized the suitability of the MIR wavelength region for quantifying soil properties such as pH, organic carbon, and sand, silt and clay contents; and reported strong correlations. They attributed what they call “superior performance” of MIR wavelength region with the high intensity and specific nature of spectral bands of materials in this wavelength region. However, the MIR wavelength region was not investigated for characterizing expansive soils.

Recently, Yitagesu et al. (2011) determined spectral characteristics of active clay minerals that dictate soil swelling and shrinkage potential; and established the potential of laboratory spectroscopy in MIR wavelength region for discriminating these clay minerals. They also quantified clay mineral contents from prepared mixtures. Their analysis on pure clay minerals and mixtures provided with essential knowledge on the spectral characteristics of active clay minerals that influence soil expansiveness. The objective in this chapter was to determine spectral characteristics of expansive soils, for analyzing soil mineralogical compositions. The soils were classified using their respective spectral characteristics in the 3-5 µm wavelength region. The classifications were then statistically compared to the soils plasticity classes (from the unified soil classification system). Spectra of bulk and fine fractions of similar soil samples were examined independently.

6.2 Materials and methods

6.2.1 Geotechnical data acquisition

In this chapter, soil samples collected from the newly planned expressway route connecting the city of Addis Ababa with the town of Nazret were used. Forty randomly selected soil samples, located in Figure 6-1 were analyzed.

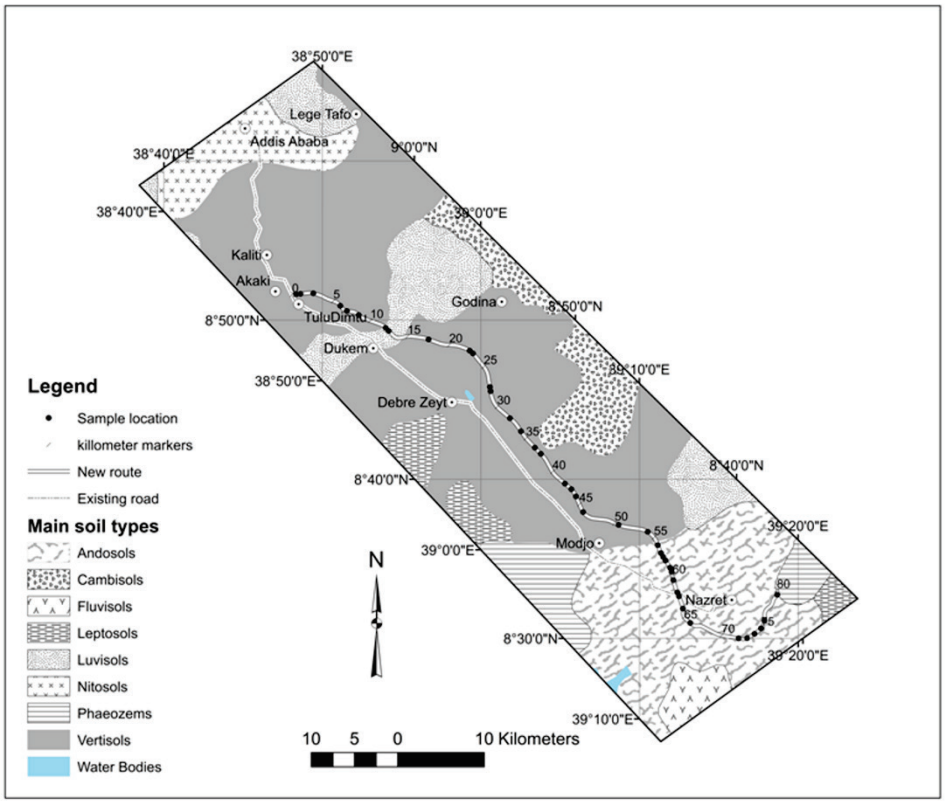

Figure 6-1 location map showing the location of 40 soil samples used in this chapter.

Identification and evaluation of the soils swelling and shrinkage characteristics was based on consistency limit tests. Geotechnical tests were conducted in accordance with the procedures described in chapter three, section 3.2.2. The soils were then classified in accordance with the unified soil classification system (USCS), ASTM D2487-10 standard practice for classification of soils for engineering purposes. Protocols for determining the mineralogical compositions, oxides and organic matter contents of the soil samples are outlined in chapter three, section 3.2.3.

6.2.2 Spectral data acquisition and processing

The soils spectra were acquired using a Bruker Vertex 70 Fourier transform infrared (FTIR) spectrometer. Chapter five, section 5.2.2 provided a detailed description of the spectrometer, configuration such as number of scans, resolution and software.

The soil samples were prepared in bulk and fine fraction (passing through the ASTM 0.075 mm sieve aperture). The ASTM 0.075 mm sieve represents the smallest commonly used practical sieve for particle size distribution analysis

of soils for most geotechnical applications (e.g., road construction). This fine fraction often consists of clay particles (Carter and Bentley, 1991), which are characterized by large specific surface area and high water affinity (Ross, 1978; Vaught et al., 2006; Yong and Warkentin, 1975). Hence, it substantially influences soil physicochemical characteristics (Chen, 1988). McCormack and Wilding (1975) published strong correlations between soil swelling potential and fine fraction. Vaught et al. (2006) on their part, showed significant correlation between COLE and soil fine fraction.

Soil spectral measurements were carried out on air-dried, loosely packed, randomly oriented samples. Spectroscopic interpretation was based on evaluation of the overall shapes and changes in characteristic absorption features (Gaffey, 1986; Van der Meer, 2004a). Continuum removal was applied to the spectra for enhancing differences in absorption features. For details of continuum removal, refer to chapter five, section 5.2.2.

6.2.3 Statistical analysis

Statistical analyses are useful to extract meaningful information for understanding spectral characteristics of soils and establishing correlations with various soil properties (Cloutis, 1996; Haaland and Thomas, 1988; Kariuki et al., 2004; Van der Meer, 1999; Yitagesu et al., 2009b). The soils spectral data and their relationships with geotechnical characteristics were explored using various statistical analyses techniques. Cluster analysis, cross tabulations with nonparametric statistical tests, box plots, and error bars were used.

6.2.3.1 The Mann-Whitney U test

The Mann-Whitney U test is one of the most widely used nonparametric statistical test (alternate to the independent t-test) to investigate whether there exist a statistically significant difference between classes (Sheskin, 1997). The assumptions in this test are: (1) samples are randomly selected from the population that they represent, (2) samples are independent of one another, (3) either ordinal, interval or ratio scale measurement, and (4) similar underlying distribution, but not necessarily a normal distribution.

The Mann-Whitney U test was used to check if there were statistically, significant differences among the mean spectra representing each plasticity categories (resulting from the USCS). The Mann-Whitney U test involves testing a null hypothesis against an alternate hypothesis (Sheskin, 1997). The null hypothesis (H0: $\eta n(i)=\eta n+1(i)$ where η is the median reflectance, n is the plasticity classes and i spectral reflectance measurements) (Farifteh et al., 2007) stipulates that the variance in reflectance between classes is equal. The alternative hypothesis (Ha:$\eta n(i)\neq \eta n+1(i)$) stipulates that the variance in reflectance between classes is different. If the test result is significant (i.e.,

at a p-value of <0.05 significance level), then it shows statistically, significant differences between classes (as it gives a strong evidence for rejecting the null hypothesis).

6.2.3.2 Cluster analysis

Cluster analysis is a procedure that identifies and categorizes homogeneous groups based on their distance from specified or computed cluster centers (Kaufman and Rousseeuw, 1990). K-means cluster analysis works based on Euclidian distance. The cluster means are iteratively approximated, and variables are assigned to a cluster for which their distance to the cluster mean is the smallest (Kaufman and Rousseeuw, 1990). In K-means clustering, the user specifies the number of clusters. Then, the algorithm starts with initial sets of means to classify variables based on their distances to these means. This step is followed by computing new sets of means using variables that are assigned to each cluster, and a classification based on the new sets of means. The process will be repeated N times until the cluster means do not vary much between successive steps, and the cluster means will be computed once more, followed by assignments of variables to their final clusters.

The soil spectral information was processed using K-means clustering analysis technique to find six homogenous groups (corresponding to the six plasticity classes of the USCS).

6.2.3.3 Cross tabulation

Cross tabulation (contingency table) is a fundamental statistical tool to compare and investigate relationships among categorical variables (Sheskin, 1997). The strength of relationship, or lack thereof, and its statistical significance, can be tested by various measures. Statistical measures such as chi-square test statistics, likelihood ratio, phi, Cramer's V, contingency coefficient, lambda, Goodman and Kruskal tau, and uncertainty coefficient (Conover, 1999; Quade and Salama, 1975; Wilson, 1989) were used associated with approximate significance levels.

The null hypothesis in Chi-square (x^2) test is that the rows and column variables in a contingency table are independent or unrelated. The actual statistics is not very informative, but its significance level is. If the statistics is significant, there is strong evidence that the variables are related. x^2 can be computed as:

$$X^2=\sum(O-E)^2/E \qquad [6\text{-}1]$$

Where: O=the observed frequency, and E=the expected frequency

The likelihood ratio, LR was computed as:

$$LR=2\sum O\ln(O/E) \quad [6\text{-}2]$$

The Phi (ϕ) was computed as the square root of the chi-square (χ^2) divided by the sample size (N):

$$\phi = \sqrt{X^2/N} \quad [6\text{-}3]$$

Cramer's V is a rescaling of the phi so that its values range between 0 and 1. This test is appropriate for contingency tables larger than 2x2 (as is the case here). The formula for computing Cramer's V is:

$$V = \sqrt{\frac{X^2}{N(k-1)}} \quad [6\text{-}4]$$

Where: N=sample size, K=the smaller of the rows and columns

The formula for computing contingency coefficient (CC) is:

$$CC = \sqrt{\frac{X^2}{N+X^2}} \quad [6\text{-}5]$$

The above mentioned statistical measures are all based on the chi-squared statistic. There are also other measures of statistical relationship such as lambda (λ), Goodman and Kruskal tau (τ), and uncertainty coefficient (UC) that are important in determining correlations among categorical data. These measures are based on the concept of proportional error reduction. Lambda is a measure of association that shows the proportional reduction in error (PRE) when values of one variable are used to predict values of the other variable (IBM, 2010). A lambda value of 1 shows a perfect match. A lambda value of 0, on the other hand, indicates a complete lack of relationship. Lambda is based on modal distribution, and can be calculated as:

$$\lambda = \frac{[\sum(fi)-(fd)]}{(n-fd)} \quad [6\text{-}6]$$

Where: fi=the largest frequency in each class of the independent variable, fd=the largest marginal value of the dependent variable, and n=the sample size

The Goodman and Kruskal tau (τ) is a measure of proportional increase in accurately predicting one variable from the other, assuming that the predictions are based on the overall proportions of the two variables.

$$\tau = (\Sigma C - \Sigma D)/(\Sigma C + \Sigma D) \quad [6\text{-}7]$$

Where: C=concordant observations, and D=discordant observations

The Uncertainty coefficient (UC) also reflects a proportional reduction in error when one variable is used to predict the values of the other variable (IBM, 2010). UC varies from 0 to 1, and it takes the entire distribution into account.

$$UC(R|C) = [H(X) + H(Y) - H(XY)]/H(Y)$$
$$UC(C|R) = [H(Y) + H(X) - H(XY)]/H(X)$$
$$UC\ symmetric = 2[H(X) + H(Y) - H(XY)]/[H(X) + H(Y)] \quad [6\text{-}8]$$

Where: R=row and C=column
X is the column variable, Y is the row variable, n is sample size, rj are the row, totals (marginals) for rows 1...j, ck are the column totals (marginals) for rows 1...k, njk is the cell count for row j, column k, ln is the symbol for the natural log function,

$H(X) = -\sum_j [(r_j/n)*\ln(r_j/n)]$ = entropy for UC(C|R),
$H(Y) = -\sum_k [(c_k/n)*\ln(c_k/n)]$ = entropy for UC(R|C),
$H(XY) = -\sum_j \sum_k [(n_{jk}/n)*\ln(n_{jk}/n)]$

The six statistically homogenous groups from the k-means clustering analysis were compared with the six plasticity classes of the soils from plasticity chart using cross tabulation techniques. Spectra of bulk and fine soil samples were treated independently.

6.2.3.4 Box plots and error bars

Box plots are important statistical data exploratory tools, providing illustrative information on data distribution and structure. Box plots were used to examine the mean and ranges of variability of the k-means clusters, thereby compare the clusters from spectra of bulk and fine fraction soil samples.

In addition, error bars showing a 95% confidence interval (Cumming et al., 2007), were used to examine how different or similar the K-means clusters and plasticity classes were. The error bars were also used to illustrate the level of confidence that the mean in each cluster represented the true mean values of the plasticity classes, as well as the uncertainty or error in the clusters. Testing statistical significance by the overlap among confidence intervals is conservative (Schenker and Gentleman, 2001). However, as described by Cumming et al. (2007), confidence intervals can be directly used to infer significance levels. The statistical analyses were done in the SPSS software (IBM, 2010).

6.3 Results

6.3.1 Geotechnical characteristics

The selected soil samples were characterized by a wide range of variability in their plasticity (Figure 6-2). Majority of the samples plotted above the 'A' line and exhibited high to extremely high plasticity. Soils that plot above the 'A' line belong to the inorganic clay soil varieties. Thus, their swelling and shrinkage potential is also high. Some soil samples plotted below the 'A' line; and belong to inorganic silt soil varieties. These inorganic silt soils are elastic silts that are of high, very high and extremely high plasticity. Accordingly they are also susceptible to large swelling and shrinkage potential.

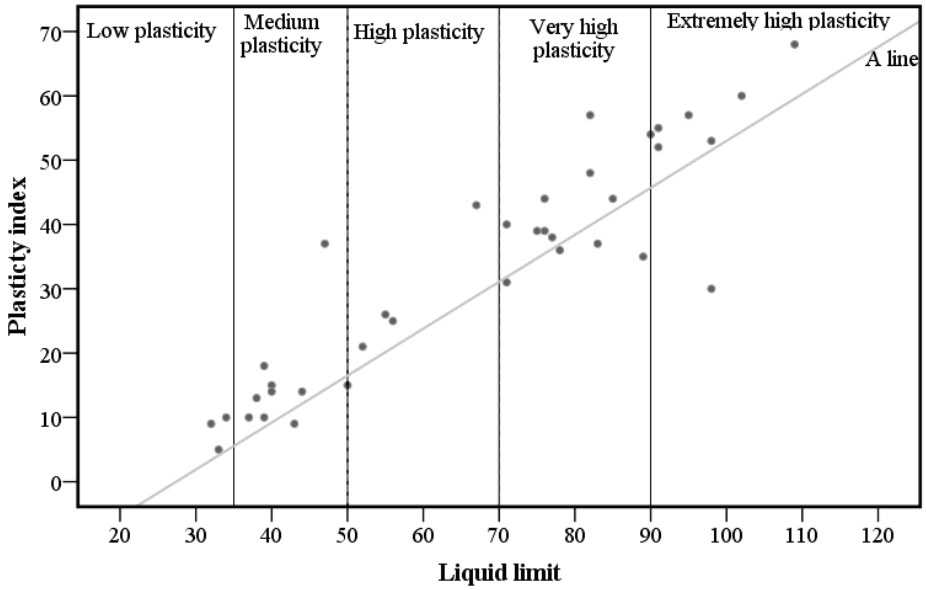

Figure 6-2 Distribution of the soil samples on plasticity chart showing their plasticity. Majority of the soil samples fall above the 'A' line, which indicates that their composition is dominated by active clay minerals.

As shown in chapter three, the soils were predominantly fine grained with high clay content. Although the soil samples were mostly fine grained, individual particles were agglomerated forming large grain aggregates in the bulk soil samples, which is typical of expansive soils containing smectite group clay minerals and a high percentage of colloids (Chen, 1988; Snethen, 1975).

6.3.2 Spectral characteristics of expansive soils

Continuum removed spectra of selected soil samples (fine fraction) are presented in Figure 6-3. The spectra showed the presence of active clay minerals in the soils. Montmorillonite and illite were identified by the characteristic absorption features that they exhibited at ~3.1 µm and a doublet with absorption minima at ~3.84 µm and ~3.98 µm (Yitagesu et al., 2011a). In some soil spectra, probably of samples containing illite-montmorillonite and illite-kaolinite interstratified clay minerals, the doublet feature that is typical of illite (Yitagesu et al., 2011a) was resolved as a single absorption feature (Figure 6-3). In the spectra where the absorption features at ~3.1 µm and ~4.3-5 µm were deep, the feature at ~3.98 µm was interpreted as an indicator of the presence of illite-montmorillonite interstratified clay mineral. For instance, illite-montmorillonite interstratified clay mineral was identified as a major constituent in the sample from km 79.5. The spectra of this sample exhibited a single absorption feature at ~3.98 µm. In the spectra where the absorption features at ~3.1 µm and ~4.3-5 µm appeared shallow, the absorption features at ~3.98 µm was considered to show the presence of illite-kaolinite interstratified clay mineral.

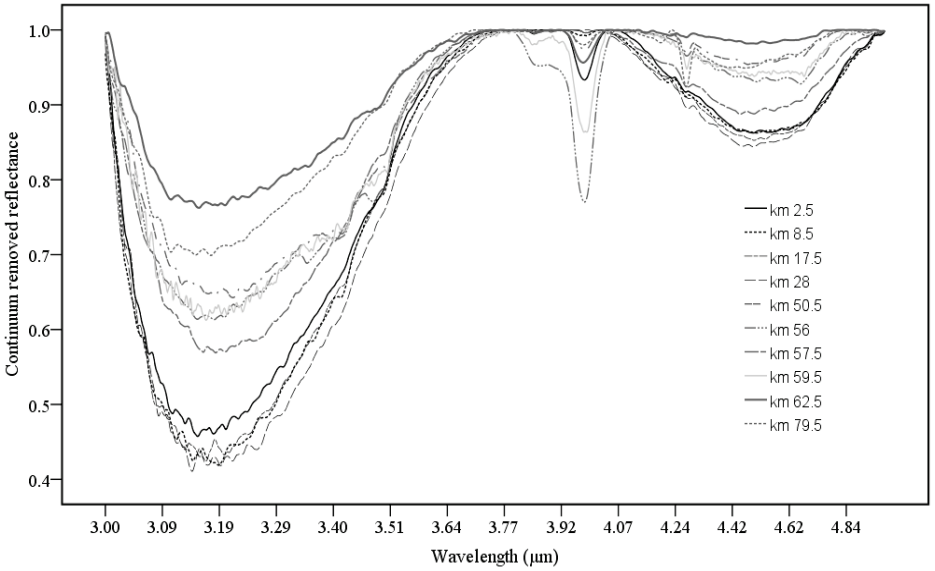

Figure 6-3 Typical spectra showing the presence clay minerals such as montmorillonite, illite, and kaolinite in the soil samples.

Quartz is the most abundant and common soil forming mineral (Fitzpatrick, 1980). Presence of quartz is evident in the soil samples as shown in the XRD and XRF analyses results. The absorption feature near 4.3 µm seen in the spectra of some soils (mostly exhibiting low, medium and high plasticity)

might be related to quartz as described by Salisbury and D'Aria (1994) as the weaker overtone or combination tone absorption features of quartz appeared in the 3-5 µm wavelength region, near 4.29 µm, 4.48 µm, 4.69 µm and 4.95 µm. The spectrum of a sample from km 79.5, which contained a high percentage of SiO2 (62.9%), exhibited a feature near 4.3 µm (Figure 6-3) that might be related to an overtone of the Si-O stretching vibration. This feature appeared in the spectrum of a sample from km 57.5 (with 50.8% SiO2), but not seen in the spectrum of a sample from km 28, which showed a comparable amount of SiO2 (50.1%).

The spectra of bulk and fine fraction soil samples differed in reflectance, spectral contrast and absorption feature intensities. Overall, the spectra of fine fraction soil samples showed higher reflectance, spectral contrast and more pronounced absorption features than the bulk soil samples.

Grouping the spectra of soil samples by plasticity classes and computing mean spectrum for each class showed differences among the six groups that seemed to correspond to differences in plasticity. Plots of continuum removed mean spectra of the bulk (Figure 6-4A, and fine fraction soil samples (Figure 6-4B) for the six plasticity classes, depicted characteristic variations. Each mean spectrum is statistically, significantly different from one another (Mann-Whitney U test, at a p-value of <0.05 significance level). Therefore, as described by Sheskin (1997), it can be concluded that there is a high likelihood that each mean spectrum is representative of groups of soil samples with distinct plasticity characteristics.

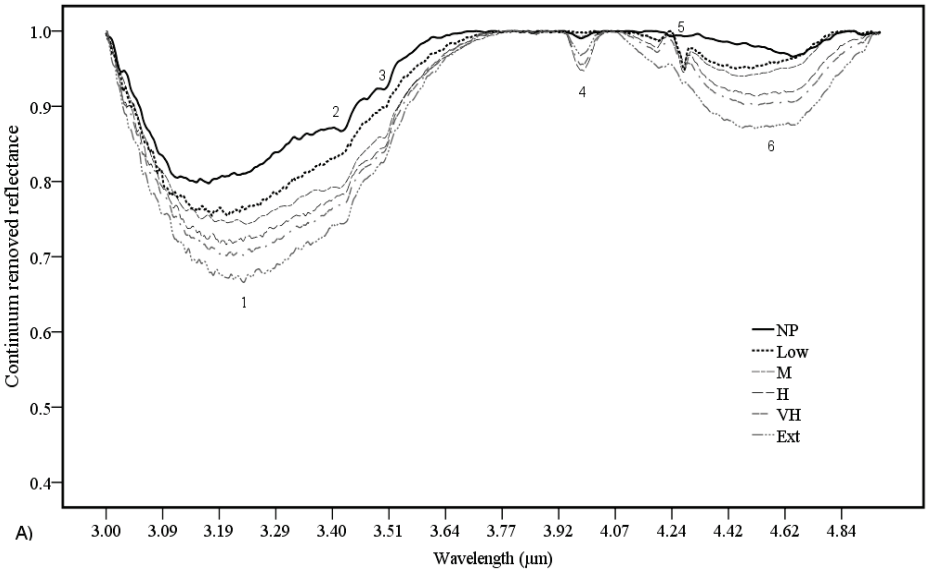

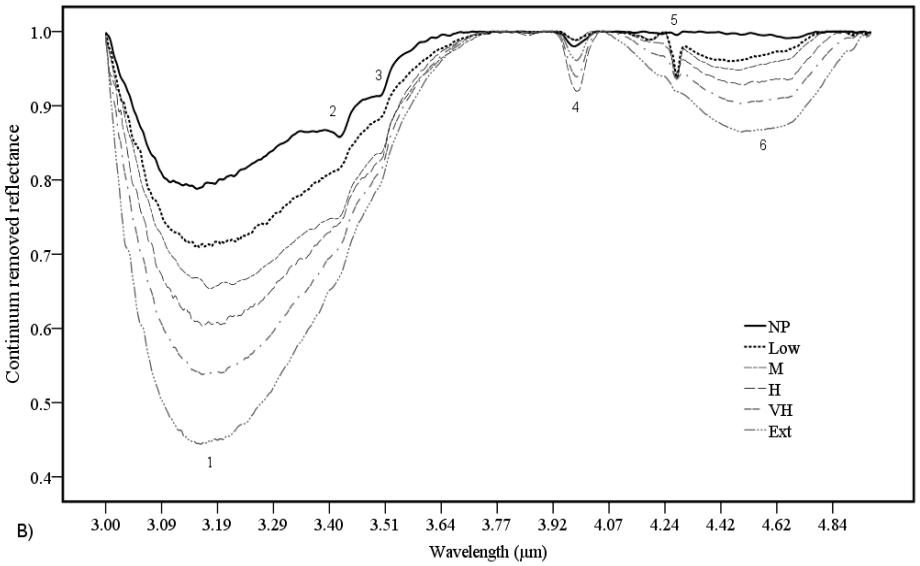

Figure 6-4 Mean continuum removed spectra: NP (non-plastic), Low, M (medium), H (high), VH (very high) and Ext (extremely high) plasticity characteristics of (A) bulk, and (B) fine fraction soil samples. Annotation numbers indicating absorption features due to the presence of (1) montmorillonite or illite, (2) and (3) illite, (4) either illite/montmorillonite or illite/kaolinite interstratified clay minerals, (5) quartz (SiO_2), and (6) montmorillonite, illite, or kaolinite.

Variation in spectral characteristics appeared to show larger similarity in pattern among the spectra of bulk and fine fraction soil samples. The number of absorption features, their appearance and changes in absorption feature parameters are similar, but the absolute values such as depth of the absorption features differed. The absorption feature annotated with number one, which was ascribed to the presence and high contents of montmorillonite or illite (Yitagesu et al., 2011a) decreased in depth intensity, width and area as plasticity gradually changed from extreme to very high, high, medium, low and non-plastic categories (Figure 6-4A and 6-4B). In both bulk and fine fraction soil spectra, the appearance of features of illite was pronounced. The absorption feature centered at ~3.98 µm also varied in depth intensity, which appeared to correspond to changes in plasticity (becoming deeper with increasing plasticity). The feature near 4.3 µm to 5 µm wavelength region, which appeared as broad, rounded feature in extremely plastic soils tended to be shallower, and flat in soils exhibiting low plasticity, and those that are non-plastic. No particular kaolinite features appeared. The only indication of its presence is related to a shallow depth at ~3.1 µm combined with a flat appearance ~3.98 µm and ~4.3-5 µm. Yitagesu et al. (2011) presented spectra of kaolinite containing samples

showing weak absorption features ~4.7 µm that disappeared with deceasing kaolinite content.

6.3.3 Relationships among plasticity and spectral reflectance of soils

Statistical relationships among the six plasticity classes and clusters resulted from the K-means clustering analyses, where distance to mean was used as a measure of determining similarity or dissimilarity among the samples, are presented in contingency tables (Tables 6-1A and 6-1C). For the spectra of bulk soil samples, a chi-square (χ^2) test statistics of 87 and a likelihood ratio (LR) of 72 were attained. Both the χ^2 and LR were significant at a p-value of <0.01 significance level. For the spectra of fine soil samples, a chi-square test statistics of 148 and a likelihood ratio of 99 were achieved. Again, both statistics were significant at a p-value of <0.01 significance level. These results signified that the classes obtained from the K-means clustering analyses and plasticity categories were associated than is expected due to chance.

Additional investigation on the pattern and number of joint occurrences of classes in the contingency tables (Tables 6-1A and 6-1C), showed for instance, all non-plastic soils fall in the same cluster, majority of extremely plastic soils fall in one cluster and so on. The symmetric measures such as Phi, Cramer's V and contingency coefficient (Tables 6-1B and 6-1D) that are based on the chi-square test statistics showed strong correlations among the classes. The correlations were statistically significant, as shown by the accompanying significance levels (at a p-value of <0.01). Table 6-2A and Table 6-2B also showed that there is a strong and statistically significant association among the k-means clusters and the plasticity classes. The values of lambda, Goodman and Kruskal tau, and uncertainty coefficients are stronger for the fine soil fractions than the bulk soil samples, indicating the accuracy (proportional reduction in error) while predicting one variable from the other (i.e., K-means and plasticity classes) was better in the case of fine fraction soils. Nonetheless, in both cases, all statistical measures are highly significant at a p-value of <0.01 significance level, suggesting strong correlation among soil geotechnical and spectral characteristics.

Table 6-1 K-means cluster classes from the spectra of (A) bulk and (C) fine fraction soil samples in the 3-5 µm wavelength region, cross tabulated with soil plasticity classes; and accompanying statistical measures showing the strength and significance of the relationship between k-means cluster and plasticity classes of (B) bulk and (D) fine fraction soil samples.

A) Bulk soil samples

		Plasticity classes						
		EXT	VH	H	M	L	NP	Total
K-means clusters	1	-	-	-	-	-	3	3
	2	-	-	1	2	1	-	4
	3	-	1	2	3	2	-	8
	4	-	-	-	4	-	-	4
	5	1	5	2	-	-	-	8
	6	7	6	-	-	-	-	13
Total		8	12	5	9	3	3	40

B) Bulk soil samples

		Value	Approx. Sig.
Nominal by Nominal	Phi	1.473	0.000
	Cramer's V	0.659	0.000
	Contingency coefficient	0.827	0.000
Number of valid cases		40	

C) Fine fraction soil samples

		Plasticity classes						
		EXT	VH	H	M	L	NP	Total
K-means clusters	1	-	-	-	-	-	3	3
	2	-	-	-	-	3	-	3
	3	-	-	-	7	-	-	7
	4	-	3	5	2	-	-	10
	5	-	6	-	-	-	-	6
	6	8	3	-	-	-	-	11
Total		8	12	5	9	3	3	40

D) Fine fraction soil samples

		Value	Approx. Sig.
Nominal by Nominal	Phi	1.922	0.000
	Cramer's V	0.859	0.000
	Contingency coefficient	0.887	0.000
Number of valid cases		40	

Table 6-2 Summary of directional measures of association among the k-means clusters and (A) bulk soil samples, and (B) fine fraction soil samples.

A) Bulk soil samples

			Value	Asymp. Std. Error[a]	Approx. T[b]	Approx. Sig.
Nominal by Nominal	Lambda	Symmetric	.418	.090	3.742	.000
		K means clusters Dependent	.407	.095	3.895	.000
		plasticity Dependent	.429	.138	2.535	.011
	Goodman and Kruskal tau	K means clusters Dependent	.401	.051		.000[c]
		plasticity Dependent	.402	.039		.000[c]
	Uncertainty Coefficient	Symmetric	.537	.051	8.559	.000[d]
		K means clusters Dependent	.538	.052	8.559	.000[d]
		plasticity Dependent	.537	.052	8.559	.000[d]

a. Not assuming the null hypothesis.

b. Using the asymptotic standard error assuming the null hypothesis.

c. Based on chi-square approximation

d. Likelihood ratio chi-square probability.

B) Fine fraction soil samples

			Value	Asymp. Std. Error[a]	Approx. T[b]	Approx. Sig.
Nominal by Nominal	Lambda	Symmetric	.719	.099	5.339	.000
		Plasticity Dependent	.714	.108	4.264	.000
		K-means clusters Dependent	.724	.094	5.254	.000
	Goodman and Kruskal tau	Plasticity Dependent	.667	.054		.000[c]
		K-means clusters Dependent	.667	.055		.000[c]
	Uncertainty Coefficient	Symmetric	.746	.053	9.956	.000[d]
		Plasticity Dependent	.749	.054	9.956	.000[d]
		K-means clusters Dependent	.743	.055	9.956	.000[d]

a. Not assuming the null hypothesis.

b. Using the asymptotic standard error assuming the null hypothesis.

c. Based on chi-square approximation

d. Likelihood ratio chi-square probability.

Further, the relationships among plasticity classes and K-means clusters for bulk and fine soil fractions were summarized in box plots (Figure 6-5). The means of the clusters for bulk soil samples do not differ pronouncedly particularly among clusters 2, 3 and 4. Although the extreme cases seemed separable, the ranges of variation in liquid limit values of member samples in four of the clusters (2, 3, 5 and 6) appeared to be large (Figure 6-5A). On the other hand, the means of the K-means cluster classes for fine fraction soil samples are markedly different from one another. In addition, each class exhibited a narrower variability in liquid limit values except for cluster 4, which showed a larger variability than was apparent in the other clusters (Figure 6-5B).

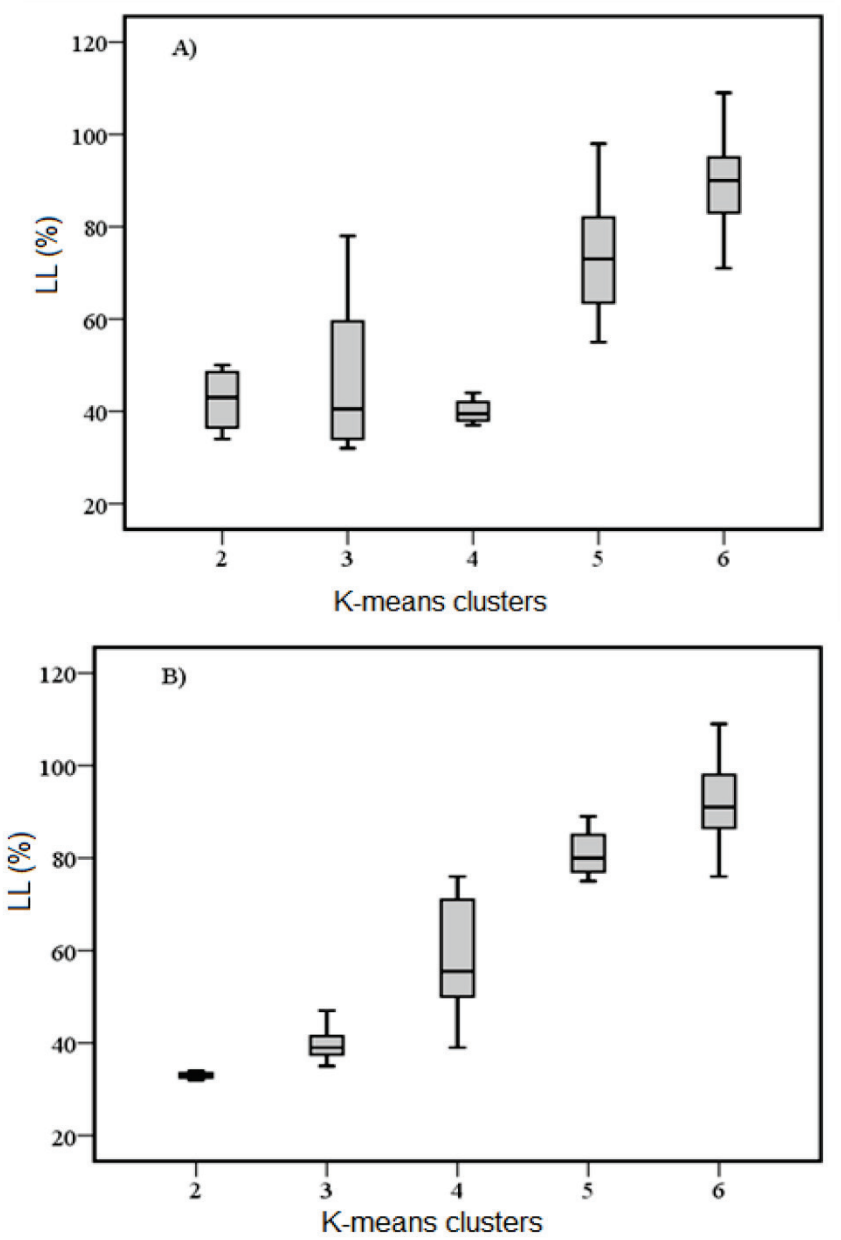

Figure 6-5 Box plots showing the range and distribution of liquid limit (LL) values of soil samples grouped by K-means clusters of (A) bulk and (B) fine fraction soil samples. The mean of each cluster for the fine fraction soils appeared distinct. The clusters also showed smaller variability in liquid limit. Whereas, for bulk soil samples particularly the means of clusters 2, 3 and 4 appeared to be not as distinctly different as in the clusters from spectra of fine fraction soils, with wider spread in values of liquid limit that they represented.

A larger range of liquid limit above and below the mean (marked by black dots), which produced wider error bars implied higher uncertainty in clusters of member soil samples with respect to the variation in spectral characteristics and the actual variation in their plasticity (Figure 6-6). On the contrary, narrower ranges of liquid limit above and below the mean produced tighter error bars, implying higher confidence that the variation in spectral characteristics that was summed in the clusters represented the actual variation in plasticity of member soil samples. The means and range of liquid limit in each cluster appeared to overlap for the bulk soil samples, while it showed distinct differences for the fine fraction soil samples. Therefore, there appeared to be a lower level of confidence that the K-means clusters for spectra of bulk soil samples particularly of clusters 2, 3 and 4 (Figure 6-6A) are significantly different from one another. Whereas, there is a higher level of confidence that the cluster for spectra of fine soil fraction samples are significantly different from one another (Figure 6-6B). Note that there is no overlap among the whiskers of error bars of the clusters for spectra of fine fraction soil samples. The larger the whiskers of the error bars extended from the mean, the higher are the standard errors about the mean values of liquid limits that the classes represented; hence larger estimation uncertainty of the mean in the classification (Cumming, 2009).

Overall, K-means clusters for the spectra of fine fraction soil samples showed a higher level of agreement with the classification from plasticity chart, than K-means clusters for the spectra of bulk soil samples.

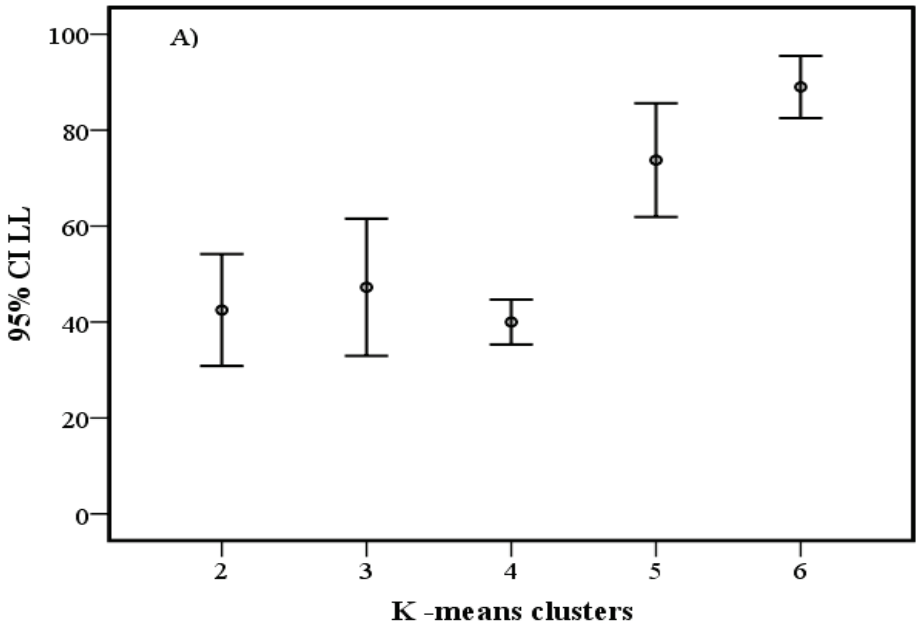

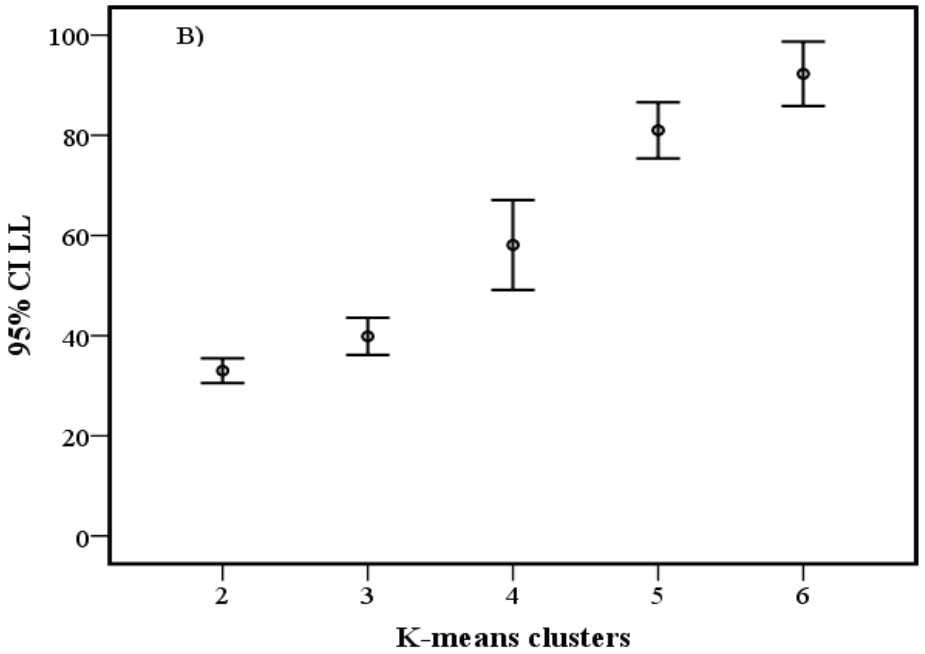

Figure 6-6 Error bars showing the 95% confidence interval of liquid limit (Y-axes) that each K-means cluster classes represented (A) of bulk and (B) fine fraction soil samples. Note the wider and overlapping error bars in the (A) bulk soil samples and (B) tighter and non-overlapping error bars in the fine fraction soil samples.

6.4 Discussion

The overall similarities in shapes of spectra of bulk and fine soil fractions are attributed to similarity in mineralogical compositions of the soil samples as expanding clay minerals dominate the soils compositions in both bulk and fine fractions. Refer to the XRD analyses results in Table 3-2A and Figure 3-4; and spectra of the soils samples (Figure 6-3 and Figure 6-4). However, absorption feature parameters such as absolute depth intensity of individual absorption features differed among the spectra of bulk and fine fraction soil samples. The statistical analyses results are suggestive of the possibility that soil spectral and plasticity characteristics are influenced by similar causative factor (i.e., clay mineralogical compositions). It appeared that the strength of the relationship between plasticity classes and k-means clusters (Tables 6-1 and 6-2) obtained from spectra of fine fraction soil samples are higher than those of the bulk soil samples. Differences in correlations signified influence from other sources of variation than mineralogical composition, affecting the spectral characteristics of soils (Gaffey, 1986). Stronger associations among fine fraction soil spectra and plasticity can be ascribed to: (1) the presence of more clay particles and may be more clay minerals in the finer fraction soil samples than in the bulk soil samples (Carter and Bentley, 1991; Ross,

1978), accordingly their strong influence on the spectral behavior of the soils; (2) the relative homogeneity of the fine fraction samples and thus lesser interference of soil texture such as grain size and porosity, on the spectral characteristics of the soils.

The larger variability in plasticity exhibited by the K-means cluster classes of bulk soil samples (Figures 6-5 and 6-6) can be attributed to interfering factors contributing to the spectral variability of the soils. Several researchers (Bras and Erard, 2003; Gaffey, 1986; Salisbury and D'Aria, 1994; Salisbury and Eastes, 1985) demonstrated that factors such as particle size differences and porosity can induce variation in the MIR spectral characteristics of materials, which are not related to changes in mineralogical compositions. Therefore, for optimal results and comprehensive applicability of the MIR spectroscopic technique, it is essential to establish a standard for sample preparation, and a method of addressing such interfering factors.

6.5 Conclusions

Optimal design of structures and formulation of appropriate measures for counteracting geotechnical problems associated with volume changes in expansive soils require identification of clay mineral composition of soils. In this chapter, the potential application of spectroscopy in the 3-5 µm wavelength region for compositional analysis and classification of expansive soils, was established. The soils exhibited characteristic spectral features, which enabled identification of constituent clay minerals. Spectra of bulk and fine fraction soil samples showed differences, which might be attributable to textural variations among the soil samples. Absorption features in the spectra of fine fraction soil samples were more pronounced than in the spectra of bulk soil samples. Differences in the soil spectral characteristics appeared to vary with the soils plasticity. The Mann-Whitney U test signified spectral differences among the mean spectra representing each plasticity class. Classification of soils based their spectral characteristics and comparison of these classes with soils plasticity showed strong and statistically significant correlations. As shown by the statistical measures of associations, spectra of fine soil fraction samples exhibited a closer match with plasticity classes than the spectra of bulk soil samples. On this account, it is clear that sample homogenization is necessary. With proper standard sample preparation, the approach can contribute a great deal in geotechnical investigation and routine analyses of expansive soils.

Chapter 7*

Mapping soil geotechnical parameters: multispectral remote sensing

Abstract: Multispectral image data was investigated for estimating geotechnical characteristics of expansive soils and mapping their spatial variation. A geotechnical parameter (weighted plasticity index) and soil spectra derived from Advanced Spaceborne Thermal Emission and Reflection Radiometer (ASTER) imagery were linked. A multivariate statistical calibration, partial least squares regression analysis was used to establish the relationship. The model performance indices such as a coefficient of determination (R^2) of 0.71, and accompanying small root mean square error of prediction and standard error of performance (6.3), negligible bias (-0.004) and small offset (5.9) showed a significant correlation between weighted plasticity indices and soil reflectance spectra, with moderate model prediction ability. Measured and predicted values of weighted plasticity indices showed a similar spatial trend of variation. Therefore, ASTER data are useful for estimating and thereby mapping variation in magnitude of soil expansiveness. The presented approach can substantially contribute to geotechnical applications. Especially to obtain information on soil swelling and shrinkage potential in a reconnaissance and technical feasibility studies, preliminary site investigation schemes and basic assumption of parameters, which in turn influence the initial choice of possible road alignment, structures and associated cost estimates. However, for optimization of the approach, further research, accounting for the influence of factors that affect spectral characteristics of soils at a multispectral image level is essential.

Keywords: Expansive soil, swell-shrink, weighted plasticity index, spectra, ASTER, PLS.

* This chapter is based on:
Yitagesu, Fekerte Arega, Van der Meer, F.D., and Van der Werff, H., 2011, Multispectral Remote Sensing for Estimating and Mapping Soil Expansiveness: Engineering Geology (in review after revision).

7.1 Introduction

The first stage of any major civil engineering project involves a reconnaissance study of a project site followed by detailed geotechnical investigation. Primary aim of such a study is to collect data concerning ground conditions in order to assess their likely influence or vice versa on design, construction and performance of infrastructures. Potential problems that could affect design, construction, performance and life time of infrastructures are best determined during pre-design phases when compromises can be made between structural, architectural, mechanical, and other aspects of design without disrupting design processes. Changes during the design phase or construction will probably delay activities and pose economic disadvantages. Therefore, it is critical to ensure that material conditions are properly assessed in a geotechnical investigation scheme. Since geotechnical properties of expansive soils change with variation in moisture content, potential heave prediction, in such soils is required. A number of qualitative and quantitative, direct and indirect, in-situ and laboratory testing procedures are available to identify and characterize expansive soils. Consistency limits are commonly used as indicators of soil swelling and shrinkage potential, due to their simplicity and significant correlation with other geotechnical characteristics including soil expansion potential (Carter and Bentley, 1991; Wan et al., 2002). The more soil testing is done before hand, the easier it is to reduce risk in design of infrastructure. However, it is impractical to analyze many samples over short distances for it is costly and time consuming. Remote sensing can potentially provide with a continuous representation of a site under investigation, other than discrete sampling points. Soil swelling and shrinkage potential depends, among other factors, on clay content and mineralogical compositions of soil (Al-Rawas, 1999; Nelson and Miller, 1992; Ramana, 1993), which also determine their spectral characteristics (Chabrillat et al., 2002; Kariuki et al., 2003; Van der Meer, 1999; Yitagesu et al., 2009b).

Researchers in soil science well explored the basic relationships among spectral response and soil characteristics, and established the role of remote sensing for characterizing and mapping soil and soil properties. Stoner and Baumgardner (1981) presented spectral reflectance and variation in spectral reflectance characteristics of different soils. Bendor and Banin (1994) established the potential of near infrared spectroscopy for estimating soil properties. Shepherd et al. (2005) used a multivariate calibration technique, partial least squares (PLS) regression analysis to predict soil properties from their respective reflectance spectra. Van der Meer (1999) outlined the potential of remote sensing for mapping soils susceptible to volume changes based on diagnostic clay mineral spectral signatures. Chabrillat et al. (2002) demonstrated capability of hyperspectral remote sensing for detecting and mapping expansive clay minerals. Bourguignon et al. (2007) mapped clay

minerals that are fundamental with respect to soil expansiveness, such as kaolinite, illite, and smectite from an ASTER image. One-to-one relationships among selected geotechnical parameters and laboratory acquired soil reflectance spectra were established by Kariuki et al. (2003 and 2004). They published empirical relations using known, clay mineral diagnostic absorption features at ~1.4 µm, ~1.9 µm, and ~2.2 µm wavelengths, and soil geotechnical characteristics. Waiser et al. (2007) predicted clay content from visible-near infrared spectra of soils using PLS regression models. Bendor et al. (2002) mapped soil properties; such as organic matter and salinity from a hyperspectral image data. Rainey et al. (2003) mapped clay and sand content of intertidal environments of estuarine, from airborne remote sensed data with multivariate regression techniques. Yitagesu et al. (2009a, 2009b) reported the importance of laboratory spectroscopy for quantifying geotechnical parameters of expansive soils, using a multivariate statistical regression analysis. Instead of using atmospheric absorption bands, they analyzed wavelengths that fall within atmospheric windows for possible extension of the approach to multispectral remote sensing. Extension of the technique to multispectral remote sensing (for estimating geotechnical characteristics of expansive soils over a large area), on the other hand, can provide a significant input to geotechnical applications.

The objective in this chapter was to investigate the utility of multispectral remote sensing data (ASTER) for predicting and mapping variation in soil expansiveness in terms of weighted plasticity index (wPI) of soils. A multivariate statistical calibration technique, PLS, was used to examine the relationship between ASTER derived soil reflectance spectra and wPI. A simple method of estimating soil wPI from ASTER reflectance spectra of soils, and thereby mapping variations in magnitude of soil expansiveness is proposed.

7.2 Material and Methods

7.2.1 Geotechnical investigation

The study summarized in this chapter was carried out in the Addis Ababa-Nazret study site. Identification and prediction of soil swelling and shrinkage potential was based on consistency limits. This has an advantage of using parameters that are relatively easy to determine. The mineralogical compositions, oxides and organic matter content of the soil samples were determined using X-ray diffraction (XRD) and X-ray florescence (XRF) analyses. The procedures are described in chapter 3, section 3.2.3. Particle size distribution tests were conducted in accordance with ASTM D6913-04e1 standard test method using sieve analysis (for the fraction passing through 2 mm, 0.425 mm and 0.075 mm ASTM sieve openings). Grading of soils finer than 0.075 mm ASTM sieve was determined by hydrometer analysis in

accordance with ASTM D422-63(2007) standard test method. Consistency limits, such as liquid limits (LL), plasticity limits (PL), and plasticity indices (PI) were determined in accordance with the ASTM D4318-05 standard test method. Weighted plasticity indices (wPI) were calculated from plasticity indices and percentage of soil sample passing through the ASTM 0.425 mm sieve aperture as shown in equation 7-1.

$$wPI = PI * (\% \text{ material passing } 0.425 \text{ mm sieve})/100 \quad [7\text{-}1]$$

Therefore, wPI compensates for the effect of coarser grained material that is not included in testing plasticity indices of soil samples. The key factors that influence soil plasticity are clay content and clay mineralogical compositions of soils. Thus, soil plasticity and soil swelling and shrinkage potential are directly proportional; making plasticity an indirect measure of soil expansiveness (Al-Rawas, 1999; Thomas et al., 2000). In accordance with the Ethiopian Roads Authority site investigation manual (ERA, 2002), soils with wPI≥20% are potentially highly expansive. Such soils may cause serious problems when construction is undertaken, unless they are correctly identified, associated with quantification of their swelling and shrinkage potential, and proper mitigation measures are formulated accordingly during design of infrastructure. Consequently, encountering soils with wPI≥20% warrants further detailed investigation of the soils potential to swelling and shrinkage characteristics.

Natural vegetation cover, in the Addis Ababa-Nazret study site, is in general poor since most of the area is farmland; hence provides enough soil exposure for soil remote sensing in dry periods. Built-up areas follow the existing road alignment connecting Addis Ababa and Nazret. Kaliti, Akaki, Dukem, DebreZeyt, Modjo and Nazret are the main built-up areas. Deeply incised drainage patterns and gully erosion are common features in the area particularly past Modjo town towards Nazret.

7.2.2 Multispectral image analysis

The Advanced Spaceborne Thermal Emission and Reflection Radiometer (ASTER), covers the visible-near infrared (VNIR, 0.4-1 µm), short wave infrared (SWIR, 1-2.5 µm) and thermal infrared (TIR, 8-12 µm) wavelength regions of the electromagnetic spectrum. ASTER has nine bands in the VNIR and SWIR, and five bands situated in the TIR wavelength region. Some of the ASTER bands in the SWIR are placed in wavelength regions that are well known to be related to characteristic absorption features of clay minerals (Clark, 1999). Soil spectral signatures measured by many, narrow and contiguous bands of high spectral resolution instruments show well-resolved spectral features that are essential in visual, qualitative identification of clay mineral assemblage (Chabrillat et al., 2002; Kariuki et al., 2003). However,

ASTER band widths are coarse in comparison to the fine spectral resolution spectrometers. Ranges of wavelength regions covered by the ASTER sensor accompanied with their spatial resolutions are summarized in Table 7-1.

Use of ASTER data for mineral mapping and lithologic discrimination has become a common practice in recent years (Bourguignon et al., 2007; Rowan et al., 2003), for its optimal placing of bands that are sensitive to minerals, and low-acquisition costs while covering large and inaccessible areas. Apart from the availability of large archives of ASTER data, upcoming similar missions such as the ENMAP, new LANDSAT mission etc. (Hermann J. Kaufmann et al., 2010; Markham, 2011) would be of interest for future application with respect to mapping soil geotechnical parameters.

Two ASTER level (1B) scenes covering the study area (Figure 2-5 B), acquired in dry seasons (January 2008 and March 2006), were obtained from the EROS Data Center (EDC), South Dakota, U.S.A. Geo-metric correction and geo-referencing was done by the image provider. The ASTER scenes were pre-processed, which includes co-registration of the 30 m spatial resolution SWIR bands with the 15 m spatial resolution of VNIR bands. Internal average relative (IAR) reflectance calibration, built in the ENVI software (ITT Visual Information Solutions, 2009) was used to retrieve scene reflectance from the ASTER radiance data. IAR reflectance calibration normalizes images to a scene average spectrum (Kruse, 1988). The algorithm first calculates an average spectrum for the entire scene. Then, use this average spectrum as a reference spectrum, to calculate apparent reflectance for each pixel by dividing it to the pixel spectrum. IAR is particularly useful in areas where no ground measurement is available (Bendor and Levin, 2000). Its success was further demonstrated in areas where vegetation cover is sparse (Tangestani et al., 2008). The two ASTER scenes from each year (2008 and 2006) were subsequently mosaicked, and a spatial subset to the extent of the study area was then created.

Spectral responses of natural materials recorded by imaging devices are rarely homogeneous or continuous (Van der Meer, 2004b). Land cover other than soil and variation in topography are common sources of heterogeneity. Supervised classification of the imagery was performed using ground truth data having soil, vegetation, water bodies and built-up areas as surface cover classes. These classes were determined in the images by locating known surface covers such as lakes and rivers for the water bodies, forested areas for vegetation, urban structures for built-up areas, and bare farm lands for soils, which were used as endmembers (reference spectra) for performing the supervised classification. Spectral angle mapper (SAM) classification technique, built in the ENVI software (ITT Visual Information Solutions, 2009), was used to stratify the images into the specified surface cover

classes. SAM is a physically based supervised classification method (Kruse et al., 1993) where image spectra are compared and matched with reference spectra. It compares the angle between image spectra with that of reference spectra, in which smaller angles represent closer matches and larger angles represent dissimilarities. The advantage of using SAM is its insensitivity to illumination and albedo effects (Kruse et al., 1993; Mather, 1999). Non soil surface cover classes such as built-up areas, vegetation, water bodies were masked out; and only the soil classes were used for further analysis.

The thermal infrared bands were excluded since the interest in this study was on soil reflectance characteristics. While the 2008 scenes were used to develop the relationship, repeatability of the approach was tested on the 2006 scenes. Spectra of soil samples were collected from the soil class of SAM stratified ASTER image (2008). A total of 92 spectra were extracted from locations where soil samples were taken for a geotechnical characterization (of 1 m depth).

Table 7-1 Summary of image characteristics of ASTER in the VNIR, SWIR and TIR regions of the electromagnetic spectrum, after (Abrams, 2000).

Characteristics	VNIR	SWIR	TIR
Wavelength region	1*: 0.52 - 0.60 µm	4: 1.600 - 1.700 µm	10: 8.125 - 8.475 µm
	2: 0.63 - 0.69 µm	5: 2.145 - 2.185 µm	11: 8.475 - 8.825 µm
	3N: 0.76 - 0.86 µm	6: 2.185 - 2.225 µm	12: 8.925 - 9.275 µm
	3B: 0.76 - 0.86 µm †	7: 2.235 - 2.285 µm	13: 10.25 - 10.95 µm
		8: 2.295 - 2.365 µm	14: 10.95 - 11.65 µm
		9: 2.360 - 2.430 µm	
Ground Resolution	15 m	30 m	90 m

*the numbers indicate the band number
† backward looking for stereo-pair

7.2.3 Partial least squares regression analysis

PLS1 (Martens and Naes, 1989), built in The Unscrambler software (CAMO Process AS., 2005) was used to establish relationships among ASTER derived soil spectra and wPI. The distribution of variables were examined, and appropriate transformations were carried out on variables that showed skewed distributions to make their distribution symmetrical (Wold et al., 2001). Various spectral data pre-processing techniques (Martens and Naes,

1989; Selige et al., 2006) were applied on the soil spectra prior to performing the multivariate regression analysis. Pre-processing enhances spectral features so as to obtain accurate input data for the PLS regression analysis. Martens and Naes (1989) demonstrated that pre-processing improves model prediction ability and hence reduce prediction errors. According to Martens and Naes (1989), spectral data pre-processing is also essential to avoid or reduce irrelevant variation in the explanatory variables. Irrelevant variation might arise from instrument noise or physical properties unrelated to the phenomena of interest. Spectral data normalization was carried out to normalize spectral input data in order to remove uncontrollable scale variations. Normalization does not induce any change into the data except for simply rescaling it. Multiplicative scatter correction (Full MSC) was performed to avoid scatter effects from the soils texture, grain size and porosity (Dhanoa et al., 1994; Martens and Naes, 1989). In MSC, the scatter for each sample is estimated relative to that of a reference sample which can be a mean spectrum calculated from all spectra in the calibration model. The data were mean centered and scaled to unit variance before calibration, for enhancing variance in the explanatory data and removing any systematic bias (Martens and Naes, 1989). A full cross validation method was used to calibrate and validate the prediction model (Wold et al., 2001). PLS factor selection was based on evaluation of residual and explained variances, and corresponding root mean square errors. Thus, factors with low residual variance accompanied with low root mean square error were selected. Model performance indices such as the coefficient of determination (R^2), root mean square of prediction (RMSEP), standard error of performance (SEP), bias and offset were used to evaluate the validation model performance. Furthermore, graphical outputs such as loading plots, plots of the PLS regression coefficient with uncertainty limits, and scatter plots of the measured versus predicted wPI were also examined.

7.3 Results and Discussion

7.3.1 Geotechnical Characteristics

The soils exhibited a wide range of variability in their geotechnical characteristics. Weighted plasticity indices ranged from 2-67%. Figure 7-1 shows the variation in wPI of soil samples with station from the start of the newly planned route near TuluDimitu to its end at Nazret town. A trend line is fitted to show the direction of increase or decrease of wPI.

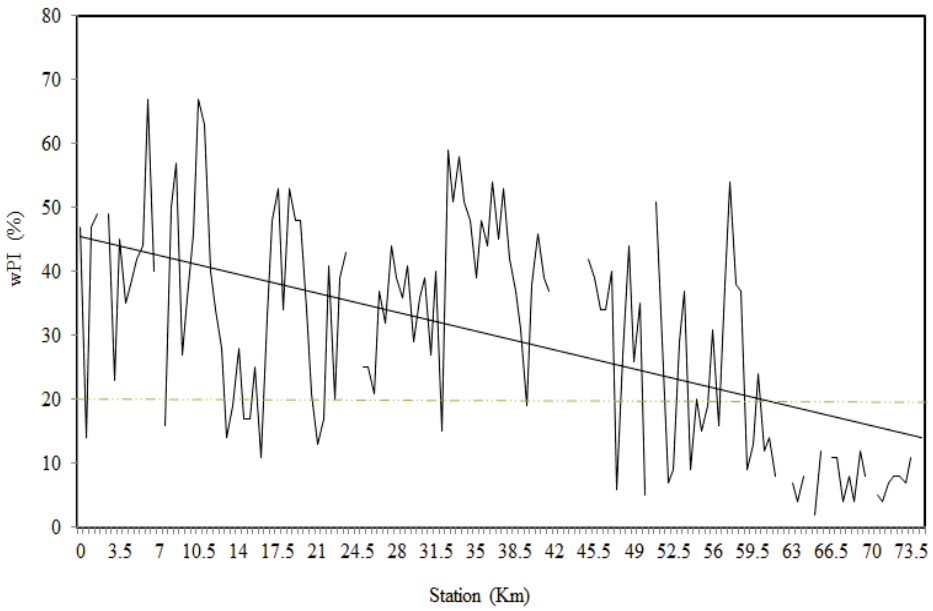

Station	Minimum	Maximum	Mean -%-	Standard deviation
0-60 km	5	67	34.8	14.3
60-80 km	2	24	8.7	4.6

Figure 7-1 Variation in wPI with a kilometer scale (station), from where the route starts till kilometer 80 where the route ends, with a line dividing high (wPI ≥20%) and low (wPI <20%) swelling and shrinkage potential; and an accompanying table presenting statistical descriptions of measurement. A trend line is fitted on the profile to show the trend of spatial variation.

Generally, wPI was high from 0-60 km of the expressway alignment with the majority of samples plotting above a wPI of 20%. Correspondingly, the swelling and shrinkage potential of soils along the 0-60 km of the alignment was high with highest peaks recorded for soil samples obtained at the beginning of the route (5-11 km). The wPI of the soils decreased from kilometer 60 onwards till the route ends at Nazret town. Soil samples from kilometer 60-80 mostly fall below a wPI of 20% line.

As described in chapter three, section 3.3.2, the mineralogical assemblage of the soils is strongly influenced by the presence of highly expanding 2:1 clay minerals such as montmorillonite, illite-montmorillonite (interstratified) and illite.

7.3.2 Relation between wPI and spectra, and mapping soil expansiveness

Overall accuracy of 70.5% with kappa coefficient of 0.62 for the 2008 image was obtained from the SAM classification. For the 2006 image, the overall accuracy was 65% with kappa coefficient of 0.56. A multivariate calibration on the 92 spectra extracted from the 2008 SAM stratified image resulted in the following equation:

wPI=(8.214+(3.595*b1)+(-3.174*b3)+(10.675*b4)+(-3.771*b7)+(-7.029*b8)+(-5.541*b9)) [7-2]

Where the b1….b9 refer to ASTER bands 1…9.

Four PLS factors were sufficient to establish the relationship. Figure 7-2A shows PLS correlation loadings of the first two factors (PC1 and PC2, at the X and Y-axis respectively). All variables plotted in-between the inner (which showed 50% of explained variance) and outer (which showed 100% of explained variance) ellipses. The bands that were statistically significant for estimating wPI are circled.

Figure 7-2B shows the PLS regression coefficients (plots of B-coefficients as no weighting is applied), with uncertainty limits (note the lines with whiskers fitted in each bar representing the bands). Coefficients close to zero with the uncertainty limits crossing the origin or zero line are unstable (Martens and Naes, 1989), hence not significant.

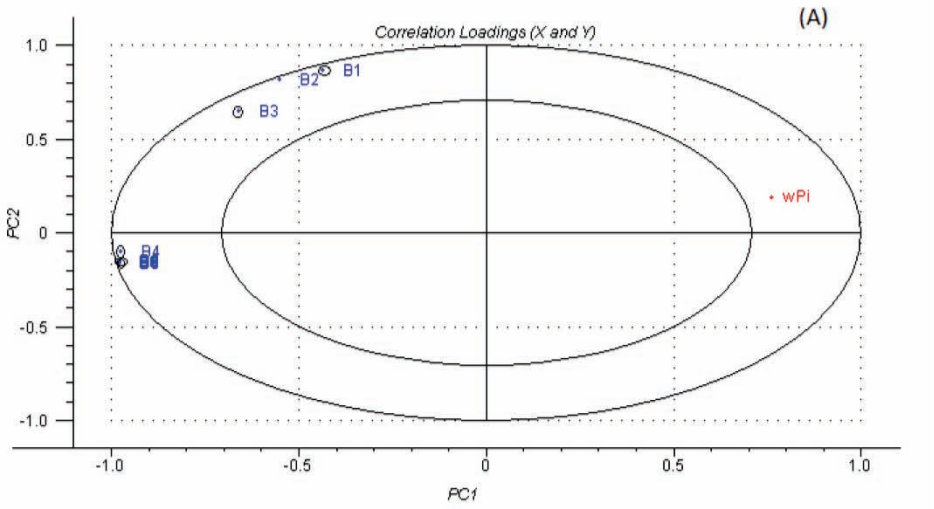

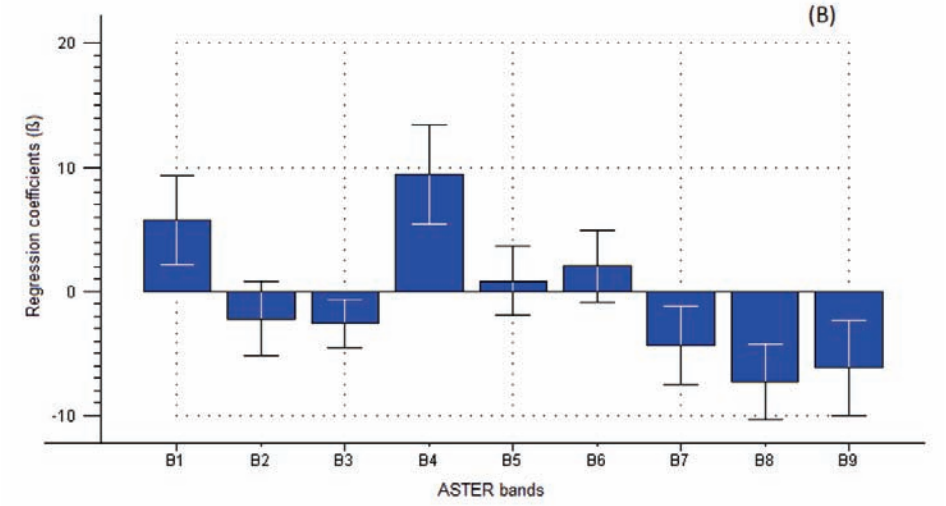

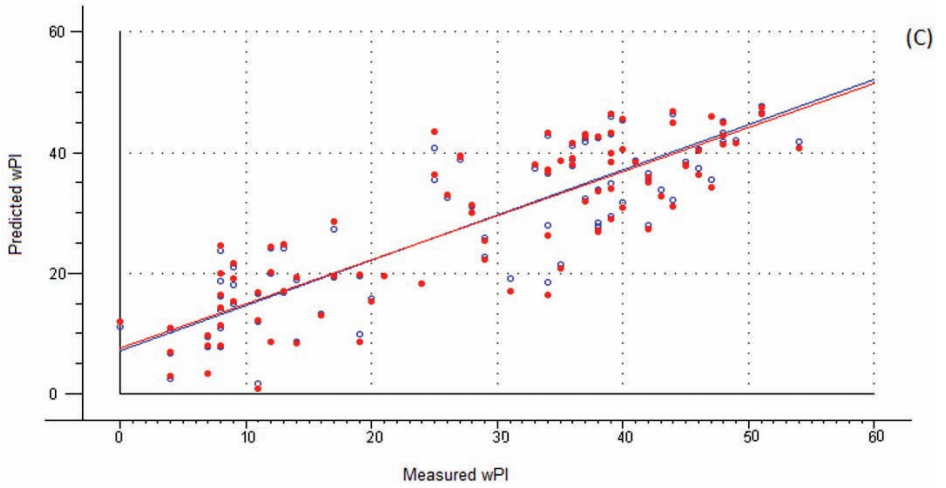

Model performance indices

	Calibration	Prediction
Coefficient of determination (R^2)	0.73	0.71
Root mean square of error of prediction (RMSE)	7.4	6.3
Standard error of performance (SEP)	7.4	6.3
Bias	-0.008	-0.004
offset	7.3	5.9

Figure 7-2 The PLS regression analysis results showing: (A) correlation loadings, (B) regression coefficients with uncertainty limits, (C) regression overview showing the relationship between measured and predicted wPI with model performance indices of the calibration and validation (prediction) stages summarized in an appending table. Open and solid circles in the regression overview represent calibration and validation (prediction) points respectively.

Among the significant predictors, ASTER bands one and four positively contributed while bands three, seven, eight and nine contributed negatively (7-2B). Organic matter and iron oxides show diagnostic spectral signatures in the VNIR wavelength region. Thus, the positive contribution from band one can be attributed to spectral signatures of organic matter and amorphous iron oxides (Bendor and Banin, 1994) that are present within the soil samples. Soils with high organic matter content are prominently sensitivity to water, which can cause high plasticity and shrinkage leading to a large compressibility and low strength (Holtz and Krizek, 1970; Odell et al., 1960). In addition, compaction is difficult in soils with appreciable amount organic matter (Malkawi et al., 1999). Malkawi et al. (1999) reported that maximum dry density (MDD) of soils with high organic matter is often extremely low, while their optimal moisture content (OMC) is high. They also noted a 100% swell increase at 20% organic matter increment, in illitic soils. This large water absorption capacity of such soils was attributed to the highly colloidal nature and thus large specific surface area of organic matter. Negative contribution of band three is probably linked to sand related spectral features, as well as absorption caused by the presence of iron oxides (Rowan et al., 2003). Positive contribution of band four, on the other hand, can be associated to spectral characteristics of kaolinite (e.g., halloysite varieties, which can exhibit some degree of swelling and shrinkage). The short wave infrared bands (bands seven, eight and nine) negative contributions might be due to absorption of clay minerals (such as montmorrilonite, nontronite, illite-montmorrilonite, illite) that showed spectral characteristics in the wavelength regions covered by these bands. Rowan et al., (2003) demonstrated that ASTER bands seven, eight and nine are dominated by metal (Fe, Mg)-OH absorption features.

Figure 7-2C shows the regression overview (of the measured versus predicted wPI) with accompanying table summarizing the model performance. A coefficient of determination (R^2) of 0.71 with accompanying root mean square error of prediction (RMSEP) of 6.3, standard error of performance (SEP) of 6.3, a bias of -0.004 and an offset of 5.9 were obtained. The result indicated that much of the variation in soil wPI could be accounted for by ASTER image derived soil reflectance spectra. The difference between calibration and validation (prediction) was not large, indicating that the model fitted the data well. According to the model performance indices, moderate prediction ability was observed over the range of samples used in this analysis.

Comparing direct measurement values of wPI (shown in Figure 7-1) with those obtained from the PLS prediction (depicted in Figure 7-3), a similar spatial trend of variation is observed. Note the trend lines showing a general decrease in wPI with station. Corresponding to the measured values, samples

from the 0-60 km stretch of the alignment showed high wPI (mostly above 20%). Most samples from kilometer 60 towards the end of the route plotted below the wPI of 20% line. Although a general similarity in spatial pattern of variations in soil swelling and shrinkage potential is observed, the prediction underestimated the wPI of soil samples from the 0-60 km stretch of the route. On the other hand, it slightly overestimated the wPI of soil samples from 60-80 km of the route.

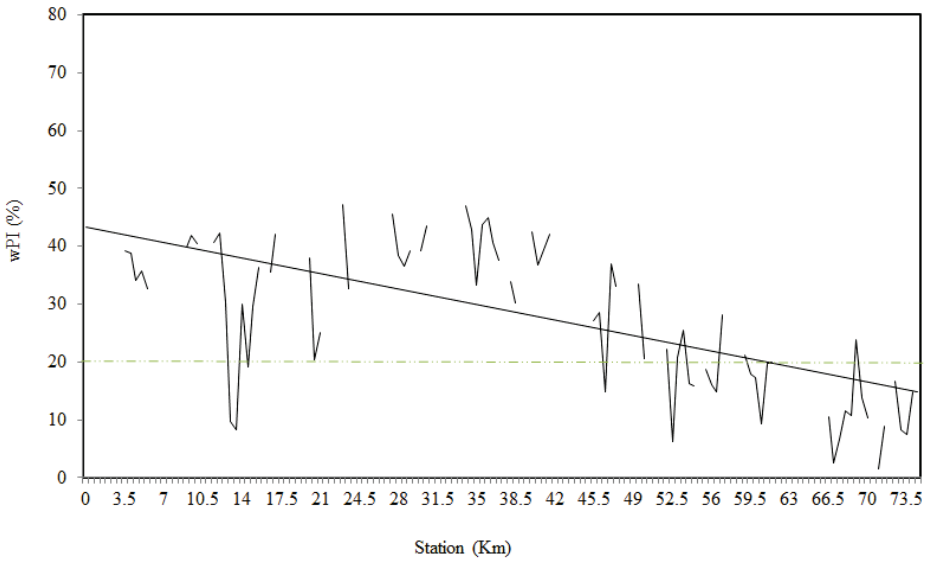

Station	Minimum	Maximum	Mean	Standard deviation
		-%-		
0-60 km	6.27	47.18	32.6	10.7
60-80 km	1.52	25.58	12.8	6.8

Figure 7-3 Variation in wPI of soil samples predicted from ASTER derived soil reflectance spectra, with a line dividing high (wPI ≥20%) and low (wPI <20%) potential expansiveness, and an accompanying table showing statistical descriptions of the prediction. A trend line is fitted on the profile that shows the trend of spatial variation.

The underestimation and overestimation is depicted in the tables summarizing descriptive statistics of measurement and prediction respectively. Mean of predicted wPI was lower than that of measured in the 0-60 km; on the other hand, mean of predicted wPI was higher than that of measured in the 60-80 km stretch of the route. Note also the differences in the minimum and maximum values. Although there was an underestimation in the 0-60 km, standard deviation of the prediction was narrow. Standard

deviation of the prediction for the 60-80 km stretch of the route was larger than that obtained for measured values.

Map of weighted plasticity indices of soils of the study area is presented in Figure 7-4. The red color indicated soils with wPI≥20%, thus potentially highly expansive. The blue color showed soils with wPI<20%, accordingly low swelling and shrinkage potential. Blue pattern around Addis Ababa city towards Kaliti in the map indicates that soils in this vicinity are of lower swelling and shrinkage potential. However, previous studies (GSE, 1990) indicated that these areas are extensively covered with black cotton soils, which exhibit a high degree of swelling and shrink potential. As the areas are urbanized places, surface soils can be influenced or contaminated with imported material (probably gravel and natural select materials, sand, crushed aggregates etc.) for construction purposes. Perhaps this is a possible explanation as to why the map showed soils of lower swelling and shrinkage potential in these areas.

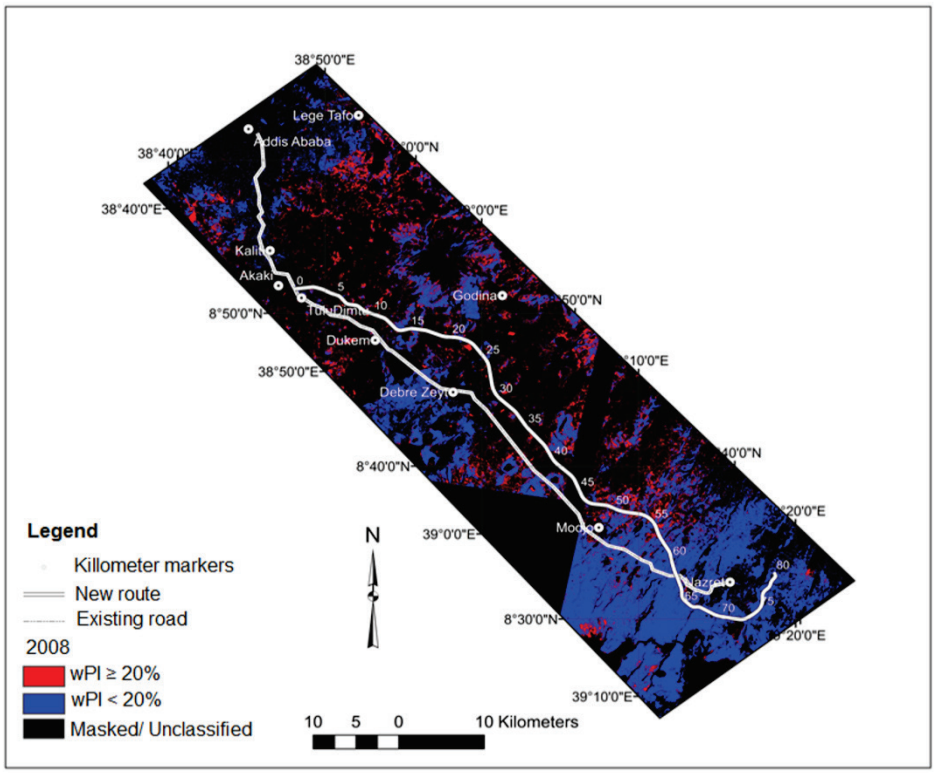

Figure 7-4 Map of weighted plasticity index of soils of the study area derived from 2008 image. The red color represents areas with wPI ≥20% and blue color those with wPI <20%. The dark color represents pixels that are either masked or unclassified (both representing non soil surface cover that are not of interest). Diagonal bar in between DebreZeyit and Modjo is an area that was not covered by the ASTER scenes.

7.3.3 Testing the prediction repeatability with a separate image

Reflectance characteristics of soils recorded in image data can be affected by several factors that might interfere with soil spectral signatures (Sullivan et al., 2005). These factors include: observing conditions, which are related to effects of atmospheric conditions and topographic variation; instrument and atmospheric calibration uncertainties, which can contribute to the difficulty of achieving accurate surface reflectance; physical conditions of soil cover such as soil moisture, texture and surface conditions; mixed pixels, which might contribute to the impurity of spectral signatures, more so in broad band imagery like ASTER; data quality or signal to noise ratio; difficulty of accounting for subtle spectral variations of soil forming minerals, which can be the cumulative result of the aforementioned factors etc.

Applying equation [7-2] on the SAM stratified 2006 ASTER image resulted in wPI map shown in Figure 7-5. The two weighted plasticity index maps outputted from ASTER scenes of different years were not in perfect agreement, similarities and differences were observed. As with Figure 7-4, majority of Figure 7-5 also falls in the high weighted plasticity index class (wPI ≥20%) denoted by red color. Spatial relationships between the two maps are presented in a profile (Figure 7-6), which showed moderate correspondence. The upper portions of both maps seemed more similar than the lower portions. The wPI values of soils from kilometer 50 onwards of those from 2006 map were generally low (wPI<20%). In the 2008 map, soils from this stretch exhibited some degree of plasticity although the wPI is mostly <20%.

Apart from differences arising from surface cover variations in the two scenes, other possible sources of discrepancy can be factors that might interfere in soil spectral responses recorded by imaging device. Spectra of soils from the 2008 and 2006 ASTER images are shown in Figure 7-7. Spectra from the 2008 scenes appeared darker than those from the 2006 scenes. Absorption features also showed subtle differences (note the differences between spectra in each pair).

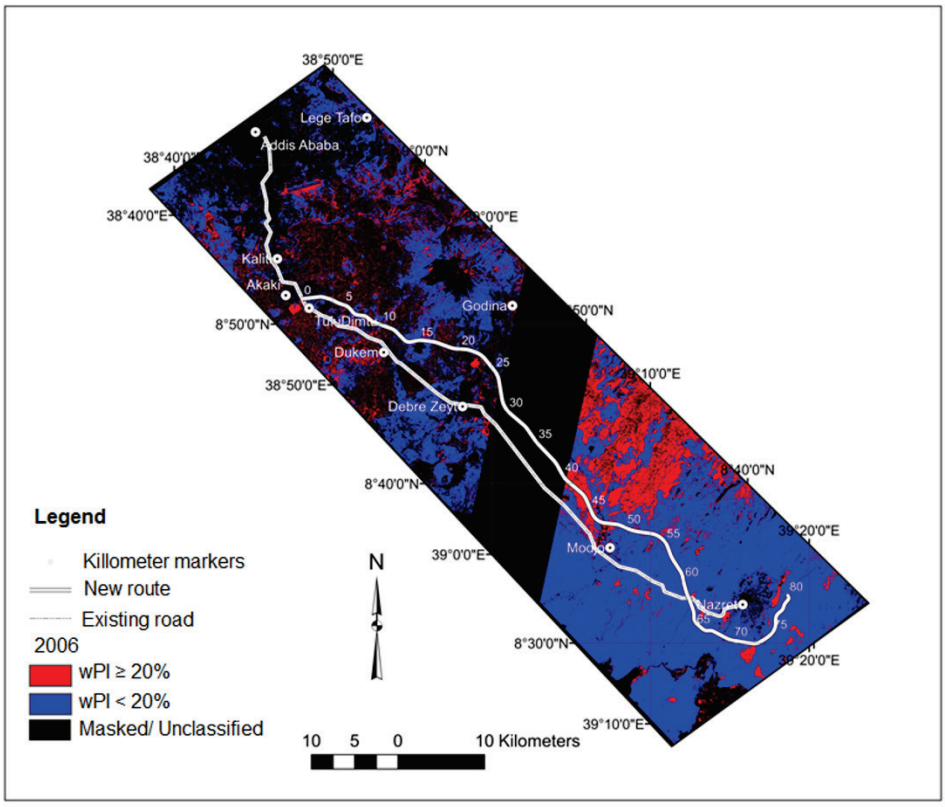

Figure 7-5 Map of weighted plasticity index of soils of the study area derived from 2006 images. The red color represents areas with wPI ≥20% and blue color those with wPI <20%. The dark color represents pixels that are either masked or unclassified (both representing non soil surface cover that are not of interest). Diagonal bar in between DebreZeyit and Modjo (wider here) is an area that was not covered by the ASTER scenes.

Aggregating wPI values from the two maps shown in Figure 7-4 and 7-5 using soil map units from Figure 2-5 clearly illustrated differences in magnitude of wPI in the 2008 and 2006 maps respectively (Figure 7-8A and 7-8B). Figure 7-8A and 7-8B was used only for the sake of illustrating similarities and dissimilarities between the two wPI maps. The figure has no implication on plasticity characteristics of different soil units due to the coarse scale of the soil map and hence generalizations of soil map units. Andosols, in both 2008 and 2006 maps, exhibited lower wPI but showed larger variability in the wPI map derived from the 2008 image than in the wPI map derived from the 2006 map. Luvisols exhibited the highest wPI values in both cases, but with larger variability and lower mean in the 2006 than in the wPI map derived from 2008 image. Mean wPI of vertisols from the 2008 map was higher than those in the 2006 map, while smaller variability was apparent in

the former. The variability towards higher wPI values was large in the wPI map derived from the 2006 image.

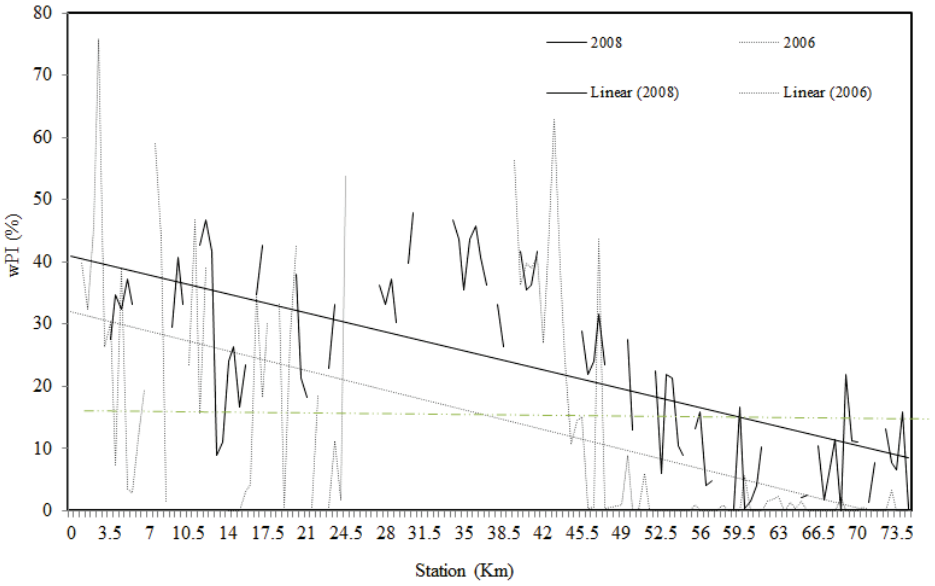

Figure 7-6 Variations in weighted plasticity indices from the two images (2008 and 2006). Although the profiles differ in absolute values of wPI, the trend lines showed a similar spatial trend of variation (that wPI decreased with station).

Further, comparison of similar locations from the 2008 and 2006 wPI maps showed a statistically highly significant, moderate degree of correspondence (Table 7-2). Although the trends of variation in wPI seemed broadly similar in both maps, differences in magnitudes and variability signified the effect of factors that may have influenced the soils spectral signatures recorded in the image data.

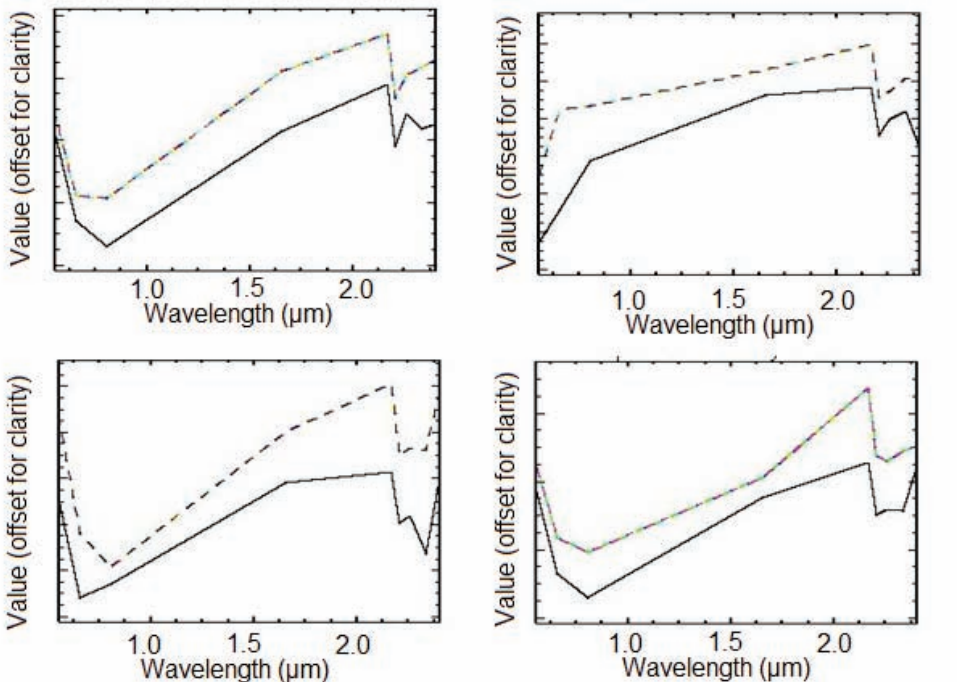

Figure 7-7 Spectra of soils from ASTER images of the year 2008 (solid lines) and 2006 (dotted line) respectively. Each pair of spectra is from similar locations in the two scenes.

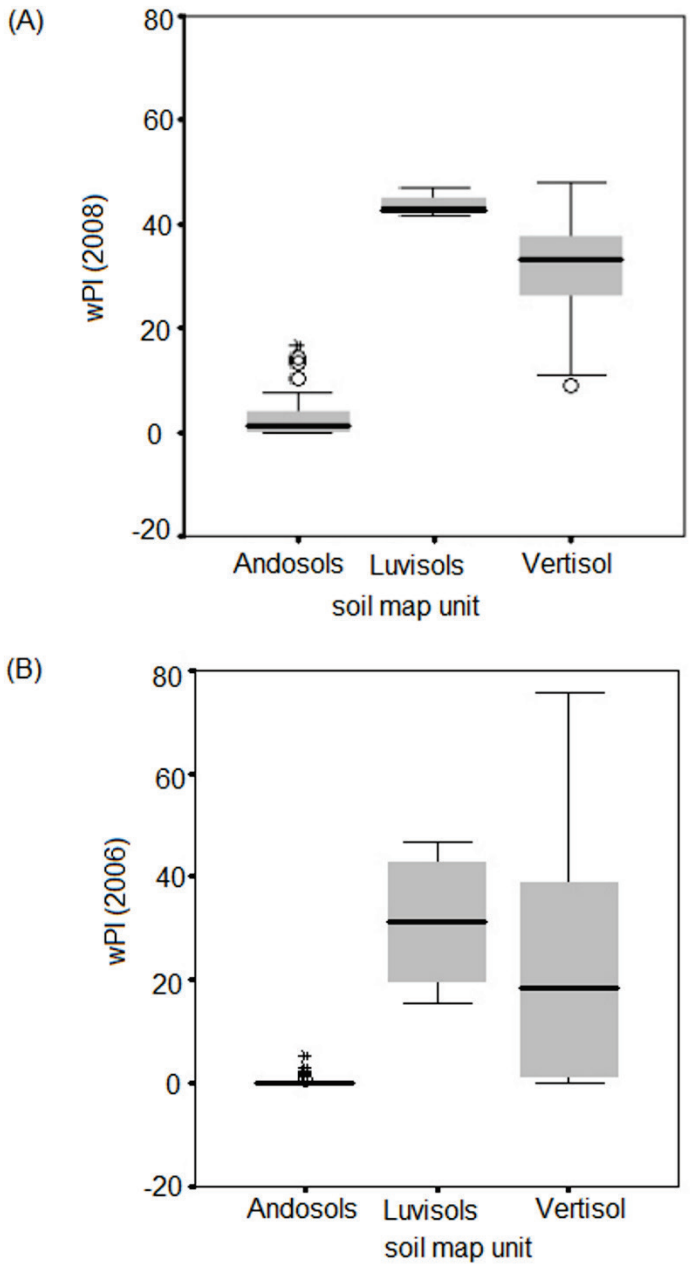

Figure 7-8 (A) Boxplots showing values of wPI aggregated by soil map units. Note the differences in means and variability (spread in magnitude of wPI) in the 2008 and (B) 2006 images respectively.

Table 7-2 Relationship between similar locations from the 2008 and 2006 wPI maps indicating a highly statistically significant moderate correlation.

Correlations

		2006	2008
2006	Pearson correlation	1	
	Sig. (2-tailed)		
	N	109	
2008	Pearson correlation	0.646**	1
	Sig. (2-tailed)	0.000	
	N	64	92

** Correlation is significant at the 0.01 level (2-tailed).

7.4 Conclusions

The use of ASTER data for mapping variation in magnitude of soil expansiveness was evaluated. A coefficient of determination R^2 of 0.71 accompanied with small RMSEP and SEP, negligible bias and small offset were obtained. These model performance indices indicated significant correlation between wPI and ASTER derived soil reflectance spectra, and a moderate prediction ability over the range of soil samples used in this study. Thus, ASTER VNIR and SWIR bands can be used for mapping geotechnical characteristics of soil that depend on clay mineralogical assemblage. A continuous surface showing quantitative variation in a geotechnical parameter of interest (wPI) rather than set of discrete point values was presented in the maps. From a geotechnical point of view, the approach can be of significance. This is in a reconnaissance and technical feasibility studies, preliminary site investigation schemes and basic assumption of parameters such as subgrade characteristics, which in turn influence preliminary choice of possible road alignments, structures and associated cost estimates, search for construction materials such as borrow and sub-base etc.

However, mapping spatial variability of soil geotechnical characteristics from multispectral remote sensing data seemed to be confounded by different factors interfering in the spectral response of soils recorded in images. Therefore, further research is required to investigate and account for factors influencing soil spectral characteristics at broad band image level; and thereby finding a way of optimizing prediction of geotechnical properties and mapping their spatial variability.

Chapter 8

Synthesis

8.1 Introduction

Geotechnical information is the basis for much of the costs (in terms of economy and time at the design, construction and maintenance stages) of engineering works. Safety of structures is also determined by the quality of the project site geotechnical information. Expansive soils in construction sites are an immense problem that require due consideration in geotechnical investigation. Therefore, detecting the presence of expansive soils and determining their geotechnical characteristics such as evaluating their potential to swelling and shrinkage are imperative to infrastructure development.

The objectives in this research were:

1) To investigate relationships among geotechnical parameters of expansive soils; and establish an empirical prediction model for estimating and rating swelling and shrinkage potential of soils from routinely determined parameters (addressed in chapter three).

2) To investigate the engineering benefits of the VNIR and SWIR laboratory spectroscopic and multispectral remote sensing techniques for identifying expansive soils and quantifying soil geotechnical characteristics; thereby producing maps showing the spatial distribution of expansive soils and variability in their geotechnical characteristics (addressed in chapter four and seven).

3) To determine spectral characteristics of (pure) active clay minerals (those that are influential in dictating soil swelling and shrinkage characteristics) and mixtures, in the mid infrared (MIR) wavelength region (addressed in chapter five).

4) To establish the potential of spectroscopy in the mid infrared (MIR) wavelength region for characterizing (i.e., identification, classification and estimation of geotechnical parameters) expansive soils (addressed in chapter six).

Investigating the geotechnical and spectral characteristics of expansive soils, and establishing relationships between the two, requires an understanding of the principal factors determining soil swelling and shrinkage potential. Although several factors contribute to soil swelling and shrinkage

characteristics, clay mineralogical composition and clay mineral content are the most fundamental (McCormack and Wilding, 1975; Mitchell, 1993; Pascal et al., 2004; Yong and Warkentin, 1975). Clay minerals also influence the spectral characteristics of soils to a large extent (Chabrillat et al., 2002; Clark, 1999; Van der Meer, 1999). Thus, analyses of soil clay mineralogical assemblage provide an opportunity to relate soil geotechnical and spectral characteristics.

A number of steps were required to accomplish the objectives of this research. An extensive fieldwork and soil sampling was carried out. Subsequently, geotechnical characteristics of the soil samples were determined following appropriate standard procedures. Apart from consistency limit tests, the soils expansion and shrinkage potential were assessed in terms of expansion index (EI). Mineralogical and chemical compositions of the soils were also analyzed by conventional methods such as X-ray diffraction (XRD) and X-ray fluorescence (XRF) analyses. Laboratory spectral analyses were carried out to determine spectral characteristics of the soils. Spectra of soil samples were acquired across the VNIR, SWIR and MIR wavelength regions (0.35-14 µm). In the VNIR and SWIR, the ASD FieldSpec full range spectrometer; and in MIR, the Bruker Vertex 70 Fourier transform infrared spectrometer was used. Relationships among the soils geotechnical parameters and spectral characteristics were explored using various statistical analyses techniques.

This chapter summarizes the main findings of the research based on the results of chapter three to seven. The issue of soil geotechnical classification and role of remote sensing techniques for identification and characterization of expansive soils are outlined. General conclusions derived from the research findings are also given. Additionally, further research directions are put forth.

8.2 Soil geotechnical classification system

The expansive soils of Ethiopia were discussed in chapter two. Problems associated to the detrimental geotechnical characteristics of expansive soils were also illustrated. The problems range from minor cracks to total structural failure in roads and buildings. Large scale instabilities and landslide problems are also common in naturally exposed and cut slopes with expansive soils or clay horizons. The environmental conditions such as geology, topography and climate of the study sites appeared to be convenient for the formation of active clay minerals, thus expansive soils (chapter two).

The issue of geotechnical characterization of expansive soils was addressed in Chapter three. Commonly, this involves establishing correlations and

classification methods; mainly from routinely determined parameters such as consistency limits and particle size distribution tests. A number of indirect relationships and evaluation procedures are available (ASTM, 2006, 2007; Cokca and Birand, 1993; Dakshanamurty and Raman, 1973; Erguler and Ulusay, 2003; Erzin and Erol, 2007; Gray and Allbrook, 2002; Kariuki and Van der Meer, 2004; Nelson and Miller, 1992; Seed et al., 1962; Thomas et al., 2000; Yilmaz, 2006). However, no single method was found to be applicable with the same degree of success for evaluating soils originated from various geographic regions. Soil forming factors such as parent material, climate, topography, time and organisms (Breemen and Buurman, 2003; Fitzpatrick, 1980) differ from one geographic region to another. These factors are responsible for variations in relative abundance of exchangeable cations such as Na, Ca, K, Mg, Fe in soils. In turn, differences in exchangeable cations among soils are attributable to a large variability in soils plasticity, cation exchange capacity and related geotechnical characteristics including swelling and shrinkage potential (Chen, 1988; Nelson and Miller, 1992).

In chapter three, expansion indices (EI) of soils were related to plasticity and grading characteristics. Consistency limits (liquid limits and plasticity indices), and of the grading characteristics, fine fraction, which is the percentage of soil samples passing through the ASTM 0.075 mm sieve aperture, were used to establish a geotechnical soil classification system. The used parameters reflect as also demonstrated by domain of experts in geotechnical engineering, the clay mineralogical composition and content in the soils. Thus, these parameters were directly relevant to differences in soil swelling and shrinkage characteristics. The newly established multivariate empirical soil geotechnical classification system is the first for soils of Ethiopia. It modeled the fuzzy interrelationship among soil geotechnical parameters and showed better prediction ability than previously proposed models (e.g., that of Zapata et al. (2006) based on univariate relations).

8.3 Remote sensing techniques

8.3.1 The VNIR and SWIR wavelength region

Problems due to soil swelling and shrinkage characteristics are mostly related to overlooking the presence of expansive soils (Al-Rawas and Qamaruddin, 1998; Gourley et al., 1993; Nelson and Miller, 1992; Paige-Green, 2008). Once the presence of such soils is ascertained and their potential for swelling and shrinkage is quantified, proper mitigating geotechnical practice can be exercised. At a broad scale, delineating the spatial occurrences of expansive soils is important for sound spatial land-use planning and management activities especially in relation to lightweight infrastructure development.

Spectroscopy in the VNIR and SWIR wavelength region showed a significant potential for characterizing expansive soils. Water absorption features such as those at ~1.4 µm and ~1.9 µm are prominent features of clay minerals and crucial in a laboratory scale application. Of importance for a field and image applications are the features that occur in the 2.1-2.5 µm (Chabrillat et al., 2002; Clark, 1999; Goetz et al., 2001; Kariuki et al., 2004; Yitagesu et al., 2010; Yitagesu et al., 2009b, 2011c) wavelength region. According to Clark (1999) and Hunt (1977), absorption features in the 2.1-2.5 µm wavelength region are due to the stretching and bending combinations of the OH group bond with metal (Al, Mg, Fe), and are diagnostic of clay minerals. Slope differences related to the influence of organic matter (Bendor and Banin, 1994) and variation in SiO_2 content (Viscarra Rossel et al., 2006) were evident in the 0.35-1 µm wavelength region. These features appeared as significant spectral indicators in estimating soil geotechnical characteristics.

Chapter seven addressed the aspect of direct, remote sensing mapping of soil geotechnical parameters. The possibilities of assessing soil geotechnical characteristics and their variations were investigated using ASTER data acquired at different times (during dry seasons in January 2008 and March 2006). ASTER has an optimal-band setting and spectral resolution that makes it suitable for surface mineral identification and mapping such as clay minerals, iron oxides, carbonates and other common rock forming silicates (Bourguignon et al., 2007; Hewson et al., 2005; Rowan et al., 2003; Tangestani et al., 2008). Recent studies (Vicente and de Souza, 2011) demonstrated strong correlations (R^2 of up to 0.80) among laboratory acquired and ASTER image pixel derived soils spectra.

Statistically significant and moderate in terms of correlation coefficient, data structure (refer to the regression overview in Figure 7-2C), and error terms (RMSEP, SEP and offset) were obtained. Coincident with the definition of weighted plasticity index, bi-color maps of division ≥20% (high potential to swelling and shrinkage) and <20% (low potential to swelling and shrinkage) were produced. The results signified the potential capability of ASTER VNIR and SWIR bands for mapping soil geotechnical characteristics. While the prediction model was developed using images acquired in 2008, the repeatability of the approach was tested with a separate scene acquired in 2006. Statistically significant (at a p-value of less than 0.01 significance level), moderate correlation was observed between the maps derived from the two images. Since soil geotechnical characteristics do not change much within such a short time span, the soils swelling and shrinkage potential is considered representative. The observed differences are probably related to factors influencing the spectral signatures of soils that were mentioned in chapter seven, section 7.3.3. For optimization of this approach, further research is required addressing the aspects of atmospheric effects, variation

in topography, differences in illumination, vegetation cover, and changes in surface conditions (heterogeneities induced by differences in soil moisture and textural or surface roughness variations), etc. In this respect, investigating datasets from different sensors, acquired in temporal bases, in areas having diverse terrain characteristics, land cover and soil surface conditions accompanied with real-time field observations might contribute towards developing reproducible procedures or results. In spite of the need of additional research, the results of this study indicated the potential of ASTER and similar multispectral missions for mapping soil geotechnical characteristics.

Mineralogical differences were observed among soil samples from Addis Ababa and Addis Ababa-Nazret study sites (chapter three and four). Smectite appeared to be dominating the most expanding soils of Addis Ababa study site. Smectite and interstratified illite-smectite clay mineral varieties constituent the highly expanding soils of the Addis Ababa-Nazret study site. Kaolinites account for the compositions of medium and low expanding soils of the Addis Ababa study site. Illite was abundant in the moderate and low expanding soils of the Addis Ababa-Nazret study site. The laboratory spectroscopic analysis on the Addis Ababa soils and multispectral remote sensing analysis on the Addis Ababa-Nazret soils revealed differences in spectral characteristics, which were reflected by the magnitude of correlations among spectral and geotechnical characteristics, and significant predictor wavelength regions. Of interest are the features at wavelengths longer than 2.2 µm, which are diagnostic of smectite and illite (Chabrillat et al., 2002; Kariuki et al., 2004). Since the features particularly of illite are normally weak, their significance reflected strong presence of this clay mineral, which according to Kariuki et al. (2004) could be assigned to be indicative of low to moderate soil swelling and shrinkage potential. The strength of correlations among the soils spectra and wPI can be attributable to the abundance and strong influence of 2:1 clay minerals that also show spectral signatures in the wavelength region longer than 2.2 µm. Yitagesu et al. (2008b) showed correlations among soil spectral and geotechnical characteristics, which were strong in smectitic soils and extremely low in soils dominated by kaolinite. Presence of substantial amount of smectite and kaolinite together tends to mask diagnostic absorption features ~2.2 µm (Kariuki et al., 2004), and result in lower correlations. It should also be noted that spectral indicators (significant wavelength regions for predicting soil swelling and shrinkage potential) may vary depending on the nature and environmental conditions (related to soil forming factors) that clay minerals are formed. As physicochemical properties of clay minerals are influenced by their origin (Galan, 2006), their spectral characteristics are also similarly influenced (Post and Noble, 1993) a conclusion, which was also shared by Kariuki et al. (2004). Post and Noble (1993) presented shifts in wavelength

positions in montmorillonite and illite spectra depending on relative abundance of Ca and Na, as well as Al and Si at ~2.2 µm. Thus, spectral-geotechnical relationships should take into account such variability that may occur due to differences related to site specific soil forming factors.

8.3.2 The MIR wavelength region

Spectral characteristics of pure active clay minerals and mixtures were determined, in the MIR wavelength region (chapter five). The established spectral characteristics provided fundamental knowledge on the spectral responses of active clay minerals and variations in mixtures. These spectral features were in turn, used to comprehend spectral manifestations of active clay minerals in expansive soils (chapter six). In the MIR wavelength region, clay minerals exhibited additional, distinct spectral features that appeared diagnostic (chapter five and six). Spectral discrimination and subsequent characterization of clay minerals and expansive soils showed a high degree of success as evidenced by the statistical measures of associations (chapter five and six). From the results presented in chapter six, closer agreement was evidenced among geotechnical parameters and spectra of fine fraction soil samples than spectra bulk soil samples.

Emphasis was given to spectral characteristics of active clay minerals and expansive soils in the 3-5 µm and 8-14 µm wavelength regions, for providing an outlook for field, airborne or satellite remote sensing applications. Several characteristic spectral signatures were observed in these two atmospheric windows. Among the most intriguing is the feature that appeared in the presence of illite. In the 3-5 µm wavelength region, spectra of illite exhibited a doublet feature (with absorption minima at ~3.84 µm and ~3.98 µm). Illite showed overlapping features with montmorillonite in the VNIR and SWIR wavelength region, due to commonality, probably in the structural arrangement. Interstratified clay mineral varieties, such as mixed layer montmorillonite-illite, showed characteristic absorption feature at ~3.98 µm. Whereas, in the VNIR and SWIR wavelength regions, these interstratified clay mineral varieties appeared as montmorillonite or illite. Thus, better differentiation of illite and interstratified clay mineral varieties can be achieved in the MIR wavelength region.

In view of active clay minerals, the presented study in the MIR wavelength region (chapter five) provided a basic understanding of spectral characteristics of clay minerals and mixtures dictating soil swelling and shrinkage characteristics. Thereby, quantitative clay mineral abundance estimations were established. The results showed that MIR spectroscopy can be an indispensable tool for analyzing clay minerals. Extending the approach for characterizing soils (chapter six) provided new insights that had not been

previously explored for a geotechnical application of spectroscopy in the MIR wavelength region.

8.4 Expansive soil characterization and mapping: an integrated approach

The approach presented in this thesis has dealt with three fundamental issues that are crucial to fully appraise the problem of soil swelling and shrinkage characteristics. These issues are:

1) Identifying potentially expansive soils
2) Quantifying geotechnical characteristics of expansive soils.
3) Delineating the spatial occurrence of expansive soils and variability in their geotechnical characteristics.

As soil swelling and shrinkage potential is an intrinsic property related to the presence and abundance of active clay minerals, soil mineralogical composition analysis is critical. Differences in compositions, structural arrangement, and related physicochemical properties are the basis for spectral discrimination of active clay minerals in expansive soils (chapters four, five and six). Clay minerals show characteristic spectral features across the VNIR, SWIR and MIR (0.35-14 µm) wavelength regions. Table 8-1 shows a summary of the spectral characteristics of clay minerals in these wavelength regions.

It has been shown that several soil geotechnical parameters can be estimated from spectra. The used geotechnical parameters are direct design inputs and are commonly used for routine quality control of construction material. Partial least squares (PLS) regression analysis was used to link spectra of soils and clay mineral mixtures to geotechnical characteristics and mineralogical content. The PLS regression coefficients showed significant wavelengths that are relevant for establishing relationships among spectra, geotechnical characteristics and abundance of clay minerals.

Apart from contributing to the knowledge required for establishing spectral-compositional and spectral-geotechnical relationships, several aspects of the practical relevance of the results of this research can be mentioned. In general, the outputs such as the new geotechnical classification and soil swelling and shrinkage potential rating system (chapter three); the spectroscopic identification and characterization methods presented in chapters four, five and six; and the wPI maps (showing the swelling and shrinkage potential of the soils) presented in chapter seven, can provide geotechnical engineers and planners with easy to use, alternate means of assessing the geotechnical behavior and performance of soils.

Table 8--1 Summary of spectral characteristics of the three clay minerals that are most influential for soil swelling and shrinkage potential: montmorillonite, illite, and kaolinite in the 0.35-14 µm wavelength region.

Clay minerals	Spectral characteristics	
	0.35 – 2.5 µm wavelength region	2.5 -14 µm wavelength region
Kaolinite	~1.4 µm & ~ 1.45 µm** ~2.17 µm & ~2.21 µm** ~ 1.9* µm	2.5-3.7 µm† ~3.69 µm ~4.7 µm ~5.2 µm & ~5.5 µm** ~6.3 µm†† ~8.6 µm ~9.4 µm†† ~9.8 µm ~10.6 µm ~11.7 µm†† ~12.4µm
Illite	~1.4 µm ~1.9 µm ~2.2 µm ~2.34 µm ~2.45 µm	2.5-3.7 µm ‡ ~3.48 µm ~4.67 µm ~3.84 µm & ~3.98 µm** ~5.56 µm ~6.1 µm
Montmorillonite	~1.4 µm ~1.9 µm ~2.2 µm	2.5-3.7 µm‡ ~4.3-5 µm ~5.1 µm & ~5.4 µm ** ~6.1 µm ~8.1 µm

* None (in kaolinite varieties due to lack of structural water molecules) to less well-resolved (in halloysite, which is water bearing variety).
** Doublet features (the doublet for halloysite variety kaolinitic clay minerals is at ~1.39 µm & ~1.41 µm, and ~2.18 µm & ~2.21 µm).
† With sharply defined absorption minima at ~2.75 µm
†† Reflectance peaks
‡ With absorption minima at ~2.75 µm and ~3.1 µm in montmorillonite; generally broad in illite.

The laboratory spectroscopic techniques were found to more precisely describe soil geotechnical characteristics than the multispectral image approach. Thus, they are more promising for integration in the routine geotechnical analyses of expansive soils than the latter. The multispectral image approach can also play a significant role for large-scale estimates of soil geotechnical parameters such as subgrade characteristics, which can be useful in site selection, route planning and the search for construction materials, such as borrow and sub-base. More important, at the early stages of project planning, preliminary site investigation, feasibility studies, and design stages, essential information can be obtained. The approach can contribute towards an appropriate scoping of the feasibility and detailed site investigation schemes, to be focused on problematic areas. Therefore, information from remote sensing techniques can be utilized to reduce the time and costly consequences related to overlooking the presence of expansive soils in construction sites.

Overall, remote sensing techniques provide a unique opportunity for identifying clay mineralogical compositions of expansive soils, estimating and mapping their geotechnical characteristics, which could be previously possible only via combining two or more techniques.

8.5 Research outlook

Four main points of research that require additional investigation are identified. These issues are suggested for furthering the understanding on various aspects that are essential to deal with the problem of soil swelling and shrinkage characteristics.

1) Currently there appears to be a lack of universal standard in employing spectroscopic techniques for various applications such as characterizing geologic materials including soils. Developing standard systems that can be universally applicable for soil spectroscopic measurement is a crucial step towards rationalizing the technique for a more comprehensive utilization. Sample preparation and number of scans are some of the issues that need additional in-depth investigation. Various researchers reported different procedures of sample preparation such as oven-drying versus air-drying and grinding versus sieving. Generally the signal to noise ratio of a spectrum is proportional to the square root of measurement time or number of scans (Griffiths and de Haseth, 2007). However, there is no single universal standard regarding the number of scans to be used. Rather, different numbers of scans (256, 320, 512, and 1000 etc.) with different spectrometers were reported (da Luz and Crowley, 2007; Johnson et al., 1998; Rivard et al., 1995; Ventura and Papini, 1999). Therefore, it is indispensable to determine these and related measurement issues in soil spectroscopic analysis.

2) Apart from crystalline clay minerals that were investigated in this research, non-crystalline clay minerals such as allophane and imogolite should also be studied. The influence of allophane and imogolite on soil properties were reported (Allbrook, 1985; Gray and Allbrook, 2002; Wada, 1977; Wan et al., 2002; Zehetner et al., 2003). These non-crystalline clay minerals are commonly found in soils developed from volcanic ashes and pyroclastic deposits (Yerima et al., 1987). Research on the influence of such non-crystalline clay minerals on geotechnical behavior and spectral characteristics of soils can contribute to advance the knowledge and understanding of the nature, geotechnical and spectral behavior of expansive soils.
3) In addition to lateral (surface) variations, soil geotechnical characteristics often show marked differences vertically (subsurface) (Bell, 2000). It is also crucial to determine the depth of the active zone, which is the depth at which moisture content fluctuations occur associated with substantial volume changes (Chen, 1988; Reznik, 1998). Below this active zone, moisture content does not change under the influence of saturation and evaporation, making the determination of this depth critical in considering counteracting remedial measures against expansive soils. Thus, the problem of soil swelling and shrinkage is three-dimensional that requires a 3D visualization of the problem. In this respect, integration of remote sensing methods proposed in this research with geophysical imagining techniques can be considered. The latter are commonly used for subsurface geotechnical exploration purposes. Geophysical imaging has a principal advantage of recording subsurface conditions from the ground surface at a relatively low cost (Hunt, 1984). Apart from the economic benefit, geophysical methods can give general information over a large area and could be suitable options for determining depth of active zone.
4) Existing knowledge on the spatial distribution and factors determining the variability in geotechnical characteristics of expansive soils of Ethiopia is limited. Research on developing a multi-criteria modeling system (such as evidential predictive modeling and logistic regression approaches) for predicting the spatial occurrences of expansive soils is critical. Combining information of environmental variables such as geology, terrain or landforms, drainage, climate and other relevant factors can add a lot into advancing an understanding of the nature, spatial distribution and variability in swelling and shrinkage potential of expansive soils. In practice, the output from such an analytical approach can support sustainable land-use planning and management activities. Despite the complexity of the problem, remote sensing data (such as multispectral images and digital elevation models, DEMs) and ancillary information collected from decades of construction activities can be utilized. Models that can be developed may also be extrapolated elsewhere with adjustments of specific parameters.

References

Abebe, B., Dramis, F., Fubelli, G., Umer, M., and Asrat, A., 2010, Landslides in the Ethiopian highlands and the Rift margins: Journal of African Earth Sciences, v. 56, p. 131-138.

Abebe, T., Franscesco, M., Fabrizio, I., and Piero, M., 1999, Geological Map of DebreZeyt Area (Ethiopia): Addis Ababa, Geological Survey of Ethiopia (GSE).

Abrams, M., 2000, The Advanced Spaceborne Thermal Emission and Reflection Radiometer (ASTER): data products for the high spatial resolution imager on NASA's Terra platform International Journal of Remote Sensing, v. 21, p. 847-859.

Ahmad, N., 1996, Vertisols and technologies for their management *in* Ahmad, N., and Mermut, A., eds., Developments in soil science Volume 24: Amsterdam, Elsevier science B.V.

Al-Mukhtar, M., Lasledj, A., and Alcover, J.-F., 2010, Behavior and mineralogy changes in lime-treated expansive soil at 20 °C: Applied clay science, v. 50, p. 191-198.

Al-Rawas, A.A., 1999, The factors controlling the expansive nature of the soils and rocks of northern Oman: Engineering Geology, v. 53, p. 327-350.

Al-Rawas, A.A., and Goosen, M.F.A., 2006, Expansive soils: recent advances in characterization and treatment: Leiden, Taylor & Francis, 526 p.

Al-Rawas, A.A., and Qamaruddin, M., 1998, Construction problems of engineering structures founded on expansive soils and rocks in northern Oman: Building and Environment, v. 33, p. 159-171.

Allbrook, R.F., 1985, The effect of allophane on soil properties: Applied clay science, v. 1, p. 65 - 69.

Arnold, G., 1991, Measurements of the Spectral Emittance of Particulate Minerals and Some Remote-Sensing Implications: Vibrational Spectroscopy, v. 2, p. 245-249.

ASD, 1995, Analytical Spectral Devices (ASD): Technical Guide, Portable Spectroradiometers, Analytical Spectral Devices, Inc.

ASTM, 2006, ASTM D2487-06 Standard Practice for Classification of Soils for Engineering Purposes (Unified Soil Classification System), American Society for Testing and Materials (ASTM).

ASTM, 2007, ASTM D4829-07 Standard Test Method for Expansion Index of Soils: West Conshohocken, PA, 19428-2959 USA, American Society for Testing and Materials (ASTM).

Ayalew, L., 1999, The effect of seasonal rainfall on landslides in the highlands of Ethiopia: Bulletin of Engineering Geology and Environment, v. 58, p. 9-19.

Babu, G.L.S., Rao, R.S., and Peter, J., 2005, Evaluation of shear strength functions based on soil water characteristic curves: Journal of Testing and Evaluation, v. 33, p. 461-465.

Baumgardner, M.F., Stoner, E.R., Silva, E.R., and Biehl, L.L., 1985, Reflectance properties of Soils, *in* N., N.B., ed., Advances of Agronomy: New York, Academic Press.

Bell, F.G., 1999, Geological hazards: their assessment, avoidance and mitigation: London etc., E & FN SPON, 648 p.

Bell, F.G., 2000, Engineering Properties of Soils and Rocks: Tokyo, Blackwell Science Ltd.

Bendor, E., and Banin, A., 1990, Near-Infrared Reflectance Analysis of Carbonate Concentration in Soils: Applied spectroscopy, v. 44, p. 1064-1069.

Bendor, E., and Banin, A., 1994, Visible and near-Infrared (0.4-1.1 µm) Analysis of Arid and Semiarid Soils: Remote Sensing of Environment, v. 48, p. 261-274.

Bendor, E., and Banin, A., 1995, Near-Infrared Analysis (NIRA) as a Method to Simultaneously Evaluate Spectral Featureless Constituents in Soils: Soil Science, v. 159, p. 259-270.

Bendor, E., and Levin, N., 2000, Determination of surface reflectance from raw hyperspectral data without simultaneous ground data measurements: a case study of the GER 63-channel sensor data acquired over Naan, Israel: International Journal of Remote Sensing, v. 21, p. 2053-2074.

Bendor, E., Patkin, K., Banin, A., and Karnieli, A., 2002, Mapping of several soil properties using DAIS-7915 hyperspectral scanner data - a case study over clayey soils in Israel: International Journal of Remote Sensing, v. 23, p. 1043-1062.

Bohn, H.L., McNeal, B.L., and O'Connor, G.A., 1985, Soil Chemistry: New York etc, Wiley & Sons, 341 p.

Bourguignon, A., Delpont, G., Chevrel, A., and Chabrillat, S., 2007, Detection and mapping of Shrink-Swell clays in SW France, using ASTER imagery: London, Geological society of London, 117-124 p.

Bowles, J.E., 1984, Physical and Geotechnical properties of soils: New York, McGraw-Hill.

Boyd, D.S., and Petitcolin, F., 2004, Remote sensing of the terrestrial environment using middle infrared radiation (3.0–5.0 micrometer): International Journal of Remote Sensing, v. 25, p. 3343-3368.

Bras, A.L., and Erard, S., 2003, Reflectance spectra of regolith analogs in the mid-infrared: effects of grain size: Planetary and Space Science, v. 51, p. 281-294.

Breemen, N.v., and Buurman, P., 2003, Formation of vertisols, Soil Formation: New York, Boston, Dordrecht, London, Moscow, Kluwer Academic Publishers.

Brereton, R.G., 2000, Introduction to multivariate calibration in analytical chemistry: Analyst, Tutorial Review, v. 125, p. 2125 - 2154.

Brigatti, M.F., Galan, E., and Theng, B.K.G., 2006, Structures and Mineralogy of Clay Minerals, *in* Bergaya, F., Theng, B.K.G., and Lagaly, G., eds., Handbook of Clay Science, Volume 1: Developments in Clay Science: Amsterdam, Elsevier.

Bruker Optik GmbH, 2007, OPUS Version 6.5: Germany, http://www.brukeroptics.com.

CAMO Process AS., 2005, The Unscrambler Version 9.2: Oslo, CAMO.

Carter, M., and Bentley, S.P., 1991, Correlations of soil properties: London, Pentech Press.

Chabrillat, s., and Goetz, A.F.H., 2000, Identification and Mapping of Expansive Clay Soils in the Western US: Using Field Spectrometry and AVIRIS Data.

Chabrillat, S., Goetz, A.F.H., Krosley, L., and Olson, H.W., 2002, Use of hyperspectral images in the identification and mapping of expansive clay soils and the role of spatial resolution: Remote Sensing of Environment, v. 82, p. 431 - 445.

Chen, F.H., 1988, Foundation on Expansive Soils: Amsterdam, Elsevier Science Publishers.

Clark, R.N., 1999, Spectroscopy of Rocks and Minerals, and Principles of Spectroscopy, *in* Rencz, A., ed., Chapter 1 in: Manual of Remote Sensing: New York, John Wiley and Sons, Inc.

Clark, R.N., King, T.V.V., and Gorelick, N.S., 1987, Automatic continuum analysis of reflectance spectra, in Proceedings, Third AIS workshop, 2-4 June, 1987: Pasadena, California, Jet Propulsion Laboratory, JPL Publication 87-30, p. 138-142.

Clark, R.N., and Roush, T.L., 1984, Reflectance spectroscopy: Quantitative analysis techniques for remote sensing applications: Journal of Geophysical Research, v. 89, p. 6329-6340.

Cloutis, E.A., 1996, Hyperspectral geological remote sensing: evaluation of analytical techniques: international Journal of Remote Sensing, v. 17, p. 2215-2242.

Cokca, E., and Birand, A., 1993, Determination of cation exchange capacity of clayey soils by the methylene blue test: ASTM Geotechnical Testing Journal, v. 16, p. 518 - 524.

Conover, W.J., 1999, Practical Nonparametric Statistics: New York, John Wiley & Sons, Inc.

Cooper, C.D., and Mustard, J.F., 1999, Effects of very fine particle size on reflectance spectra of smectite and palagonitic soil: Icarus, v. 142, p. 557-570.

Cross, S.A., and Gregory, G.H., 2007, Correlation of California bearing ratio with shear strength parameters: Transportation Research Record, p. 148-153.

Cumming, G., 2009, Inference by eye: Reading the overlap of independent confidence intervals: Statistics in Medicine, v. 28, p. 205-220.

Cumming, G., Fidler, F., and Vaux, D.L., 2007, Error bars in experimental biology: Journal of Cell Biology, JCB, v. 177, p. 7-11.

da Luz, B.R., and Crowley, J.K., 2007, Spectral reflectance and emissivity features of broad leaf plants: Prospects for remote sensing in the thermal infrared (8.0-14.0 mu m): Remote Sensing of Environment, v. 109, p. 393-405.

Dakshanamurty, V., and Raman, V., 1973, A simple method of identifying an expansive soil: Japanese Society of Soil Mechanics and Foundation Engineering, v. 13, p. 97 - 104.

Delaney, M.D., Allman, M.A., Smith, D.W., and Sloan, S.W., 1998, The establishment and monitoring of expansive soil field sites: Geotechnical Site Characterization, Vols 1 and 2, p. 551-556.

Dhanoa, M.S., Lister, S.J., Sanderson, R., and Barnes, R.J., 1994, The link between Multiplicative Scatter Correction (MSC) and Standard Normal Variate (SNV) transformations of NIR spectra: Journal of Near Infrared Spectroscopy, v. 2, p. 43-47.

Divinsky, M., Ishai, I., and Livneh, M., 1998, Probabilistic approach to pavement design based on generalized California Bearing Ratio equation: Journal of Transportation Engineering-Asce, v. 124, p. 582-588.

ERA, 2002, Site Investigation Manual: Addis Ababa, The Ethiopian Roads Authority.

Erguler, Z.A., and Ulusay, R., 2003, A simple test and predictive models for assessing swell potential of Ankara (Turkey) clay: Engineering Geology, v. 67, p. 331 - 352.

Erzin, Y., and Erol, O., 2007, Swell pressure prediction by suction methods: Engineering Geology, v. 92, p. 133 - 145.

Fall, M., and Sarr, A.M., 2007, Geotechnical characterization of expansive soils and their implications in ground movements in Dakar: Bulletin of Engineering Geology and the Environment, v. 66, p. 279-288.

FAO, 1998, World Reference Base for Soil Resources: Rome, International Society of Soil Science.

Farifteh, J., Van Der Meer, F., and Carranza, E.J.M., 2007, Similarity measures for spectral discrimination of salt-affected soils: International Journal of Remote Sensing, v. 28, p. 5273-5293.

Farmer, V.C., 1974, The layer silicates, *in* Farmer, V.C., ed., The infra-red spectra of minerals: London, Mineralogical society, p. 331-364.

Farmer, V.C., and Russell, J.D., 1964, The infrared spectra of layer silicates: Spectrochimica Acta, v. 20, p. 1149-1173.

Fityus, S., and Buzzi, O., 2009, The place of expansive clays in the framework of unsaturated soil mechanics: Applied Clay Science, v. 43, p. 150-155.

Fitzpatrick, E.A., 1980, SOILS; their formation, classification and distribution: London, NY, Longman Inc., 354 p.

Frost, R.L., Locos, O.B., J., R.H., and Kloprogge, T., 2001, Near-infrared and mid-infrared spectroscopic study of sepiolites and palygorskities: Vibrational Spectroscopy, v. 27, p. 1-13.

Fu, Z.Y., Robles-Kelly, A., Caelli, T., and Tan, R.T., 2007, On automatic absorption detection for Imaging spectroscopy: A comparative study: IEEE Transactions on Geoscience and Remote Sensing v. 45, p. 3827-3844.

Gadre, A.D., and Chandrasekaran, V.S., 1994, Swelling of black cotton soil using centrifuge modeling: Journal of Geotechnical Engineering, v. 120, p. 914 - 919.

Gaffey, S.J., 1986, Spectral reflectance of carbonate minerals in the visible and near infrared (0.35-2.55 microns): calcite, aragonite, and dolomite: American Mineralogist, v. 71, p. 151-162.

Galan, E., 2006, Genesis of Clay Minerals, *in* Bergaya, F., Theng, B.K.G., and Lagaly, G., eds., Handbook of Clay Science, Volume 1: Developments in Clay Science: Amsterdam, Elsevier.

Gillot, J.E., 1987, Clay in engineering geology: New York, Elsevier.

Goetz, A.F.H., Chabrillat, S., and Lu, Z., 2001, Field Reflectance Spectrometry for Detection of Swelling Clays at Construction Sites: Field Analytical Chemistry and Technology, v. 5, p. 143-155.

Gomez, C., Lagacherie, P., and Coulouma, G., 2008, Continuum removal versus PLSR method for clay and calcium carbonate content estimation from laboratory and airborne hyperspectral measurements: Geoderma, v. 148, p. 141-148.

Gourley, C.S., Newill, D., and Schreiner, H.D., 1993, Expansive soils: TRL's research strategy, *in* Fookes, P.G., and Parry, R.H.G., eds., First International Symposium on Engineering Characteristics of Arid Soils, Volume PA1301/93: City University, London, July 5-8, Overseas Centre, Transport Research Laboratory, Crowthorne, Berkshire, UK., p. 247-260.

Gray, C.W., and Allbrook, R., 2002, Relationships between shrinkage indices and soil properties in some New Zealand soils: Geoderma, v. 108, p. 287 - 299.

Gray, J., and Murphy, B., 2002, Parent material and world soil distribution, 17th World congress of soil science (WCSS) Bangkok, Thailand.

Griffiths, P.R., and de Haseth, J.A., 2007, Fourier transform infrared spectrometry, Wiley & Sons, 529 p.

GSE, 1990, Engineering Geological Mapping of Addis Ababa: Addis Ababa, Geological Survey of Ethiopia and the Ethiopian Ministry of Mines and Energy.

Haaland, D.M., and Thomas, E.V., 1988, Partial Least-Squares Methods for Spectral Analyses. 1. Relation to Other Quantitative Calibration Methods and the Extraction of Qualitative Information: Analytical Chemistry, v. 60, p. 1193-1202.

Hair, J.F., Anderson, R.E., and Tatham, R.L., 1987, Multivariate Data Analysis: New York, Macmillan.

Hecker, C., Van der Meijde, M., and Van der Meer, F.D., 2010, Thermal infrared spectroscopy on feldspars - Successes, limitations and their implications for remote sensing: Earth-Science Reviews, v. 103, p. 60-70.

Hermann J. Kaufmann, Karl Segl, Luis Guanter, Andreas Mueller, Stefan Hofer, and Chlebek, C., 2010, EnMAP – An Advanced Optical Payload for Earth Observation, *in* Goetz, A.F.H., ed., Proceedings of ASD and IEEE GRS; Art, Science and Applications of Reflectance Spectroscopy Symposium, www.asdi.com. , Volume II: Boulder, Colorado, p. 5.

Hewson, R.D., Cudahy, T.J., Mizuhiko, S., Ueda, K., and Mauger, A.J., 2005, Seamless geological map generation using ASTER in the Broken Hill-Curnamona province of Australia: Remote Sensing of Environment, v. 99, p. 159-172.

Holtz, R.D., and Krizek, R.J., 1970, Properties of Slightly Organic Topsoils: Journal of the Construction Division, ASCE, v. 96, p. 29-43.

Hower, J., and Mowat, C.T., 1966, The Mineralogy of illites and mixed layer illite/montmorillonites: The American Mineralogist, v. 51, p. 825-854.

Hunt, E.R., 1984, Geotechnical Engineering Investigation Manual: New York, McGraw-Hill Book Company.

Hunt, G.R., 1977, Spectral signatures of particulate minerals in the visible and near infrared: Geophysics, v. 42, p. 501-513.

Hunt, G.R., and Salisbury, J.W., 1970, Visible and near-infrared spectra of minerals and rocks: I Silicate minerals: Modern Geology, v. 1, p. 283-300.

IBM, 2010, PASW Statistics version 18.0.2, SPSS: Chicago, www.spss.com.

ITT Visual Information Solutions, 2009, ENVI Version 4.7: Boulder, Colorado, USA, www.ittvis.com.

Johnson, J.R., Lucey, P.G., Horton, K.A., and Winter, E.M., 1998, Infrared measurements of Pristine and disturbed soils 1.Spectral contrast differences between field and laboratory data: Remote Sensing of Environment, v. 64, p. 34-46.

Jones, J.D.E., and Holtz, W.G., 1973, Expansive soils - The hidden disaster Civil Engineering, ASCE, v. 43, p. 49-51.

Karathanasis, A.D., and Hajek, A.F., 1985, Shrink-Swell Potential of Montmorillonitic Soils in Udic Moisture Regimes: Soil Science Society of America, v. 49, p. 159-166.

Kariuki, P.C., and Van der Meer, F.D., 2003, Issues of effectiveness in empirical methods for describing swelling soils: International Journal of Applied Earth Observation & Geoinformation, v. 4, p. 231-241.

Kariuki, P.C., and Van der Meer, F.D., 2004, A unified swelling potential index for expansive soils: Engineering Geology, v. 72, p. 1-8.

Kariuki, P.C., Van der Meer, F.D., and Siderius, W., 2003, Classification of soils based on engineering indices and spectral data: International Journal of Remote Sensing, v. 24, p. 2567 - 2574.

Kariuki, P.C., Woldai, T., and Van der Meer, F.D., 2004, Effectiveness of spectroscopy in identification of swelling indicator clay minerals: International Journal of Remote Sensing, v. 25, p. 455 - 469.

Kaufman, L., and Rousseeuw, P.J., 1990, Finding Groups in Data: An Introduction to Cluster Analysis New York, John Wiley & Sons, Inc.

Kruse, F.A., 1988, Use of Airborne Imaging Spectrometer Data to Map Minerals Associated with Hydrothermally Altered Rocks in the Northern Grapevine Mountains, Nevada, and California: Remote Sensing of Environment, v. 24, p. 31-51.

Kruse, F.A., 1991, Spectral identification (1.2-2.5 µm) and characterization of Paris basin kaolinite/smectite clays using a field spectrometer, 5th colloquium on physical measurements and signatures in remote sensing: Courchevel, France, ESA, p. 181-184.

Kruse, F.A., Kierein-Young, K.S., and Boardman, J.W., 1990, Mineral mapping at Cuprite, Nevada with a 63 channel imaging spectrometer: Photogrammetric Engineering and Remote Sensing, v. 56, p. 83-92.

Kruse, F.A., Lefkoff, A.B., Boardman, J.W., Heidebrecht, K.B., Shapiro, A.T., Barloon, P.J., and Goetz, A.F.H., 1993, The spectral image processing system (SIPS)—interactive visualization and analysis of imaging spectrometer data: Remote Sensing of Environment, v. 44, p. 145-163.

LEA, 2006, Expansive soils characterization and remedial measures (Addis Ababa - Tarmaber road rehabilitation project): Addis Ababa, The Ethiopian Roads Authority.

Ludwig, B., Nitschke, R., Terhoeven-Urselmans, T., Michel, K., and Flessa, H., 2008, Use of mid-infrared spectroscopy in the diffuse-reflectance mode for the prediction of the composition of organic matter in soil and litter: Journal of Plant Nutrition and Soil Science-Zeitschrift Fur Pflanzenernahrung Und Bodenkunde, v. 171, p. 384-391.

Ma, C., and Eggleton, R.A., 1999, Cation exchange capacity of kaolinite: Clays and Clay Minerals, v. 47, p. 174-180.

Malkawi, A.I.H., Alawneh, A.S., and Abu-Safaqah, O.T., 1999, Effects of organic matter on the physical and the physicochemical properties of an illitic soil: Applied clay science, v. 14, p. 257-278.

Markham, B., 2011, Landsat Data Continuity Mission: Overview and Status, 10th Annual JACIE (Joint Agency Commercial Imagery Evaluation) Workshop, March 29-31, 2011 Boulder CO, USA, USGS.

Martens, H., and Naes, T., 1989, Multivariate calibration, John Wiley & Sons inc.

Mason, P., Breman, M., Warren, P., Guo, Y., Green, A., Lagerstrom, R., Bischof, L., and Huntington, J., 2011, The Spectral Geologist (TSG): Sydney, Australia CSIRO, http://www.thespectralgeologist.com.

Mather, P.M., 1999, Computer processing of remotely - sensed images: an introduction: Chichester etc., Wiley & Sons, 292 p.

McCormack, D.E., and Wilding, L.P., 1975, Soil Properties Influencing Swelling in Canfield and Geeburg Soils: Soil Science Society of America, v. 39, p. 496-502.

Michalski, J.R., Kraft, M.D., Sharp, T.G., Williams, L.B., and Christensen, P.R., 2006, Emission spectroscopy of clay minerals and evidence for poorly crystalline aluminosilicates on Mars from Thermal Emission Spectrometer data: Journal of Geophysical Research, v. 111.

Mitchell, J.K., 1993, Fundamentals of Soil behavior: New York, Wiley

Moore, D.M., and Reynolds, R.C.J., 1997, X-ray diffraction and the identification and analysis of clay minerals Oxford, Oxford University press.

Morin, W.J., 1971, Properties of African black clay soils, Fifth regional conference on soil mechanics and foundation engineering, Volume 1: Luanda, Angola, August 1971, Laboratorio de Engenharia de Angola, p. 51-65.

Morin, W.J., and Parry, W.T., 1971, Geotechnical properties of Ethiopian volcanic soils: Geotechnique, v. 21, p. 223-232.

Mustard, J.F., Murchie, S.L., Pelkey, S.M., Ehlmann, B.L., Milliken, R.E., Grant, J.A., Bibring, J.-P., Poulet, F., Bishop, J., Dobrea, E.N., Roach, L., Seelos, F., Arvidson, R.E., Wiseman, S., Green, R., Hash, C., Humm, D., Malaret, E., McGovern, J.A., Seelos, K., Clancy, T., Clark, R., Marais, D.D., Izenberg, N., Knudson, A., Langevin, Y., Martin, T., McGuire, P., Morris, R., Robinson, M., Roush, T., Smith, M., Swayze, G., Taylor, H., Titus, T., and Wolff, M., 2008, Hydrated silicate minerals on Mars observed by the Mars Reconnaissance Orbiter CRISM instrument: Nature, v. 454, p. 305-309.

Nalbantoglu, Z., and Tuncer, E.R., 2001, Compressibility and hydraulic conductivity of a chemically treated expansive clay: Canadian Geotechnical Journal, v. 38, p. 154-160.

Nelson, J.D., and Miller, D.J., 1992, Expansive Soils Problems and Practice in Foundation and Pavement Engineering, John Wiley &Sons, Inc.

Netterberg, F.D., 2001, Addis Ababa-Jimma road project Preliminary report on cracking problem: Addis Ababa, Ethiopian Roads Authority.

Odell, R.T., Thornburn, T.H., and McKenzie, L.J., 1960, Relationships of Atterberg Limits to Some Other Properties of Illinois Soils: Soil Science Society of America, v. 24, p. 297-300.

Omotosho, O., and Ogboin, A.S., 2009, Active Soils of the Niger Delta in Road Pavement Design and Construction: Geotechnical and Geological Engineering, v. 27, p. 81-88.

Paige-Green, P., 2008, Dealing with Road Subgrade Problems in Southern Africa, The 12th International Conference of International Association for Computer Methods and Advances in Geomechanics (IACMAG): Goa, India, 1-6 October, 2008.

Pandian, N.S., and Nagaraj, T.S., 1990, Critical reappraisal of colloidal activity of clays: Journal of Geotechnical and Geoenvironmental Engineering, v. 116, p. 285 - 296.

Parfitt, R.L., and Hemni, T., 1980, Structures of some allophanes from New Zealand: Clay and Clay Minerals, v. 28, p. 285 - 294.

Pascal, B., Patricia, G., and Daniel, T., 2004, Relationship between clay content, clay type, and shrinkage properties of soil samples: Soil Science Society of America, v. 68, p. 1145 - 1153.

Perloff, W.H., and Baron, W., 1976, Soil Mechanics Principles and Applications, John Wiley & Sons.

Petit, S., 2006, Fourier Transform Infrared Spectroscopy *in* Bergaya, F., Theng, B.K.G., and Lagaly, G., eds., Handbook of Clay Science, Volume 1: Developments in Clay Science: Amsterdam, Elsevier.

Pontual, S., Merry, N., and Gamson, P., 1997, G-Mex Spectral interpretation field Manual: Sydney, AusSpec international.

Popescu, M.E., 1979, Engineering problems associated with expansive clays from Romania: Engineering Geology, v. 23, p. 145-163.

Post, J.L., and Noble, P.N., 1993, The near-infrared combination band frequencies of dioctahedral smectites, micas, and illites: Clays and Clay Minerals, v. 41, p. 639-644.

Quade, D., and Salama, I.A., 1975, Minimum Chi-Square Statistics in Contingency-Tables: Biometrics, v. 31, p. 953-956.

Rainey, M.P., Tyler, A.N., Gilvear, D.J., Bryant, R.G., and P.McDonald, 2003, Mapping intertidal estuarine sediment grain size distributions through airborne remote sensing: Remote Sensing of Environment, v. 86, p. 480-490.

Ramana, K.V., 1993, Humid tropical expansive soils of Trinidad: Their geotechnical properties and areal distribution: Engineering Geology, v. 34, p. 27 - 44.

Reddy, P.V.S., Rao, K.M., and Rani, C.S., 2009, Identification of expansive soils and assessment of expansion potential by fuzzy approach: Electronic Journal of Geotechnical Engineering EJGE, v. 14 Bundle L, p. 1 - 11.

Reznik, Y.M., 1998, Deformation zones under square footings supported by clayey soils: Engineering Geology, v. 50, p. 319-327.

Rivard, B., Thomas, P.J., and Giroux, J., 1995, Precise Emissivity of Rock Samples: Remote Sensing of Environment, v. 54, p. 152-160.

Ross, G.J., 1978, Relationships of specific surface area and clay content to shrink-swell potential of soils having different clay mineralogical compositions Canadian journal of soil science, v. 58, p. 159-166.

Roush, T.L., Singer, R.B., and McCord, T.B., 1987, Reflectance Spectra of selected phyllosilicates from 0.6 to 4.6 microns: Abstracts of the Lunar and Planetary Science Conference v. 18.

Rowan, L.C., Goetz, A.F.H., and Ashley, R.P., 1977, Discrimination of hydrothermally altered and unaltered rocks in the visible and the near infrared multispectral images: Geophysics, v. 42, p. 522-535.

Rowan, L.C., Mars, J.C., and .Simpson, C.J., 2003, Lithologic Mapping in the Mountain Pass, California area using Advanced Spaceborne Thermal Emission and Reflection Radiometer (ASTER) data: Remote Sensing of Environment, v. 84, p. 350-366.

Runqiu, H., and Lizhou, W., 2007, Stability Analysis of Unsaturated Expansive Soil Slope: Earth Science Frontiers, v. 14, p. 129-133.

Salisbury, J.W., and D'Aria, D.M., 1992a, Emissivity of terrestrial materials in the 8 -14 µm atmospheric window: Remote Sensing of Environment, v. 42, p. 83 - 106.

Salisbury, J.W., and D'Aria, D.M., 1992b, Infrared (8–14 µm) remote sensing of soil particle size: Remote Sensing of Environment, v. 42, p. 157-165.

Salisbury, J.W., and D'Aria, D.M., 1994, Emissivity of terrestrial materials in the 3 -5 µm atmospheric window: Remote Sensing of Environment, v. 47, p. 345 - 361.

Salisbury, J.W., and Eastes, J.W., 1985, The effect of particle size and porosity on spectral contrast in the mid-infrared: Icarus, v. 64, p. 586-588.

Salisbury, J.W., Wald, A., and D'Aria, D.M., 1994, Thermal-infrared remote sensing and Kirchhoff's law 1. Laboratory measurements: Journal of Geophysical Research, v. 99, p. 11,897-11,911.

Schafer, W.M., and Singer, M.J., 1976, Influence of Physical and Mineralogical Properties on Swelling of Soils in Yolo County, California: Soil Science Society of America, v. 40, p. 557-562.

Schenker, N., and Gentleman, J.F., 2001, On Judging the significance of differences by examining the overlap between confidence intervals: The American Statistician, v. 55, p. 182-186.

Seco, A., Ramirez, F., Miqueleiz, L., and Garcia, B., 2011, Stabilization of expansive soils for use in construction: Applied Clay Science, v. 51, p. 348-352.

Seed, H.B., Woodward, R.J., and Lundgren, R., 1962, Prediction of swelling potential for compacted clays: Journal of the Soil Mechanics and Foundation Division Proceedings of the American Society of Civil Engineers, v. 88, p. 53 - 88.

Selige, T., Bohner, J., and Schmidhalter, U., 2006, High resolution topsoil mapping using hyperspectral image and field data in multivariate regression modeling procedures: Geoderma, v. 136, p. 235 - 244.

Shepherd, K.D., Vanlauwe, B., Gachengo, C.N., and Palm, C.A., 2005, Decomposition and mineralization of organic residues predicted using near infrared spectroscopy: Plant and Soil, v. 277, p. 315-333.

Shepherd, K.D., and Walsh, M.G., 2002, Development of reflectance libraries for characterization of soil properties: Soil Science Society of America, v. 66, p. 988-998.

Sheskin, D.J., 1997, Handbook of parametric and nonparametric statistical procedures New York, CRC press.

Shi, B., Jiang, H., Liu, Z., and Fang, H.Y., 2002, Engineering geological characteristics of expansive soils in China: Engineering Geology, v. 67, p. 63 - 71.

Site Investigation Steering Group, 1993a, Site Investigation in Construction Part 1: Without Site Investigation Ground is a Hazard, Thomas Telford Ltd, 56 p.

Site Investigation Steering Group, 1993b, Site Investigation in Construction Part 2: Planning, Procurement and Quality Management, Thomas Telford Ltd, 40 p.

Skempton, A.W., 1984, The colloidal activity of clays, *in* Skempton, A.W., ed., Selected papers on Soil Mechanics London, Thomas Telford Limited, p. 281.

Snethen, D.R., 1975, A Review of Engineering Experiences with Expansive Soils in Highway Subgrades: Washington D.C, Federal Highway Administration Office of Research and Development.

Spectronics, I., 1999, PIMAVIEW version 3.1 user manual: New South Wales, Australia, Integrated Spectronics, www.intspec.com.

Sridharan, A., and Gurtug, Y., 2004, Swelling behavior of compacted fine-grained soils: Engineering Geology, v. 72, p. 9 - 18.

Stenberg, B., Viscarra Rossel, R.A., Mouazen, A.M., and Wetterlind, J., 2010, Visible and near Infrared Spectroscopy in Soil Science: Advances in Agronomy, v. 107, p. 163-215.

Stravern, M.T.V., and Seters, A.J.v., 2004, Smart site investigation saves money *in* Hack, H.R.G.K., Azzam, R., and Charlier, R., eds., Engineering geology for infrastructure planning in Europe : a European perspective, Volume 104: Lecture Notes in Earth Sciences: Berlin etc., Springer, p. 803.

Sullivan, D.G., Shaw, J.N., and Rickman, D., 2005, IKONOS imagery to estimate surface soil property variability in two Alabama physiographies: Soil Science Society of America, v. 69, p. 1789-1798.

Sunshine, J.M., Pieters, C.M., and Pratt, S.F., 1990, Deconvolution of Mineral Absorption-Bands - an Improved Approach: Journal of Geophysical Research-Solid Earth and Planets, v. 95, p. 6955-6966.

Taboada, M.A., Lavado, R.S., Rubio, G., and Cosentino, D.J., 2001, Soil volumetric changes in natric soils caused by air entrapment following seasonal ponding and water table rises: Geoderma, v. 101, p. 49-64.

Takahashi, T., Dahlgren, R.A., Theng, B.K.G., Whitton, J.S., and Soma, M., 2001, Potassium-Selective, Halloysite-Rich Soils Formed in Volcanic Materials from Northern California: Soil Science Society of America, v. 65, p. 516 - 526.

Tangestani, M.H., Mazhari, N., Agar, B., and Moore, F., 2008, Evaluating Advanced Spaceborne Thermal Emission and Reflection Radiometer (ASTER) data for alteration zone enhancement in a semi-arid area, northern Shahr-e-Babak, SE Iran: International Journal of Remote Sensing, v. 29, p. 2833-2850.

Thomas, P.J., Baker, J.C., and Zelazny, L.W., 2000, An Expansive Soil Index for Predicting Shrink–Swell Potential: Soil Science Society of America, v. 64, p. 268 - 274.

Van Den Eeckhaut, M., Moeyersons, J., Nyssen, J., Abraha, A., Poesen, J., Haile, M., and Deckers, J., 2009, Spatial patterns of old, deep-seated landslides: A case-study in the northern Ethiopian highlands: Geomorphology, v. 105, p. 239-252.

Van der Meer, F.D., 1995, Spectral Reflectance of Carbonate Mineral Mixtures and Bidirectional Theory: Quantitative Analysis techniques for Application in Remote Sensing: Remote Sensing Reviews, v. 13, p. 69-94.

Van der Meer, F.D., 1999, Can we map swelling clay with remote sensing?: International Journal of Applied Earth Observation & Geoinformation (JAG), v. 1, p. 27-35.

Van der Meer, F.D., 2004a, Analysis of spectral absorption features in hyperspectral imagery: International Journal of Applied Earth Observation and Geoinformation, v. 5, p. 55-68.

Van der Meer, F.D., 2004b, Remote sensing image analysis: including the spatial domain, *in* Van der Meer, F.D., and De Jong, S.M., eds., Remote Sensing and Digital Image Processing: Dordrecht, Kluwer Academic Publishers, p. 539.

Vaught, R., Kristofor, R.B., and Miller, D.M., 2006, Relationships among Coefficient of Linear Extensibility and Clay Fractions in Expansive, Stony Soils: Soil Science Society of America, v. 70, p. 1983-1990.

Ventura, C., and Papini, M., 1999, Diffuse reflection spectroscopy study of granular materials and their mixtures in the mid-infrared spectral range: Vibrational Spectroscopy, v. 21, p. 17-26.

Verhoef, P.N.W., 1992, The Methylene Blue Adsorption Test Applied to Geo-materials, Delft, Delft University of Technology.

Vicente, L.E., and de Souza, C.R., 2011, Identification of mineral components in tropical soils using reflectance spectroscopy and advanced spaceborne thermal emission and reflection

radiometer (ASTER) data: Remote Sensing of Environment, v. 115, p. 1824-1836.

Viscarra Rossel, R.A., Cattle, S.R., Ortega, A., and Fouad, Y., 2009, In situ measurements of soil colour, mineral composition and clay content by vis-NIR spectroscopy: Geoderma, v. 150, p. 253-266.

Viscarra Rossel, R.A., Walvoort, D.J.J., McBratney, A.B., Janik, L.J., and Skjemstad, J.O., 2006, Visible, near infrared, mid infrared or combined diffuse reflectance spectroscopy for simultaneous assessment of various soil properties: Geoderma, v. 131, p. 59 - 75.

Wada, K., 1977, Allophane and Imogolite: Madison, Soil Science Society of America (SSSA), 948 p.

Waiser, T.H., Morgan, C.L.S., Brown, D.J., and Hallmark, C.T., 2007, In situ characterization of soil clay content with visible near-infrared diffuse reflectance spectroscopy: Soil Science Society of America, v. 71, p. 389 - 396.

Wan, Y., Kwong, J., Brandes, H.G., and Jones, R.C., 2002, Influence of Amorphous Clay - Size Materials on Soil Plasticity and Shrink - Swell Behavior: Journal of Geotechnical and Geoenvironmental Engineering, v. 128, p. 1026 - 1031.

Wilson, J.R., 1989, Chi-Square Tests for Overdispersion with Multiparameter Estimates: Applied Statistics-Journal of the Royal Statistical Society Series C, v. 38, p. 441-453.

Wold, S., Sjostrom, M., and Eriksson, L., 2001, PLS-regression: a basic tool of chemometrics: Chemometrics and Intelligent Laboratory Systems, v. 58, p. 109-130.

Yeniay, O., and Goktas, A., 2002, A comparison of partial least squares regression with other prediction methods: Hacettepe Journal of Mathematics and Statistics, v. 31, p. 99 - 111.

Yerima, B.P.K., Calhoun, F.G., Senkayi, A.L., and Dixon, J.B., 1985, Occurrence of Interstratified Kaolinite-Smectite in El Salvador Vertisols: Soil Science Society of America, v. 49, p. 462-466.

Yerima, B.P.K., Wilding, L.P., Calhoun, F.G., and Hallmark, C.T., 1987, Volcanic Ash-influenced Vertisols and Associated Mollisols of El Salvador: Physical, Chemical, and Morphological Properties: Soil Science Society of America, v. 51, p. 699-708.

Yilmaz, I., 2006, Indirect estimation of the swelling percent and a new classification of soils depending on liquid limit and cation exchange capacity: Engineering Geology, v. 85, p. 295 - 301.

Yitagesu, F.A., Van der Meer, F., and Van der Werff, H., 2010, Mapping variation in soil volumetric shrinkage using ASTER imagery, AARSE 2010 : 8th international conference African Association of Remote Sensing of the Environment, AARSE, on

earth observation for Africa's development agenda: Addis Ababa, Ethiopia.

Yitagesu, F.A., Van der Meer, F., Van der Werff, H., and Hecker, C., 2011a, Spectral characteristics of clay minerals in the 2.5-14 µm wavelength region: Applied Clay Science, v. 53, p. 581-591.

Yitagesu, F.A., Van der Meer, F., Van der Werff, H., and Seged, H., 2011b, Evaluation of Soil Expansion Index from routinely determined geotechnical parameters: Soil Science Society of America, v. 75, p. 1641-1652.

Yitagesu, F.A., Van der Meer, F., Van der Werff, H., and Zigterman, W., 2008a, Assessing expansive soil engineering parameters using spectroscopy, Geoscience and Remote Sensing Symposium, 2008. IGARSS 2008. IEEE International: Boston, MA, p. II-1255 - II-1258.

Yitagesu, F.A., Van der Meer, F.D., and Van der Werff, H., 2009a, Prediction of Volumetric Shrinkage in Expansive Soils (Role of Remote Sensing), *in* Jedlovec, G., ed., Advances in Geoscience and Remote Sensing: Vukovar, Croatia, In-Tech, p. 347-370.

Yitagesu, F.A., Van der Meer, F.D., and Van der Werff, H., 2009b, Quantifying engineering parameters of expansive soils from their reflectance spectra: Engineering Geology, v. 105, p. 151 - 160.

Yitagesu, F.A., Van der Meer, F.D., and Van der Werff, H., 2011c, Multispectral Remote Sensing for Estimating and Mapping Soil Expansiveness: Engineering Geology.

Yitagesu, F.A., Van der Meer, F.D., Van der Werff, H., and Zigterman, W., 2008b, A multivariate regression analysis for deriving engineering parameters of expansive soils from spectral reflectance The International Archives of the Photogrammetry, Remote Sensing and Spatial Information Sciences, Volume XXXVII, Part B7: Beijing, China, ISPRS, p. 1319-1324.

Yong, R.N., and Warkentin, B.P., 1975, Soil properties and behavior: Amsterdam, Oxford, New York, Elsevier scientific publishing company.

Young, R.A., 1995, The Rietveld Method International Union of Crystallography - Monographs on Crystallography, Oxford University Press, p. 312.

Zapata, C.E., Houston, S.L., Houston, W.N., and Dye, H., 2006, Expansion index and its relationship with other index properties, *in* Miller, G.A., Zapata, C.E., Houston, S.L., and G.Fredlund, D., eds., 4th International Conference on Unsaturated Soils, Volume 2: Reston, VA, ASCE, p. 2133–2137.

Zehetner, F., Miller, W.P., and West, L.T., 2003, Pedogenesis of volcanic ash soils in Andean Ecuador: Soil Science Society of America, v. 67, p. 1797 - 1809.

Publications of the author

ISI journal articles:

Yitagesu, Fekerte Arega, Van der Werff, H., Van der Meer, F.D, and Hecker, C., 2012, On the relationships between plasticity and spectral characteristics of Expansive soils: the 3-5 µm wavelength region: Applied clay science (accepted with minor corrections).

Yitagesu, Fekerte Arega, Van der Meer, F.D, Van der Werff, H., and Seged, H., 2011, Evaluation of Soil Expansion Index from routinely determined geotechnical parameters: Soil Science Society of America v. 75 (5), p. 1640-1651.

Yitagesu, Fekerte Arega, Van der Meer, F.D, Van der Werff, H., and Hecker, C., 2011, Spectral characteristics of clay minerals in the 2.5-14 µm wavelength region: Applied Clay Science, v. 53 (4), p.581-591.

Yitagesu, Fekerte Arega, Van der Meer, F.D., and Van der Werff, H., 2011, Multispectral Remote Sensing for Estimating and Mapping Soil Expansiveness: Engineering Geology (in review after revision).

Yitagesu, Fekerte Arega, Van der Meer, F.D., and Van der Werff, H., 2009, Quantifying engineering parameters of expansive soils from their reflectance spectra: Engineering Geology, v. 105, p. 151-160.

Other Peer-reviewed journal articles:

Yitagesu, Fekerte Arega, 2007, Remote sensing in assessing geotechnical properties of expansive soils: a case study in Addis Ababa. In: EACE Bulletin: Ethiopian Association of Civil Engineers, Special issue, v. 7 (2), p. 30-38.

Yitagesu, Fekerte Arega and Belew, M., 2007, GIS and remote sensing in highway route selection: a case study in Ethiopia, selection of the Addis Ababa - Nazret expressway alignment. In: EACE Journal: Ethiopian Association of Civil Engineers, v. 4 (3), p. 17-27.

Full conference proceedings (peer-reviewed):

Yitagesu, Fekerte Arega, Van der Meer, F.D, and Van der Werff, H., 2010, Mapping variation in soil volumetric shrinkage using ASTER imagery, AARSE 2010 : 8th international conference African Association of Remote Sensing of the Environment, AARSE, on earth observation for Africa's development agenda: Addis Ababa, Ethiopia.

Yitagesu, Fekerte Arega., Van der Meer, F.D, Van der Werff, H., and Zigterman, W., 2008, Assessing expansive soil engineering parameters using spectroscopy, Geoscience and Remote Sensing

Symposium, 2008. IGARSS 2008. IEEE International: Boston, MA, p. II-1255 - II-1258.

Yitagesu, Fekerte Arega., Van der Meer, F.D., Van der Werff, H., and Zigterman, W., 2008, A multivariate regression analysis for deriving engineering parameters of expansive soils from spectral reflectance The International Archives of the Photogrammetry, Remote Sensing and Spatial Information Sciences, Volume XXXVII, Part B7: Beijing, China, ISPRS, p. 1319-1324.

Yitagesu, Fekerte Arega., Van der Meer, F.D., Van der Werff, H., and Zigterman, W., 2007, Spectroscopy to characterize expansive soils, Geoscience and Remote Sensing Symposium, 2007. IGARSS 2007, IEEE International: Barcelona, Spain, IEEE International, p. 1250 - 1254.

Yitagesu, Fekerte Arega, and Belew, M., September 17-21, 2007 Remote sensing and GIS in Highway route selection (A case study in Addis-Nazret express highway), In AFRICAGIS 2007 Conference and Exhibition: Ouagadougou, Burkina Faso.

Yitagesu, Fekerte Arega, 30 October - 2 November, 2006, Predicting Soil Engineering Parameters from Spectral Data Using PLSR, In AARSE 2006 Conference & Exhibition: International conference on Earth Observation and Geo-information Science in support for Africa's Development: Egypt, Cairo.

Book chapter:

Yitagesu, Fekerte Arega, Van der Meer, F.D., and Van der Werff, H., 2009, Prediction of Volumetric Shrinkage in Expansive Soils (Role of Remote Sensing), in Jedlovec, G., ed., Advances in Geoscience and Remote Sensing: Vukovar, Croatia, In-Tech, p. 347-370.

Presentations:

Yitagesu, Fekerte Arega, Van der Meer, F.D., and Van der Werff, H., Seged, Hadush., September 13, 2011, Expansive soils: geotechnical characterization: ESA research lunch talk: Enschede, the Netherlands, ITC, p. 32.

Kusnierek, K., Nocita, M., Opitz, R., Yitagesu, Fekerte Arega., and Zamolyi, A., 2011, Improving the soil organic carbon and pH VisNIR calibrations within the field of uniform soil cover by extending the model with the samples from the nearby locations: Geophysical Research Abstracts, v. 13, EGU2011-13391.

Yitagesu, Fekerte Arega, Van der Meer, F.D., and Van der Werff, H., Seged, Hadush., Remote Sensing and Geotechnical Investigation of Expansive Soils: Integrated approach for Understanding and

Estimating Swell-Shrink Parameters. Presented at the: 1st European Facility for Airborne Research (EUFAR) training Course on advanced digital remote sensing in ecology and earth summer school (ADDRESSS), August 19-28, 2010, Tihany, Hungary, p. 13.

Yitagesu, Fekerte Arega, Van der Meer, F.D., and Van der Werff, H., April 7, 2010, Thermal Infrared (TIR) Spectroscopy for clay mineral characterization: ESA research lunch talk: Enschede, the Netherlands, ITC, p. 24.

Yitagesu, Fekerte Arega, Van der Meer, F.D., and Van der Werff, H., Seged, Hadush., February 18, 2010, Geotechnical Investigation and spectral characteristics of Expansive Soils: ESA PhD day: Eden dish hotel, Enschede, the Netherlands, p. 16.

Yitagesu, Fekerte Arega, Van der Meer, F.D, Van der Werff, H., and Hecker, C. Remote Sensing: role in linear Infrastructure Planning and Development. Invited presentation at the 2nd national workshop on preparation of Design Manual, Specifications and Standard Bidding Documents for Low Volume Roads of Ethiopia, January 18-20, 2010, Blossom Hotel, DireDawa, Ethiopia, p. 28.

Yitagesu, Fekerte Arega, Drainage provision in Ethiopia. Invited presentation at the 2nd national workshop on preparation of Design Manual, Specifications and Standard Bidding Documents for Low Volume Roads of Ethiopia, January 18-20, 2010, Blossom Hotel, DireDawa, Ethiopia, p. 27.

Yitagesu, Fekerte Arega, The Role of Female Earth Scientists in their Country, In: Innovative application for Remote Sensing and GIS for female professional in the Earth Sciences, November 3 – 16, 2006, Cairo, Egypt, p.12.

Summary

Expansive soils are weak and unstable when subjected to changes in moisture content either due to significant seasonal, climatic variations (alternate dry and wet periods) or artificial causes. Their presence in construction sites is challenging, as it is one of the critical factors that can substantially affect the overall cost, especially of lightweight engineering infrastructure development. Increase in volume (swelling) of expansive soils often exceeds the downward pressure exerted from lightweight structures, causing deformations and formation of cracks. Considerable decrease in volume (shrinkage) associated with drying, on the other hand, is responsible for differential settlement. According to literature, soil swelling and shrinkage cause damage to infrastructure that cost billions of dollars each year in various parts of the world. Thus, it is rated as one of the most costly natural geo-hazards. The areas that are predominantly prone to soil swelling and shrinkage problems are those located in arid and semiarid regions of tropical and temperate climate zones, where the annual evapotranspiration exceeds precipitation. Expansive soils also occur in Ethiopia and are notorious for posing a wide range of problems in the construction sector.

As investment in infrastructure development forms a significant portion of the global economy, expansive soils are a prime focus of research in geotechnical engineering and soil science. Two foremost topics in expansive soil research are (1) characterization and (2) treatment or stabilization. While the first deals with identification and quantitative analysis of expansive soils, the second strives to improve their geotechnical characteristics (such as reducing their swelling and shrinkage potential). Site characterization is a prerequisite at the onset of any construction, also to promote a better land-use planning. A comprehensive geotechnical investigation ensures an optimal planning, design, construction and satisfactory functionality of structures. Confronted by prohibitively expensive customary testing procedures, use of advanced techniques such as remote sensing is highly sought for characterizing expansive soils.

In recent years, significant development has been made to improve geotechnical characterization of expansive soils and better account their spatial variability, by taking advantage of remote sensing techniques. Wavelength coverage and spectral resolution of spectrometers are continually enhanced. Prices of spectrometers have decreased. Portable spectrometers are available. Spatial and spectral resolutions of sensors are also continuously improved apart from the availability of large archives of remotely sensed data sets. In addition, advances in spectral and image data processing techniques have created the opportunity to extract soil geotechnical information from remote sensing data.

In this research, geotechnical and spectral characteristics of expansive soils are described. The main aim was to investigate interrelationships between these two aspects of expansive soils across the visible-near infrared (VNIR), short wave infrared (SWIR), and mid infrared (MIR) wavelength regions (0.35-14 µm). Expansive soil geotechnical and spectral characteristics are determined by the mineralogical assemblage, principally the presence and abundance of active clay minerals, which provides a prospect to link the two. Emphasis was put on establishing new techniques for characterization including identification, estimation of commonly used geotechnical parameters, and mapping spatial variability in geotechnical characteristics of expansive soils.

On a laboratory scale, expansive soils can be identified and characterized from their spectra. The technique requires a small amount of material per sample, minimal sample preparation and time for analyses. Thus, opposed to the arduousness to accomplish using conventional techniques, a dense sampling can be achieved. In addition to the VNIR and SWIR wavelength regions, spectral characteristics of active clay minerals and expansive soils were also established in the MIR wavelength region. This has given new insights as there was a little understanding of the spectral responses of active clay minerals and expansive soils in the MIR wavelength region. Several spectral and statistical analyses techniques were used to derive compositional information, and relate soil spectral characteristics to routinely determined geotechnical parameters such as consistency limits. Statistical techniques such as a multivariate calibration, partial least square (PLS) regression analysis, were effective for deriving quantitative estimation of soil geotechnical characteristics from spectral data. Spectra of clay minerals in the MIR wavelength region are found to provide additional remarkable information for identification and subsequent characterization of clay minerals. Statistically significant correlations are observed between geotechnical and spectral characteristics of expansive soils.

The potential of multispectral images in combination with a multivariate statistical analysis (PLS) for mapping variation in soil geotechnical characteristics was also investigated. To date, no direct remote sensing maps of soil geotechnical parameters have been published. The approach presented in chapter seven highlighted the potential of multispectral remote sensing in mapping geotechnical characteristics of expansive soils. It is possible to acquire large-scale (covering a wide area) estimate of soil geotechnical parameters such as those indicating subgrade characteristics. Availability of such maps during project planning can give a reasonable indication of soil geotechnical characteristics. Identification of problematic sites for narrowing down the need for detailed assessment is of significance. Furthermore,

important contribution is anticipated as a constraining factor in spatial infrastructure planning such as choice of optimal road alignment.

Remote sensing allows for mineralogical composition analyses and quantitative estimation of various soil geotechnical characteristics, which was previously possible through a combination of at least two methods. In practice, this unique capability can provide information necessary for planning and design of infrastructure. Overall, remote sensing can substantially contribute to the understanding of active clay minerals and play a significant role in geotechnical investigation of expansive soils. Therefore, integrating these techniques with routine geotechnical analyses of soils is highly beneficial, as it can serve as basic means for recognizing the presence of expansive soils. Finally, the issue of standardizing remote sensing techniques requires further research and collaboration among the domain of experts in the discipline to universalize the approach.

Samenvatting

Bodems kunnen opzwellen en onstabiel worden door verandering in vochtgehalte. Veranderingen in vochtgehalte zijn het gevolg van bijvoorbeeld natuurlijke variatie in verschillende seizoenen en door klimaat, maar kennen ook niet-natuurlijke oorzaken. Zwellende bodems vormen een uitdaging voor de bouwsector, aangezien bodemstabiliteit een kritische factor is in bouwkosten vooral bij het ontwikkelen van lichtgewicht infrastructuur. De toename in volume van zwellende bodems door opname van vocht is vaak groter dan de neerwaartse druk uitgeoefend door het gewicht van lichte bouwstructuren, hetgeen leidt tot deformatie en scheuren. Grote afname van volume door opdrogen van een bodem leidt daarentegen tot verschillen in het zetten van een bodem. Uit literatuur blijkt dat wereldwijd deze toename en afname van bodemvolume jaarlijks resulteert in miljarden dollars schade aan infrastructuur. Daarmee behoren zwellende bodems tot de kostbaarste natuurlijke gevaren (geohazards). De gebieden die het meest blootgesteld zijn aan zwellen en krimpen van de bodem zijn de aride en semi-aride regio's in tropische en gematigde klimaatzones, waar de jaarlijkse evapo-transpiratie groter is dan de neerslag. Zwellende bodems komen onder meer voor in Ethiopië, en zijn ook daar berucht om een wijds scala aan problemen in de bouwsector.

Aangezien investeringen in infrastructuur een significant deel zijn van de globale economie, hebben zwellende bodems een primaire focus in geotechnische engineering en bodemkundig onderzoek. De twee belangrijkste onderwerpen in onderzoek naar zwellende bodems zijn (1) karakterisering en (2) behandeling, of stabilisatie. Het eerste punt behelst identificatie en kwantitatieve analyse van zwellende bodems, terwijl het tweede punt gaat over het streven naar verbeteren van geotechnische kenmerken van een bodem (zoals het verminderen van zwel en krimp potentieel). Karakterisering van bouwgrond is daarom al in een vroeg stadium benodigd bij een bouwproject, maar is ook nodig voor een beter landgebruik. Een compleet geotechnisch onderzoek verzekert een optimale planning, ontwerp, bouw en bevredigende functionaliteit van bouwsels. Geconfronteerd met beperkende hoge kosten van gebruikelijke onderzoek methodes, is er een grote belangstelling voor vernieuwende technieken in het karakteriseren van zwellende bodems, zoals aardobservatie.

In de laatste jaren zijn er, door het gebruik van aardobservatie technieken, significante ontwikkelingen geweest in het verbeteren van geotechnische karakterisering van zwellende bodems, en in het voorspellen van hun ruimtelijke variabiliteit. Het golflengte bereik en spectrale resolutie van spectrometers verbeteren continu. Prijzen van deze instrumenten zijn gedaald, en draagbare spectrometers zijn nu beschikbaar. Naast de

beschikbaarheid van grote archieven met beeldmateriaal verkregen door aardobservatie, zijn ook de ruimtelijke en spectrale resolutie van deze sensoren continu verhoogd. De daar nog bij komende verbeteringen in spectrale en ruimtelijke beeld analyse hebben geleid tot de mogelijkheid om geotechnische informatie over bodems te karteren.

In dit onderzoek werden geotechnische en spectrale kenmerken van zwellende bodems beschreven. Het hoofddoel was om de relatie tussen deze twee aspecten van zwellende bodems te bestuderen, in het zichtbare en nabij-infrarode (visible near infrared, VNIR), het kortgolvig-infrarode (shortwave infrared, SWIR) en het mid-infrarode (mid infrared, MIR) golflengtebereik (0.35-14 µm). Geotechnische en spectrale kenmerken van zwellende bodems worden beide bepaald door de mineraal samenstelling, voornamelijk door aanwezigheid of afwezigheid van actieve klei mineralen, hetgeen de mogelijkheid biedt om beide kenmerken te relateren. Nadruk werd gelegd op het ontwikkelen van nieuwe methodes voor karakterisering, waaronder identificatie, schattingen van standaard geotechnische parameters, en het karteren van ruimtelijke variatie in geotechnische kenmerken van zwellende bodems vallen.

In een laboratorium kunnen zwellende bodems geïdentificeerd en gekarakteriseerd worden met spectra. Deze techniek vereist maar weinig materiaal per bodem monster, een minimale preparatie en minimale tijd voor analyse. In vergelijking met het vele werk dat benodigd is bij een conventionele analyse, kan zo in een hogere dichtheid gemeten worden. Naast metingen in het nabij en kortgolvig infrarood, werden ook de spectrale kenmerken van actieve klei mineralen vastgesteld in mid-infrarode golflengtes. Dit heeft geleid tot nieuwe inzichten, aangezien er voorheen weinig begrip was over de spectrale karakteristieken van actieve klei mineralen en zwellende bodems in mid-infrarode golflengtes. Verscheidene spectrale en statistische technieken werden gebruikt om bodemsamenstelling te bepalen en spectrale kenmerken te relateren aan standaard geotechnische parameters zoals Attenberg consistentie grenzen (consistency limits). Statistische technieken zoals multivariate calibratie en partial least square (PLS) regressie analyse bleken effectief in het verkrijgen van kwantitatieve schattingen van geotechnische bodemkenmerken uit spectra. Spectra in het mid-infrarode golflengte bereik bleken kenmerkende informatie te kunnen verschaffen voor identificatie en karakterisering van klei mineralen. Statistisch significante correlaties werden waargenomen tussen geotechnische en spectrale kenmerken van zwellende bodems.

Het potentieel van multispectrale aardobservatiebeelden in combinatie met een multivariate statistische analyse (PLS) voor het karteren van variatie in geotechnische bodemkenmerken werd ook onderzocht. Tot nu toe waren er

nog geen geotechnische bodemkaarten gepubliceerd op basis van aardobservatie. De methode die in hoofdstuk 7 uitgelegd wordt, laat het potentieel van multispectrale aardobservatie voor het karteren van geotechnische kenmerken van zwellende bodems zien. Het is nu mogelijk om een grootschalige (een groot gebied bedekkende) schatting maken van geotechnische bodemkenmerken die, bijvoorbeeld, wijzen op een ondermaatse staat van een bodem. De verkrijgbaarheid van zulke kaarten bij een projectplanning kan een redelijke inschatting geven van geotechnische bodemkenmerken. Van significant belang is dat er identificatie is van problematische gebieden, die nadere bestudering behoeven. Verder is een belangrijke rol voorzien in het plannen van infrastructuur, bijvoorbeeld in de keuze van een optimaal tracé in de wegenbouw.

Met aardobservatie kunnen minerale samenstellingen en kwantitatieve schattingen van verscheidene geotechnische bodem karakteristieken gemaakt worden, hetgeen voorheen alleen mogelijk was door een combinatie van ten minste twee methodes te gebruiken. Dit unieke kenmerk kan in de praktijk informatie verschaffen die nodig is voor de planning en ontwerp van infrastructuur. Aardobservatie kan substantieel bijdragen aan ons begrip van actieve kleimineralen en een significante rol spelen in geotechnisch onderzoek van zwellende bodems. Het integreren van deze techniek met gebruikelijke geotechnische analyse van bodems heeft een hoge toegevoegde waarde, aangezien het een praktisch bruikbare methode is om het voorkomen van zwellende bodems te detecteren. Ten slotte moet nog opgemerkt worden dat een standaardisering van aardobservatie technieken, door meer onderzoek en intra disciplinaire samenwerking, nodig zal zijn om deze methode universeel toepasbaar te maken.

Biography

Fekerte Arega Yitagesu was born on the 16th of February 1975 in Addis Ababa, Ethiopia. She obtained her BSC. degree (in Geology) from Addis Ababa University (AAU), Faculty of Natural Science (1997). She joined the International Institute for Geo-information and Earth observation (ITC) in September 2004, and graduated with a master of science (MSC.) degree in geo-information science and earth observation, specialization Geological engineering in March 2006 (with distinction).

Since October 2007, she is working on her PhD research at the University of Twente, faculty of Geo-information and Earth observation (ITC). Her study is focused on identification, characterization and mapping expansive soils using remote sensing techniques.

Fekerte has several years of experience in geotechnical site investigation, geotechnical mapping, earthworks, rock mass classification, slope stability analyses, sampling, in-situ and laboratory testing of various construction materials, geophysical survey, environmental impact assessment (EIA), strategic environmental assessment (SEA). Her experience includes assessing geotechnical and geo-environmental inputs for preparation and review of road projects, tender and construction document, quality control and management (supervision), preparation of geotechnical investigation and material reports, preparation of environmental impact assessment reports and environmental management plans for road projects etc. She also gained an ample experience in remote sensing and GIS in relation to infrastructure development and various aspects of environmental applications. Other than expansive soils, Fekerte is keenly interested in ground improvement research and the application of remote sensing and geo-information technologies for analyzing and mapping other problem soil and geo-hazards such as mass movements.

ITC Dissertation List

http://www.itc.nl/Pub/research_programme/Graduate-programme/Graduate-programme-PhD_Graduates.html